UNIVERSITY OF TRENTO - Italy

International PhD Program in Biomolecular Sciences

XXVI Cycle

Silk fibroin-based injectable hydrogels for brain tissue engineering applications

Tutor: Prof. Alessandro Quattrone

Centre for Integrative Biology (CIBIO), University of Trento, Trento, Italy

Advisor: Prof. Antonella Motta

Department of Industrial Engineering and Biotech Research Center, University of Trento, Trento, Italy

European Institute of Excellence on Tissue Engineering and Regenerative Medicine, Trento, Italy

PhD thesis of

Wei Sun

Centre for Integrative Biology (CIBIO), University of Trento

Department of Industrial Engineering and Biotech Research Center University of Trento

European Institute of Excellence on Tissue Engineering and Regenerative Medicine, Trento,Italy

Academic Year 2012-2013

DECLARATION

I, Wei Sun , confirm that this is my own work and the use of all material from other sources has been properly and fully acknowledged.

PhD candidate:

Wei Sun

Tutor:

Prof. Alessandro Quattrone

Date: 16/05/2014

Abbreviations

Ang-1	Angiopoietin-1
bFGF	Basic fibroblast growth factor
BM-MSCs	Bone marrow mesenchymal stem cells
BMPs	Bone morphogenetic proteins
BMP-4	Bone morphogenetic protein 4
BSA	Bovine serum albumin
CNS	Central nervous system
CD31	Cluster of differentiation 31
DAPI	4',6-diamidino-2-phenylindole
DMEM	Dulbecco's modified Eagle's medium
DMEM/F12	Dulbecco's Modified Eagle Medium: Nutrient Mixture F-12
ECs	Endothelial cells
ECM	Extracellular matrix
EDC	1-Ethyl-3-(3-dimethylaminopropyl)carbodiimide
EGM-2	Endothelial cell growth medium-2
EPCs	Endothelial progenitor cells
ESCs	Embryonic stem cells
FE-SEM	Field Emission Scanning Electron Microscope
FGF	Fibroblast growth factors
FT-IR	Fourier Transform Infrared
GFAP	Glial fibrillary acidic protein
GMEM	Glasgow Minimum Essential Medium
HNSCs	Human neural stem cells
IKVAV	Isoleucine-Lysine-Valine-Alanine-Valine
KSR	Knockout Serum Replacement
MAP2	Microtubule-associated protein 2
MES	2-(N-Morpholino)ethanesulfonic acid hydrate
mESCs	Mouse embryonic stem cells
MT-MMPs	Membrane-type matrix metalloproteinases
NSCs	Neural stem cells
OCT-4	Octamer-binding transcription factor 4
OEC	Outgrowth endothelial cells
PBS	Phosphate buffered saline
PCR	Polymerase chain reaction
PEG	Polyethylene glycol
PHA	Polyhydroxyalkanoates
PHPMA	Poly[N-2-(hydroxypropyl) methacrylamide]
PI	Propidium iodide
PNS	Peripheral nervous system
RT-PCR	Real-time polymerase chain reaction
QRT-PCR	Quantitative real-time polymerase chain reaction
RGD	Arginine-Glycine-Aspartic
SF	Silk fibroin

SM-actin	Smooth muscle actin
Sulfo-NHS	N-Hydroxysulfosuccinimide sodium salt
SVZ	Subventricular zone
TBI	Traumatic brain injury
TCP	Tissue culture plate
TGF-β	Transforming growth factors-β
VE-Cadherin	Vascular endothelial cadherin
VEGF	Vascular endothelial growth factor
VZ	Ventricular zone
2D	Two dimensional
3D	Three dimensional

Contents

Abstract

Stroke and traumatic brain injury are among the leading causes of death in the world. Until now, there are no effective treatments available. Current pharmaceutical treatments have limited benefits to repair the damaged tissue. Brain tissue engineering is a promising strategy to help brain regeneration after the damage induced by stroke or traumatic brain injury. In this thesis, our work focused on designing and evaluating appropriate silk fibroin-based hydrogels combined with stem cells therapy for brain tissue regeneration.

The work initially started from looking for appropriate silk fibroin-based hydrogel substrates which can support the viability and neural differentiation of pluripotent cells. Mouse embryonic stem cells (mESC) were used as a model. Different processing procedures of silk fibroin-based hydrogel substrates were prepared by chemical genipin crosslinking and physical sonication crosslinking. The viability and neural differentiation of pluripotent cells on these hydrogel substrates were evaluated, using tissue culture plates (TCP) as control. Different crosslinking processes were found to modulate the neural differentiation of pluripotent cells. Chemical genipin crosslinked hydrogel substrates could inhibit the neural differentiation of mESC compared to control TCP, while the physical sonication crosslinked hydrogel substrates could support the neural differentiation as TCP.

According to the results obtained in the first stage, the physically sonication-crosslinked 3D silk fibroin hydrogel was produced to encapsulate human neural stem cells (hNSC). In order to improve the hNSC attachment and neuronal differentiation, the isoleucine-lysine-valine-alanine-valine (IKVAV) peptide derived from laminin was covalently conjugated to the silk fibroin. The viability and neural differentiation of hNSC were evaluated in the unmodified and IKVAV

peptide modified silk fibroin hydrogels. We found that the IKVAV peptide modified silk fibroin hydrogel could increase the viability, proliferation and neuronal differentiation of hNSC.

Furthermore, the angiogenesis potential of sonication-induced 3D silk fibroin unmodified and modified with IKVAV and a scramble peptide VVIAK (as control) were evaluated in a human outgrowth endothelial cells (OEC) mono-culture system and a co-culture system in which OEC were cultured with human bone marrow mesenchymal stem cells (BM-MSC). Both the silk fibroin unmodified and modified with IKVAV peptide could not induce angiogenesis in the mono-culture system under the VEGF condition. However, in the co-culture system, we found that unmodified, IKVAV-modified and VVIAK-modified silk fibroin hydrogels all could support angiogenesis. Furthermore, there were no significant differences among unmodified, IKVAV modified and VVIAK modified silk fibroin hydrogels influencing on angiogenesis structure and gene expression related to angiogenesis.

The thesis will introduce the detailed work in three different chapters (from chapter 3 to chapter 5) respectively.

Chapter 2: General introduction

2.1 Tissue engineering and regenerative medicine

In adult human body, tissues and organs could be damaged and their functions could be lost by a wide range of diseases and injuries which include trauma, degenerative diseases, inflammation, or other conditions. The self-repair ability of the body is usually limited without medical intervention. Many damaged tissues can not be regenerated by themselves, such as central nervous system. Moreover, the repair process might involve producing scar tissues instead of restoring the normal structure and function of tissues (*1*, *2*).

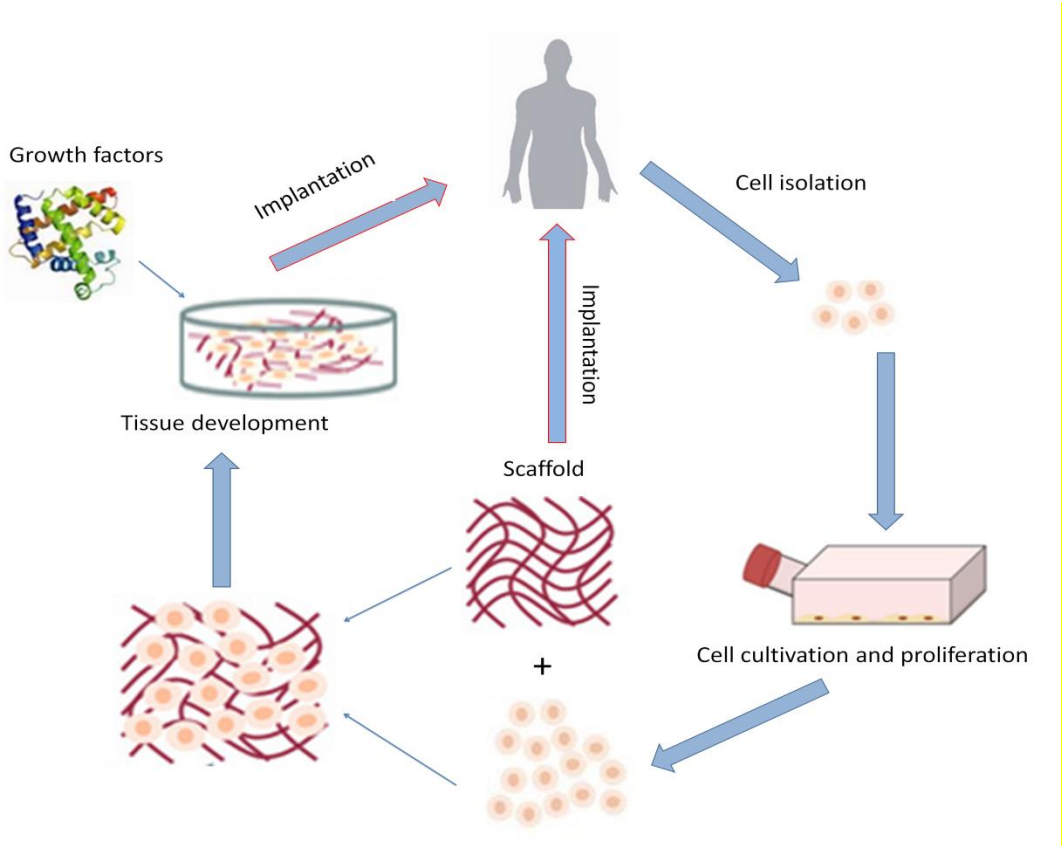

Fig 2.1 Principle of tissue engineering.

Therefore, to induce regeneration of damaged tissue, the concept of tissue engineering occurred. In 1993, Langer and Vacanti provided the definition of tissue engineering as "an interdisciplinary field that applies the principles of engineering and life sciences toward the development of biological substitutes that restore, maintain, or improve tissue function or a whole organ" (*3*). Then in 2006, David F. Williams defined tissue engineering as "Tissue engineering is the creation of a new tissue for the therapeutic reconstruction of the human body, by the deliberate and controlled stimulation of selected target cells, through a systematic combination of molecular and mechanical signals " (*2*) (Fig 2.1).

2.1.1 Key elements

To regenerate the damaged tissues, there are two main strategies in tissue engineering (Fig 2.1). The first approach is named *in situ* regeneration, and involves the design of an inductive scaffold (with or without growth factor/drug delivery system) which should interact with the implantation environment, guiding cells from surrounding tissue to adhere and migrate in the scaffold and trigger new tissues formation. This approach relies on the development of a target-specific scaffold system that can effectively mobilize host stem/progenitor cells to target tissues. (*4*) *In situ* tissue regeneration has been applied to various therapeutic applications. For example, the scaffold made by calcium phosphate, calcium sulfate and hydroxyapatite were widely used for *in situ* bone regeneration (*4*). Scaffolds consisting of biodegradable PLGA polymer were incorporated with plasma and hyaluronic acid, then were implanted into micro-fractured cartilage tissue (*5*). Besides, this *in situ* regeneration concept was also translated to regeneration of other tissues, such as skeletal muscle, brain, cardiovascular, spine and skin (*4*). However, when the damaged tissues have poor regenerative ability (such as brain and myocardium) and the defect size is critical, the first approach is limited because it relies on the body's own regenerating

capacity. Therefore, a complex cells-based tissue engineering strategy has emerged as a promising approach to overcome these limitations. In this approach, to specifically guide tissue regeneration and stimulate the specific target tissue cell population, the scaffold can be cultured in the hybrid-system *in vitro* to synthesize new tissue or can be implanted in vivo. These scaffolds not only induce surrounding cells growth but also serve as templates for the implanted cells to attach, grow, migrate or differentiate. The desired tissue regeneration can be developed via proliferation and differentiation of the host cells and transplanted cells. This strategy has been applied in tissues such as bone (*6*), cartilage (*7*), liver (*8*), blood vessels (*9*), and nerve (*10*).These two approaches could be utilized separately depending on the application and could also be combined as a promising strategy in tissue engineering. The three components: scaffold, cells and signals are usually described as a tissue engineering triad (Fig 2.2) (*11*).

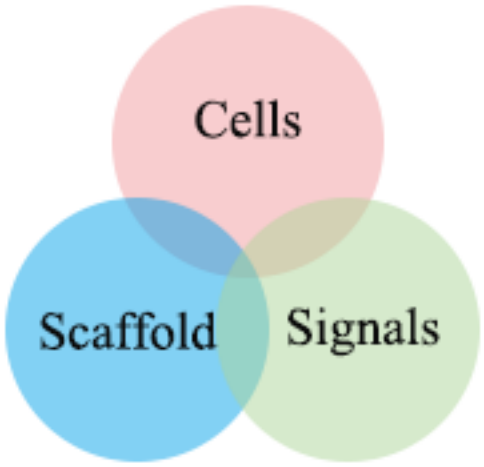

Fig 2.2 Key elements in Tissue engineering and regenerative medicine

2.1.1.1 Scaffold

Scaffold is a basic three-dimension (3D) bioactive framework for cell activity and subsequent tissue regeneration. Human tissues reside in the extracellular matrix (ECM), which are an

instructive physical environment and a structure supporting for cells in the tissues to attach, grow and migrate (*12*). Therefore, the natural ECM represents an appealing model to design bioactive scaffolds (*13*). Regardless of different tissue engineering applications, the scaffold must be biocompatible, the cells in the implanted environment or the pre-seeded cells should be able to adhere, proliferate and migrate in the scaffold before producing new matrix. After implantation, the inflammatory responses should be guided to the transition of tissue repair. Then, the scaffold should have porous architecture, which allows cells proliferation and migration, nutrients and oxygen diffusion, as well as new capillary formation. Scaffolds should also have the bioactivity to interact with host tissue facilitating and regulating the cell activities. They also need to be endowed with biological cues to influence cell adhesion, proliferation and/or stem cells differentiation. Upon the implantation site, the scaffold must be controlled biodegradable so that the cells could produce their own ECM that can eventually replace the implantation scaffolds (*14*). Depending on the different tissue regeneration application, the mechanical properties should be varied when designing specific scaffolds to match the host tissue. Different tissue cell types like fibroblasts, myocytes, neurons, and other cell types reside in the ECM of different stiffness. These cells can just sense the matrix whose stiffness are similar to their resident tissues (*15*). Furthermore, the stiffness of scaffolds can also affect the stem cells differentiation to specific lineages, consistent with the resident elasticity of differentiated cell types (*16*).

Biomaterials are the starting point to fabricate artificial 3D frameworks referred as scaffolds, matrices, or constructs (*17*). At the conference of European Society for Biomaterials (ESB) in 1976, the biomaterial was firstly defined as “a nonviable material used in a medical device, intended to interact with biological systems”. Then, the definition is evolved to “a material intended to interface with biological systems to evaluate, treat, augment or replace any tissue,

organ or function of the body" (*14*). Until now, biomaterials have been widely used as implants in the form of sutures, bone plates, joint replacements, ligaments, vascular grafts, heart valves, intraocular lenses, dental implants, and medical devices like pacemakers, biosensors, and so forth (*17*, *18*).

Polymers, synthetic and naturally-derived, are widely used as biomaterials to fabricate scaffolds for tissue engineering. Natural polymers and synthetic polymers are the main types used in designing scaffolds. Both of them have advantages and disadvantages in the application of tissue engineering.

Synthetic polymers are widely used in tissue engineering because they can be tailored in a range of properties (such as strength, flexibility and degradation) compared to natural polymers. Besides, they are much cheaper than natural polymers and can be widely produced in uniform quantities and have a long shelf time. However, their biocompatibility and biodegradability are the disadvantages, limiting their potential use in the clinical side. (*17*). Many synthetic polymers such as PLA (*19*), PCL(*20*), PLGA (*21*) PEVA (*22*) have been widely used in tissue engineering.

Natural polymers are derived from natural living creature sources. Unlike synthetic polymers, natural polymers are biologically active because of the inherent bio-recognition. They are able to support excellent cell adhesion and growth. Furthermore, most of them are biodegradable and therefore allow host cells, or pre-seeded cells, to produce their own ECM (*14*). Natural-derived polymers are usually classified into three groups (*23*):

(i) Protein-origin polymers (such as collagen, gelatin, fibrinogen, silk, elastin, keratin, actin, myosin and so on) can mimic aspects of natural protein in ECM and thus have the potential to guide the attachment, growth, migration and differentiation of cells in tissue regeneration and

wound healing, as well as for stabilization of encapsulated and transplanted cells. Protein-origin polymers structures are composed by distinct amino acids linked by amide (or peptide) bonds. Amino acids are the building blocks of polypeptides and proteins, which consist of a central carbon linked to an amine group, a carboxyl group, a hydrogen atom, and a side chain (*23*). For examples, collagen is a naturally occurring matrix polymer, which is regarded as an ideal scaffold or matrix for tissue engineering (*24*). It is the major protein component of the extracellular matrix, providing support to connective tissues such as skin, tendons, bones, cartilage, blood vessels, and ligaments (*25*). Gelatin is a denatured, biodegradable protein obtained by acid and alkaline processing of collagen (*26*), and is commonly used for pharmaceutical and medical applications because of its biodegradability and biocompatibility in physiological environments (*27*).

(ii) Polysaccharides are a class of biopolymers constituted by sugars as monomers (*28*). They can be obtained from different sources such as microbial, animal and vegetal (*29*) Polysaccharides are non-toxic, which show interaction with living cells and usually have low costs in comparison with others biopolymers such as collagen (*30*) Furthermore, polysaccharides show good hemocompatibility properties because of the chemical similarities with heparin. Different polysaccharides such as aginate, chitosan, hyaluronan, Chondroitin sulphate cellulose, amylose, dextran, chitin, carrageenans, glycosaminoglycans, and so on have been widely utilized as scaffold materials in tissue engineering applications as well as carriers for drug delivery systems.

(iii) Bacterially synthesized polyhydroxyalkanoates (PHAs) have attracted much attention because they can be produced from a variety of renewable resources, and are truly biodegradable and highly biocompatible thermoplastic materials (*31*)

Although natural origin materials also present some drawbacks such as limited processability, the difficulties in controlling the mechanical properties and the variability from batch to batch, their advantages clearly surplus the drawbacks and they are still very attractive candidates for biomedical applications because of their biocompatibility, degradability, low cost and availability, similarity with the ECM and intrinsic cellular interaction for tissue engineering applications. Furthermore, in order to overcome the disadvantages of synthetic or natural polymers in tissue engineering application, composite materials by blending both materials have arisen growing interests to improve the scaffold properties, controlled degradation and biocompatibility (*17*).

2.1.1.2 Cell sources

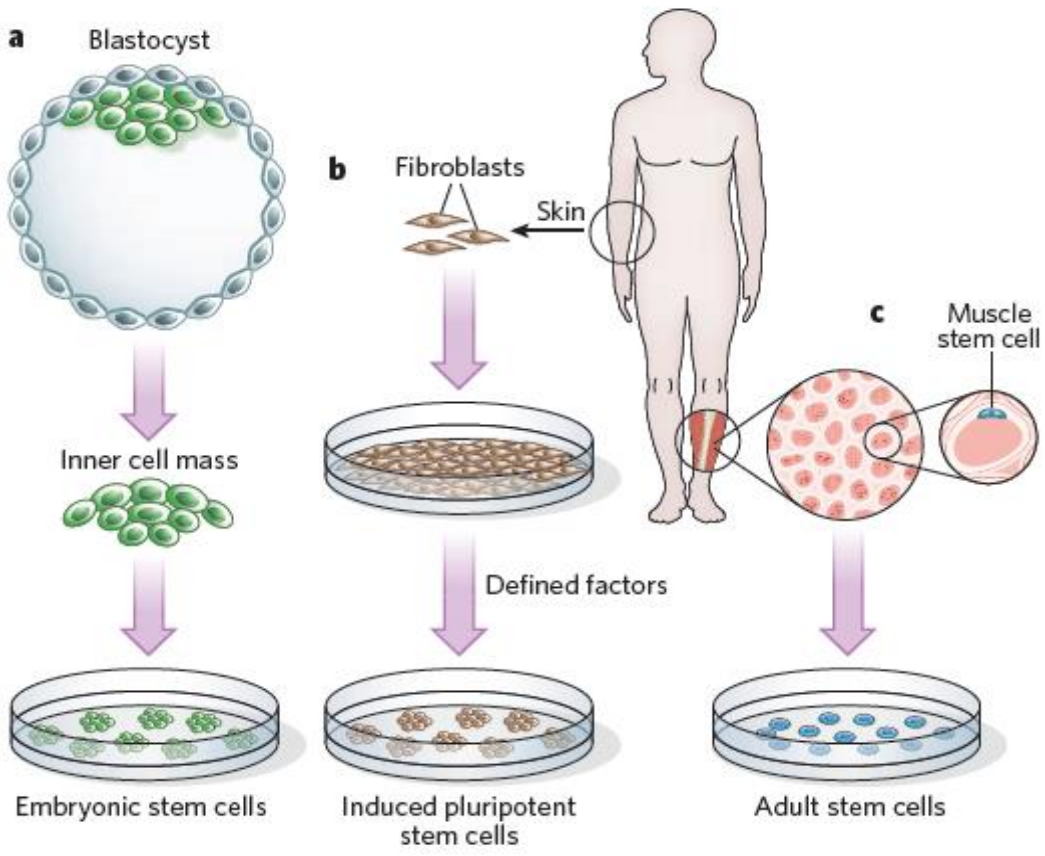

Fig 2.3 Stem cells resources for tissue engineering and regenerative medicine: Embryonic stem cells(a), Induced pluripotent cells(b) and Adult stem cells(c) (*32*).

In the second strategy of tissue engineering that combines cells and scaffolds, the sources of cells are important. Some successes have come from the use of autologous cells, taken from the patient, and used in conjunction with scaffolds to produce tissues for re-implantation. However, this strategy has limitations, because of the invasive nature of cell collection and the potential for cells to be in a diseased state (*11*). Therefore, in such situations, stem cells are considered as an important alternative cell sources because of their ability to self-renew and to produce specialized progeny. Embryonic stem cells, adult stem cells and induced pluripotent stem cells are obtained from three different sources and have different advantages and limitations (*32*) (Fig 2.3).

Embryonic stem cells (ESCs) are pluripotent cells, which can proliferate in self-renewal stage and can be differentiated into many specialized cell types (*33*). Human embryonic stem cells (hESCs), firstly derived by Thomson in 1998 (*34*), aroused great interest in tissue engineering and regenerative medicine because of their multi-ability to differentiate into any adult tissue cell type (*35*). However, hESCs are restricted to their clinical application due to the ethical problems and regulations. Furthermore, when implanted in an animal model, hESCs can possibly give rise to teratoma, tumor-like formations containing tissues belonging to all three germ layers (*36*). In parallel, stem cells derived from adult tissues (adult stem cells) have also a promising potential in tissue engineering with considerable advantages. They are immunocompatible and are not associated with ethical concerns. However, challenges remain related to optimization of isolation techniques that avoid contamination, permanently maintain the desired cell types following differentiation, and produce a large number of cells that are adequate for the construction of a

tissue or organ (*37*). Adult stem cells have been isolated from different tissues such as bone marrow (*38*), adipose tissue, peripheral blood, amniotic fluid or umbilical cord blood (*39*). Finally, induced pluripotent stem cells have all of the properties of embryonic stem cells, overcoming the problem of immune tolerance and the ethical issues faced by the use of human embryonic stem cells. However, the currently available methods to reprogram somatic cells and to generate induced pluripotent stem cells are extremely slow and inefficient (*32*).

2.1.1.3 Signaling molecules delivery

Growth factors are soluble-secreted signaling polypeptides capable of instructing specific cellular responses in a biological environment (*40*). They could trigger a wide range of cell responses, which include cell survival, cell migration, proliferation or differentiation of a specific subset of cells (*41*). Growth factor could bind to specific transmembrane receptors of the target cells. Then the growth factor-binding signals are conducted to the cell nucleus, which results in a complex array of events involving cytoskeleton protein phosphorylation, ion fluxes, changes in metabolism and gene expression, protein synthesis and ultimately an integrated biological response (*42*). The specific growth factor can be chemically conjugated and/or physically encapsulated in the scaffold to release in the target tissue or they can be added in the culture conditions *in vitro.* Many growth factors have been applied in tissue engineering. For example, vascular endothelial growth factor (VEGF), fibroblast growth factor (FGF) and angiopoietin-1 (Ang-1) are required for the angiogenesis of pre-existing blood vessels, as well as for promoting the proliferation and migration of new cells to form new immature vessels (*43*), bone morphogenetic proteins-2 (BMP-2) and transforming growth factor-β3 (TGF-β3) in alginate hydrogels, VEGF and BMP-2 from gelatin microparticles have been reported to enhance healing effects (*44, 45*).

Consequently, tissue engineering is a multidisciplinary field that involves the principles and methods of engineering, life science and clinics. Successful strategies in tissue engineering require the optimization of the combination of scaffolds, cells and growth factors which is still a complex process. Even though there are still many challenges in developing the regenerated tissue, results now are still promising.

2.2 Brain tissue engineering

The nervous system is composed of peripheral nervous system (PNS) and central nervous system (CNS). In contrast to the PNS, the CNS and especially the adult brain possess a very limited ability to regenerate after damages.

2.2.1 Brain injuries

Many physical injuries and neurological disorders can result in brain damage: (i) stroke, which can be categorized as hemorrhagic, ischemic, or embolic in origin, is the third leading cause of death in the world. (*46*). Ischemic stroke accounts for 80% of all brain strokes which is the death of an area of brain tissue (cerebral infarction) resulting from an inadequate supply of blood and oxygen due to the blockage of an artery. (ii) Traumatic brain injury (TBI) is another major cause of brain health problems, more than 1.4 million new cases are reported annually in the USA. Like stroke, TBI causes severe disability and there is still no effective clinical treatment available worldwide to repair the damaged tissues (*47*). Besides, neurodegenerative diseases are also consistently increasing, like Parkinson's disease. All these damages, often result in the loss of neuronal cell bodies and axons (*46*), which also involving the recruitment and activation of astrocytes, macrophages, and microglia and ultimately forming a glial scar, a physical and chemical barrier for regeneration (*48, 49*). Most treatments currently use pharmacological agents

aiming to reduce the sequelae of injury in the acute phase and to enhance the remaining brain tissue function during the chronic stage of the injury process. This occurs, however, without eliciting tissue regeneration (*50*).

Therefore, brain tissue engineering is a promising strategy to repair the injured brain tissue. Scaffolds act as artificial environments to support the long-term growth of endogenous and therapeutic cells pre-seeded in the scaffolds, facilitating cell regeneration but also preventing further damage to adjacent tissues. Combination of cell therapy in brain tissue engineering is also a main research area to replace the lost neural cells.

2.2.2 Neural stem cells

One promising approach is the use of stem cells, especially neural stem cells (NSCs) for damaged brain tissue regeneration. NSCs are present both in the developing and adult brain. They can self-renew and generate both neurons and glial cells in the developing brain and therefore are potential cell sources for regeneration of the adult brain (*51*). At early embryonic stages, NSCs exist as neuroepithelial stem cells in the embryonic neural tube. In this stage, NSCs expand their population by symmetric cell divisions, before they start to produce neurons. Subsequently, the neuronal lineages are generated by NSCs through asymmetric cell divisions in the germinal ventricular zone (VZ). After this major neurogenic period, NSCs acquire gliogenic competency and produce glial progenitor cells, which proliferate mostly in a second germinal zone, the subventricular zone (SVZ). By the postnatal stage, the radial glial have transformed into astrocytes and the VZ has disappeared, but some portions of the SVZ remain into adulthood, to become sites of adult neurogenesis. Adult endogenous NSCs can be found in the two principal adult neurogenic regions, the hippocampus and the SVZ, indicating that possible regenerative capabilities are preserved in the adult mammalian brain (*51*). However, although endogenous

NSCs are presented in the adult brain, the mechanism that regulates their self-renewal and differentiation after injury is still poorly understood. Furthermore, the brain regions to which their progeny migrate in order to differentiate remain unresolved.

Thus, besides the activation of endogenous NSCs, NSCs transplantation is a more promising strategy to regenerate the damaged brain tissue. NSCs can be derived from many sources, including embryonic stem cells, fetal stem cells, adult stem cells and induced pluripotent stem cells (*46*). NSCs have been isolated from many regions of the embryonic nervous system (*52*) and adult brain tissue (*53*). In the beginning stages of NSCs transplantation, cells were directly injected into the lesion sites, which resulted in low cell viability of the transplanted cells and the further damage to the host tissue (*46*). Furthermore, NSCs transplanted into the brain in the absence of a supporting niche largely differentiated into glial cells (*54*).

Therefore, to support the functions of NSCs, an important niche, the NSCs microenvironment must be provided. Adult NSCs microenvironment in mammalian, usually contains resident stem cells, vessels, stromal cells, and a specialized ECM (Fig 2.4) (*55*). Although some signaling molecules can control the functions of NSCs, ECM is a long-term structure niche to maintain the functions of NSCs. The structure, mechanical and chemical properties, as well as the signaling molecules in ECM could all contribute to controlling the behavior and differentiation fate of NSCs. Brain tissue engineering aims at creating such a specialized scaffold to mimic the microenvironment ECM for NSCs and help damaged brain tissue regeneration. More specifically, this scaffold should enhance the viability of transplanted NSCs and control their differentiation fate.

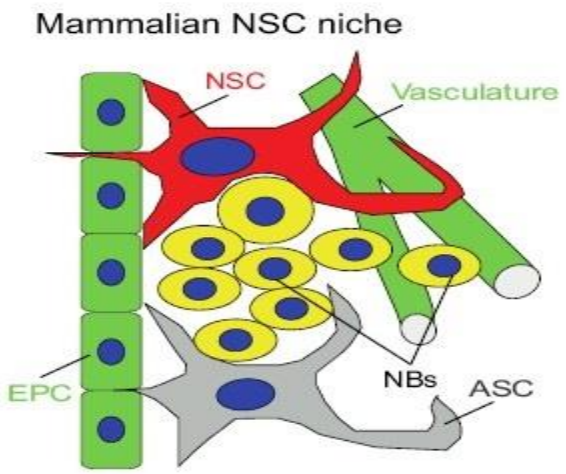

Fig 2.4: NSCs niche in the mammalian SVZ: ASC, astrocyte; EPC, ependymal cell; NBs, neuroblasts; NSC, neural stem cell; (*55*)

2.2.3 Hydrogel design

The natural brain is a very unique tissue, as it has unusual ECM components such as lecticans, proteoglycans, hyaluronic acid and tenascin family proteins (*56*), as well as its soft physical properties. Therefore, although many different kinds of scaffolds are used in brain tissue engineering such as nanofibers (*57*), much of the research efforts focused on the development of hydrogels (*58*). Hydrogels are high water content polymers, which can be produced by both natural and synthetic materials such as collagen (*59*), hyaluronic acid (*60*), alginate (*61*), chitosan (*62*) and Polyethylene glycol (PEG) (*63*). Easy diffusion of nutrients, oxygen and cellular metabolites are permitted in hydrogels (*64*). Furthermore, hydrogels are mainly used, as they display similar mechanical properties (such as rheology behavior) to those of the central nervous system ECM (*46*). Many different types of hydrogel have been fabricated and evaluated for brain application by mimicking the biochemical and mechanical properties of brain. Synthetic hydrogels such as poly[N-2-(hydroxypropyl) methacrylamide] (PHPMA), Polyethylene glycol (PEG) and so on. PEG has many excellent qualities for this application, including being highly hydrophilic, biocompatible, non-immunogenic, and neuroprotective. However, due to the

polyether backbone, it is non-degradable in the body (*65*). Biological derived hydrogels such collagen, hyaluronic acid (HA) chitosan, agarose, alginate, methyl cellulose, xyloglucan, Matrigel, fibrin, PolySia-based hydrogels, peptide hydrogels are widely used in the CNS regeneration (*46*). These natural polymers have biocompatibility, intrinsic biological activity, as well as degradability, by the naturally occurring enzymes. To better mimic the brain tissue ECM and control the differentiation fate of NSC, many aspects of the hydrogel design should be considered.

(i) Hydrogel stiffness

In the human body, different kinds of cells reside in tissues of different stiffness ranging from soft tissue to stiff tissue, like neurons in the soft brain tissue while osteoblasts in the hard bone tissue (Fig 2.5). Meanwhile, stem cells differentiation to specific lineages is also greatly effect by the specific microenvironment. Soft matrices that mimic brain are neurogenic, stiffer matrices that mimic muscle are myogenic, and comparatively rigid matrices that mimic collagenous bone improve osteogenic responses (*66*). For example, on photopolymerizable methacrylamide chitosan hydrogel surfaces of different stiffness, it had been demonstrated that neuronal differentiation was favored on the softest surfaces with Young's elastic modulus less that 1 kPa which highlights the importance of mechanical properties to the success of scaffolds designed to engineer the NSCs differentiation fate (*62*).

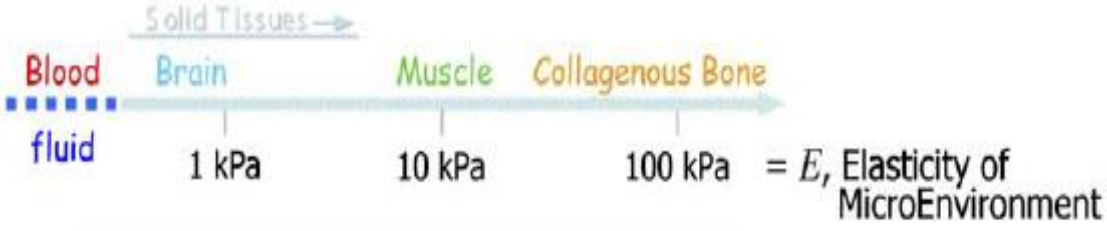

Fig 2.5 Solid tissues exhibit a range of stiffness, as measured by the elastic modulus, E. (*16*)

(ii) Hydrogel structure

In stem cells transplantation strategy, hydrogels are usually used to embed cells. Therefore, it is critical to create 3D porous hydrogels to facilitate the mass transport of oxygen, nutrients and waste. The porous structure is also important for the cells proliferation and migration. Porous hydrogels could be produced and different methods could enhance the porosity of hydrogels. For example, some components (progen) can be incorporated into the starting solution that can be removed after the hydrogel formation, in order to create a construct with tuned pore size and distribution. Li et al. reported that D-mannitol crystals were mixed with photocrosslinkable methacrylamide chitosan as a porogen to enhance pore size during hydrogel formation (*67*). Mahony and coworkers created a network of interconnected pores within a PEG hydrogel by incorporating a fibrin network that was later enzymatically degraded (*65*).

(iii) Signal cues in hydrogels

Hydrogels for brain tissue engineering should not only just be a supporting frame to transfer drugs or cells, they should also include biological cue to activate the cells in the host brain tissue and the encapsulated transplanted stem cells, guiding their proliferation, migration or differentiation.

In stem cells transplantation, the cells viability is a key factor for the success of regeneration. In order to increase the cell viability, the cells attachment is usually the first consideration. Many ECM components such as laminin, fibronectin, and collagen, are the common choices to be physically blended with hydrogel or can be chemically conjugated to the hydrogel backbones. For example, laminins are known as a family of heterotrimeric large basement membrane proteins consisting of a α-chain, a β-chain, and a γ- chain. Laminins mediate a variety of biological activities, and have been implicated in cell adhesion, cell migration, cell differentiation, and neurite outgrowth during brain development (*68, 69*). Laminins could be

blended, physically absorbed and covalently conjugated to biomaterials (*70*). Furthermore, peptides, instead of whole ECM protein, have garnered much attention because of their synthesis process, easier than the isolation of ECM proteins, and their stable conjugating to other materials (*71*). For example, a variety of potential cell-binding sequences exist in the laminin, and seventeen different cell-adhesion sites have been reported in the α1, β1 and γ1 chains. Some cell surface proteins binding to laminin-1 have been reported as follows: a non-conserved RGD site in the α1 chain interacts with integrin α3β1 and α6β1; the GD-6 in the α1 chain interacts with α3β1; two peptides, YIGSR and LGTIPG, in the β1 chain probably interact with a 67kDa binding protein; peptide IKVAV in the α1 chain interacts with a 110kDa protein (*72*) (Fig 2.6). These different peptides have been reported for using in biomaterials modification for neural tissue engineering (*10, 48, 73*)

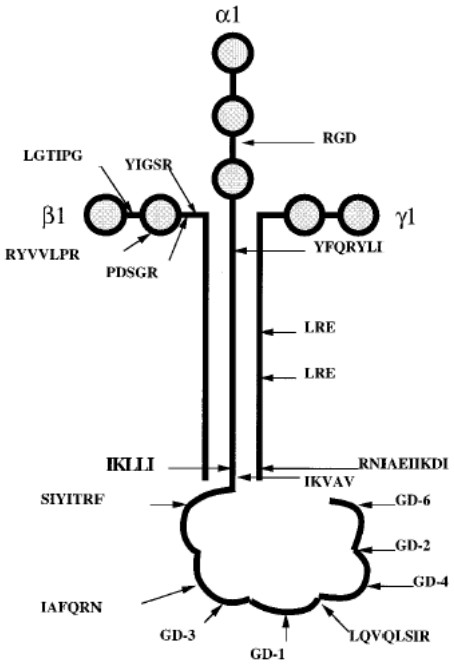

Fig 2.6 Structural model of laminin and cell binding sites (*72*)

Although some successes have been obtained in the past years for brain tissue regeneration, there are still many challenges in this field. How to integrate the building blocks of these complex

systems in brain which including the physical properties of hydrogels, the spatial and temporal control of signaling molecules, and the presentation of key ECM motifs, into modular and scalable platforms for clinical translation also need to be taken into consideration (*46, 74*).

2.2.4 Vascularization in brain tissue engineering

Stroke is the one of the leading cause of serious, long-term disability in the world, in which about 80% belong to the class of ischemic stroke. Besides the neuronal cell death during brain injury, also regenerative responses are also triggered in the tissue around the ischemic core area, including angiogenesis, vascular remodeling and neurogenesis. Migration of neuroblasts was induced after stroke into regions of degenerating striatum that border the SVZ and neuroblasts develop closely associated to vascular endothelial cells in an environment termed the neurovascular niche. In this neurovascular niche, newly born, immature neurons are closely associated with the remodeling vasculature. Neurogenesis and angiogenesis are causally linked during brain recovery through specific vascular growth factors and adhesion molecules (*75, 76*).

Angiogenesis is defined as the generation of blood vessels from the existing vasculature through activation of proliferation and sprouting mechanism in adult endothelial cells, which was for a long time considered as the exclusive pathway for blood vessels formation in an adult organism (*77*). After Asahara discovered the so-called endothelial progenitor cells (EPCs), they assumed that endothelial progenitor cells are responsible for de novo formation of blood vessels in a process termed vasculogenesis which was also referred to as a collateral mechanism in neovascularization (*78*). EPCs are defined by surface markers such as CD133 and CD34 (*79*), as well as other characteristics such as staining for von Willebrand factor, incorporation of acetylated low-density lipoprotein (*80*) and binding of ulex europaeus agglutinin (*81*). EPC can be isolated from several sources, such as bone marrow, bone marrow-derived mononuclear cells,

human umbilical cord blood cells and human peripheral blood mononuclear cells (*82*). The key function of EPC includes forming vascular structures in pro-angiogenic matrices *in vitro,* as well as the potential to contribute to the vascularization *in vivo* (*77*). In human peripheral blood, two types of EPC were isolated from the mononuclear cells: early EPC and late EPC (*83*). Some synonyms of late EPC include outgrowth endothelial cells (OEC), late OEC, blood OEC and endothelial colony forming endothelial cells (*77*).

In response to ischemia, many pathophysiologic changes occur in the brain microvasculature. Subsequently immediate events include the breakdown of the blood-brain barrier (BBB), with transudation of plasma, cytokines (*84*) and vascular matrix degradation (*85*). In the meantime, active angiogenesis is induced after focal cerebral ischemia (*86*) and many angiogenic factors are up-regulated (*87*). Moreover, the circulating EPCs are reduced in the stroke patients (*88*). Therefore, therapeutic enhancement of angiogenesis is a strategy for a series of different vascular-related diseases. Recently, therapeutic potential of EPCs has been highlighted in experimental cerebral ischemia. Some groups have demonstrated the EPC administration could restore the blood flow and enhance the tissue regeneration in experimental cerebral ischemia models. Furthermore, the EPC could secret several growth factors that enhance neuronal survival, neurogenesis, and vascular regeneration (*89, 90*). In addition, vascular endothelial growth factors are also widely used in experimental cerebral ischemia models because they can increase cerebral angiogenesis, but also enhance neuroprotection and neurogenesis (*86*). Although still a lot of questions remain unclear, these results are promising and provide initial ideas for treatment of the ischemic stroke by means of therapeutical relevant cells and suitable tissue engineering approaches.

2.3 Natural polymer: Silk fibroin

Silk is generally defined as protein polymers which are spun fibers by some Insects larvae such as silkworms and flies, Arthropods such as spiders and scorpions, or Mollusks as mites. Silk proteins are usually biosynthesized in epithelial cells of these organisms and produced within specialized glands (*91*). Silks produced by silkworms are well known and used in biomedical applications particularly as sutures and in the textile industry because of its luster and peculiar mechanical properties. Although some delayed chronic inflammatory reaction to suture were observed (*92*), this biological responses could be overcome by removing the sericin, the glue-like proteins and by changing the protein conformation. *Bombyx mori* silkworm silk, the most common source of commercially available silk, have shown tunable mechanical properties, biocompatibility, and controlled biodegradability (*93-96*). Silk fibers are composed of a two filament: a structure protein (silk fibroin) and a gummy substance that glues the two filaments together (silk sericin) (Fig 2.7). The sericin coated outside of silk fibroin is a hydrophilic protein (~20-310kDa), which could be removed in the de-gumming process (*97*).

Fig 2.7 Scanning electron micrograph of a silk filament partially degummed (data not published from lab).

2.3.1 Structure

Silk fibroin filament has a diameter from 10um to 15um, which is composed of a heavy chain (~390kDa) and a light chain (~26kDa) at 1:1 ratio. These two chains are linked by a single disulfide bond (*97*) (Fig. 2.8)

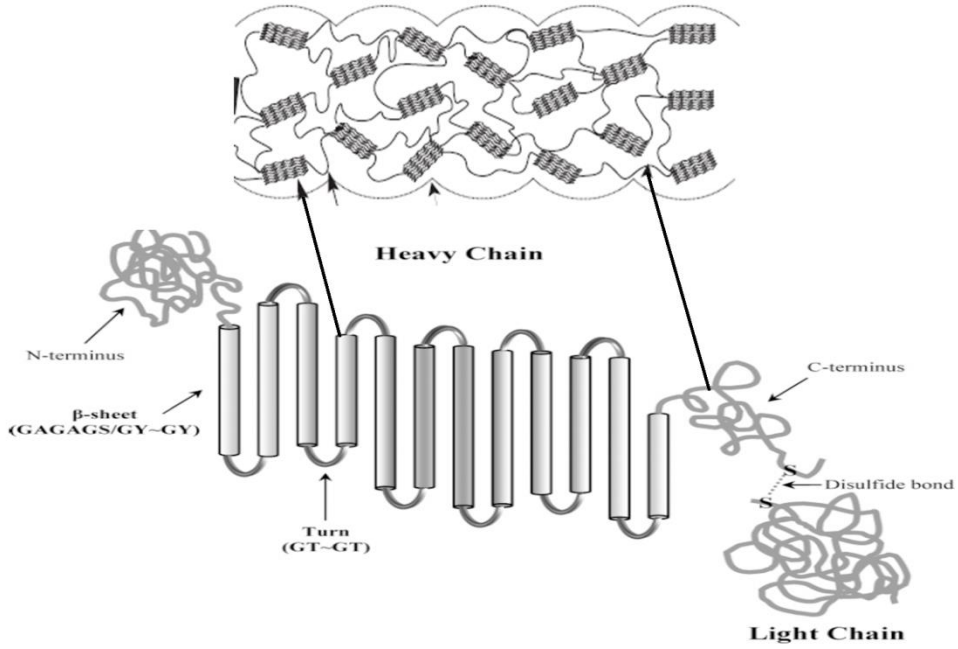

Fig 2.8 Silk fibroin filament composition

The amino acid composition of *Bombyx mori* silk fibroin includes more than 16 amino acids whose ratio varies between different areas of the supramolecular structure of fibroin. The amino acid composition of silk fibroin from *Bombyx mori* consists primarily of glycine (Gly) (49.9%), alanine (Ala) (27.7%) and serine (Ser) (7.9%) (Table 2.1).

Table 2.1 Amino acid composition of *Bombyx mori* silk fibroin analyzed by HPLC

(data not published from lab)

Amino Acid	Amino acid composition (%)
Glycine	49.9
Alanine	27.7

Serina	7.9
Tyrosine	5.3
Valine	2.7
Threonine	0.8
Isoleucine	1.2
Phenylalanine	0.8
Lysine	0.3
Aspartic Acid	1.0
Leucine	0.6
Arginine	0.6
Glutamic Acid	0.9
Proline	0.4
Methionine	0
Cysteine	0
Histidine	0

The heavy chain of silk fibroin is composed of the 12 small hydrophilic domains (amorphous region) and 12 large hydrophobic domains (crystalline region). In the crystalline regions, each domain consists of sub-domain hexapeptides including: GAGAGS, GAGAGY, GAGAGA or GAGYGA in which G is glycine, A is alanine, S is serine and Y is tyrosine. These subdomains end with tetrapeptides such as GAAS or GAGS. In the amorphous region, they are between 42 and 44 amino acid residues in length. All the linkers have an identical 25 amino acid residue (non-repetitive sequence), which is composed of charged amino acids absent in the crystalline regions (*98*).

Some different secondary structures of silk fibroin are reported: α-helical (silk I) and β-sheet (silk II) structures in crystalline areas, and disordered conformation of random globules in amorphous areas. The silk I structure is stabilized by intra-molecular hydrogen bonds, with the hydrophobic fragments displaced to the periphery (Fig 2.9a). Silk I is a water-soluble state (can be obtained *in vitro* in aqueous conditions) and easily converts to the silk II structure when exposed to physical stresses or heating. The β-sheet structures are asymmetrical with one side

occupied with hydrogen side chains from glycine and the other occupied with the methyl side chains from the alanines. Antiparallel β-sheets of silk fibroin are packed in the face-to-face, back-to-back mode (Fig 2.9b). The silk II structure is water insoluble in several solvents including alkaline conditions, mild acid and several chaotropes (*97*, *99*).

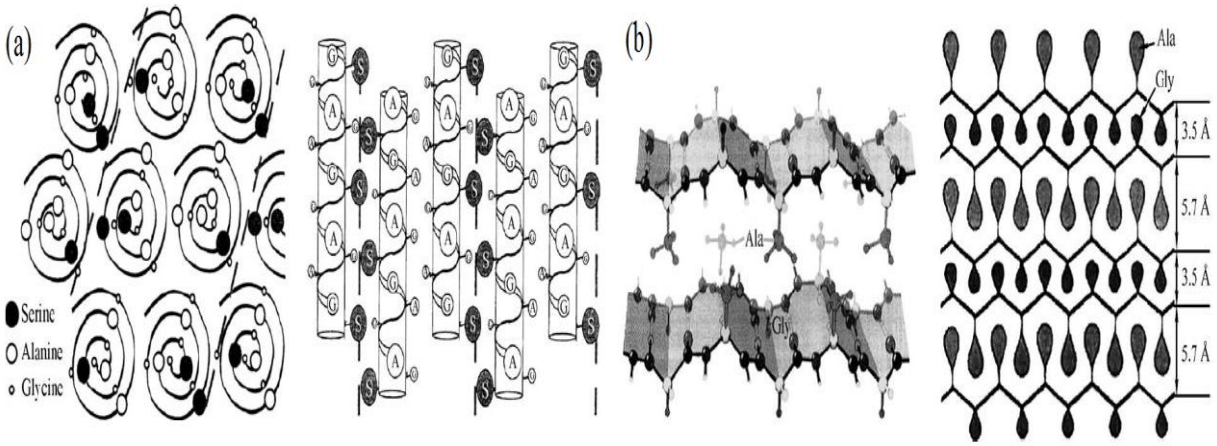

Fig 2.9. α-Helical structure of fibroin macromolecules in two projections (a) β-sheet structure of fibroin (b). (*99*)

2.3.2 Tissue engineering application

Silk fibroin has the great potential to be applied in tissue engineering and regenerative medicine. Bio-recognition ability of silk fibroin is the basic contribution to induce regeneration of various mammalian tissues. Two different active sequences VITTDSDGNE and NINDFDED, recognized by the integrin that promoting fibroblast growth, were localized in the N-terminal region of the heavy chain (*100*). Besides, silk fibroin could be processed into many different kinds of materials which enable its extensive application in tissue engineering and regenerative medicine (Fig 2.10). All these diverse kinds of materials start from the protocol to obtain aqueous silk fibroin solution (Fig 2.11) (*101*). Then, this silk fibroin solution can be prepared into films, sponges, fibers and gels (*102-104*). Depending on the procedure of processing and the source of silk, the silk fibroin could have different secondary conformation and molecule assembling, which result in different mechanical and biological functions (*102*).

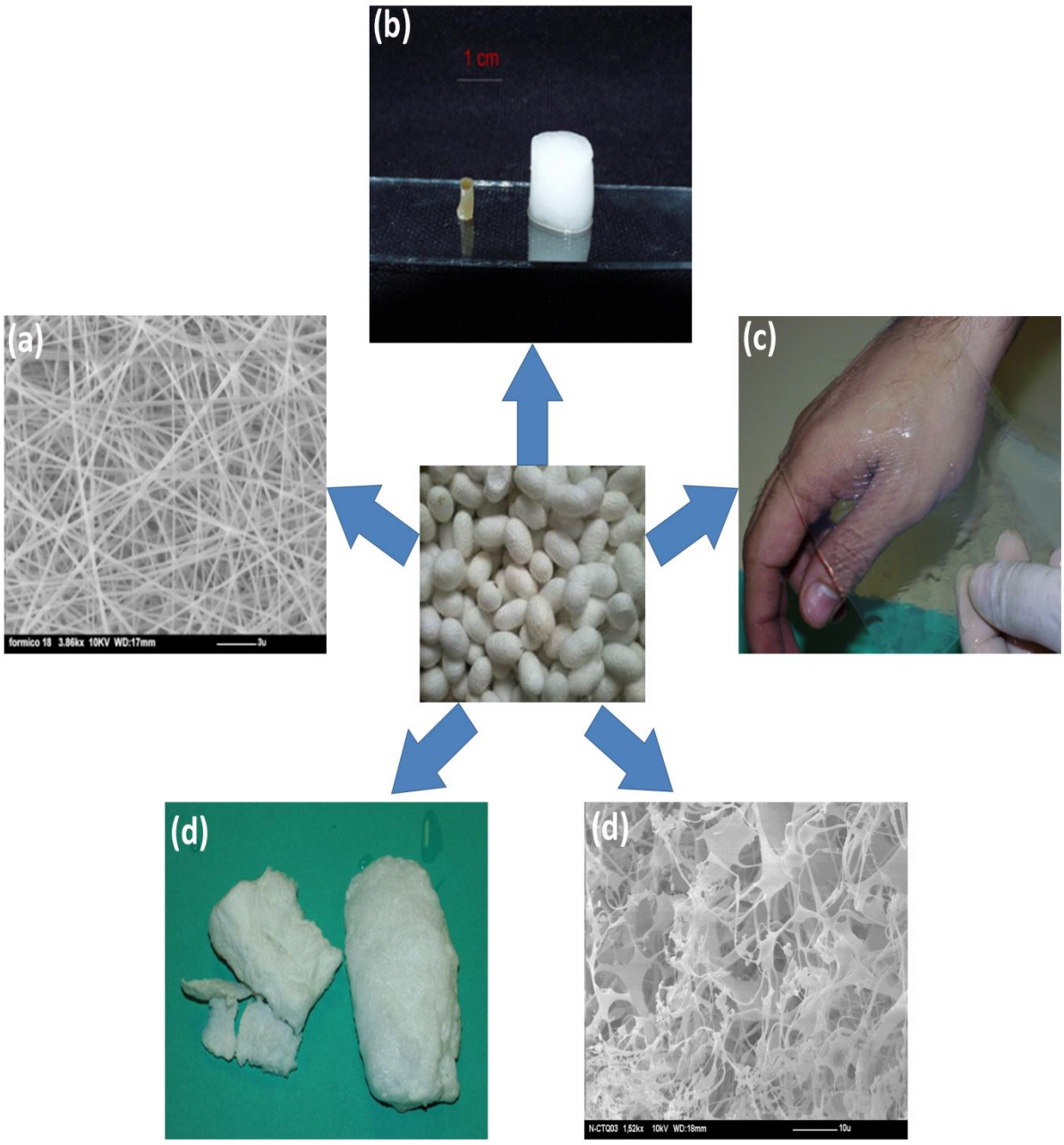

Fig 2.10 Diverse material forms fabricated from silk fibroin: (a) fiber (b) gel (c) film (d) sponge. (Figures are not published data from lab)

These different forms of silk fibroin materials are widely applied in tissue engineering:

(i) For skin would healing, fibroin films and fibroin-alginate sponges have been reported to enhance skin wound healing *in vivo* compared to clinically used materials (*105, 106*). Oral keratinocytes also proliferate on woven fibroin meshes (*107*), a form that is likely to be used for

wound healing applications. Both studies concluded that fibroin-based materials promoted epithelialisation.

(ii) For vascular tissue regeneration, sulphonated and heparinised silk fibroin films were reported for use as artificial blood vessels by adjusting suitable mechanical properties (*108*). The studies showed these films have good anticoagulant activity and platelet response and support endothelial cell spreading and proliferation. Besides, nano-fibrous and micro-fibrous silk fibroin nets have good compatibility with endothelial cells, maintaining their endothelial characteristics and functions (*94*). Biohybrid multilayer nanofiber composed of silk fibroin and poly(ε-caprolactone) were prepared using double-electrospinning technique, displaying both an endothelial-conductive surface with anisotropic mechanical properties (*109*).

(iii) In neural tissue engineering, especially in the peripheral nervous system, the dorsal root ganglia and schwann cells cultured on silk fibroin maintain their viability and keep their normal phenotype or functionality without any cytotoxic effects (*110*). Silk-Carbon nanotubes composite scaffolds were able to improve the neuron differentiation of human embryonic stem cells, which is applicable for efficient supporting matrices for stem cell-derived neuronal transplants (*111*).

(iiii) Most of the research of silk fibroin has carried out for bone tissue engineering. Films, electrospun scaffolds and salt-leaching 3D-porous scaffolds are processed in bone tissue engineering (*112-114*). Some previously work showed that silk fibroin hydrogels and membranes/nets without pre-seeded cells have been used for guided bone regeneration (*115, 116*). However, recently 3D porous silk fibroin scaffolds combined with MSCs resulted advance bone formation for the repair of critical-sized bone defects (*117*). Furthermore, the silk fibroin scaffold also modified with RGD to increase the cell attachment and slowdown the degradation in bone tissue engineering. RGD-silk scaffolds were demonstrated to be suitable for autologous

bone tissue engineering, probably because of their stable macroporous structure, tailorable mechanical properties matching those of native bone, and slow degradation (*118*).

Furthermore, Silk fibroin are also applied in cartilage, cardiac, skin, spinal cord tissue engineering and so on (*119*). In the future, with the development of understanding of silk fibroin and optimization of processing, the silk fibroin could be more widely and successfully used in tissue regeneration.

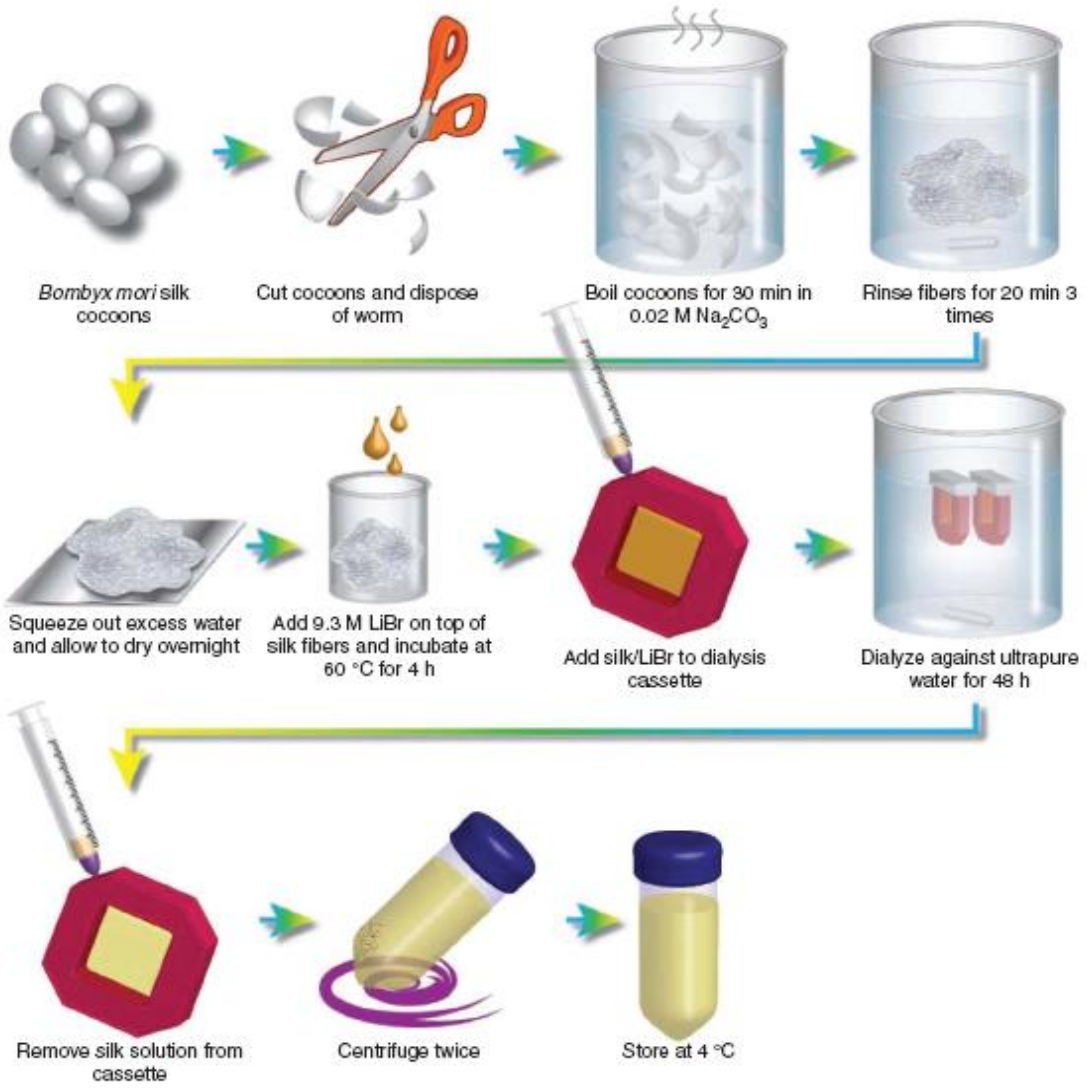

Fig 2.11 Silk fibroin aqueous solution preparation (*101*).

2.3.3 Hydrogel

Silk fibroin solution can be assembled into hydrogels by using different processing methods. The sol-gel transition can be induced by physical or chemical factors. In the presence of low pH, high temperatures, or high ionic strength which induce self-assembly into β-sheet-rich networks and concomitant hydrogelation of silk fibroin (*120, 121*). Usually, with an increase in silk fibroin concentration, temperature, concentration of additives like Ca^{2+}, glycerol and poly (ethylene oxide), or a decrease in pH, gelation time decreases. In the gelation process, silk fibroin structure changed from random coil to β-sheet due to enhanced hydrophobic interactions and hydrogen bond formation (*103, 122-124*). In addition, silk fibroin hydrogel can also be prepared by genipin chemically crosslinking (Fig 2.12) (*125*). Genipin preferentially reacts with the amino acids lysine and arginine of certain proteins. However, the silk fibroin chain contains a very low percentage of these amino acids (0.6% for both), mainly in the hydrophilic blocks. Therefore, the kinetic of gelation is a slow process because the existed cross-linking sites are few in the silk fibroin (*126*). In this process, genipin can also induce the β-sheet formation of silk fibroin (*127, 128*). However, the silk fibroin gelation was very slow under these physiologically stimuli and genipin crosslinking, which were more suitable for 2D *in vitro* study of cells behavior instead of 3D encapsulation system. Recently, relatively new protocols have been explored to induce the gelation of silk fibroin, such as using sonication (*129*) or votex (*130*) in which the hydrogelation kinetics could be easily manipulated by changing the sonication and vortex time, assembly temperature and protein concentration, suggesting proper techniques of 3D silk fibroin for cells encapsulation. This method makes it possible for new tissue engineering applications in 3D hydrogel constructs without harsh solution conditions that may be detrimental to cell behavior (*129*).

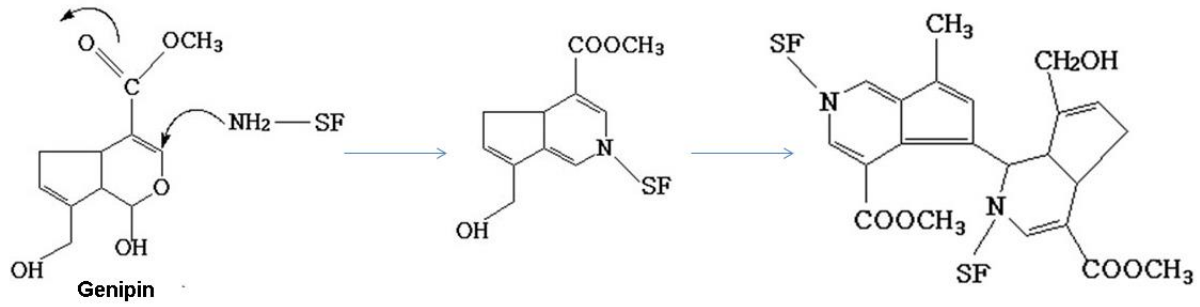

Fig 2.12 The mechanism of genipin crosslinking silk fibroin by reacting with the primary amino acid group (*125*).

2.4 Aim of this thesis

In order to solve the problem of brain injury caused by stroke and traumatic, brain tissue engineering is a promising strategy to provide appropriate biocompatible and bioactive scaffolds to help the damaged brain tissue regeneration. When the damaged part is large, the combination of stem cells is necessary to replace the lost neural cells because of the limited regeneration ability of the brain tissue.

To this aim, our work is to design and evaluate an instructive injectable scaffold combined with stem cells for brain tissue regeneration. The stem cells (embryonic stem cells or neural stem cells) will be provided as cell sources to replace the lost cells in the brain damage, and the scaffold should induce the proliferation and neural differentiation of the implanted stem cells.

To define which form of materials should be applied in brain tissue engineering, hydrogels were taken into prior consideration in the brain tissue engineering application as they have comparable physical characteristics to soft tissues. Moreover, the injectable hydrogel can avoid invasive

surgical procedures. Many natural polymers could be processed into hydrogels. Among these, silk fibroin is a natural bioactive polymer, which has been used in many different tissue engineering applications because of its tunable mechanical properties, biocompatibility and controllable degradation rates. Silk fibroin could be processed using a number of techniques to obtain diverse forms of materials including the hydrogel. Chemical and physical crosslinking are the main ways to obtain silk fibroin hydrogel. However, few studies have focused on the application of silk fibroin hydrogel for neural tissue engineering application, especially for brain tissue engineering. Therefore, we chose silk fibroin as our main material to produce hydrogels. Furthermore, to improve the bioactivity of hydrogel, gelatin which is the denatured collagen was considered to combine with silk fibroin. Different combination and crosslinking ways were performed to obtain hydrogels which aimed to find the optimized hydrogel for supporting stem cells viability and neural differentiation. Even though our final aim is to build a 3D scaffold, we decided to use hydrogel substrates as our starting step to choose the appropriate crosslinking and combination of hydrogels. Different processing of silk fibroin/gelatin hydrogel substrates were prepared by chemical genipin crosslinking and physical sonication crosslinking. Furthermore, different composition of silk fibroin and gelatin were prepared to vary structures, protein conformations and mechanical properties of hydrogels. Mouse embryonic stem cells (mESC) were used as a model to investigate the effects of these hydrogel substrates to the viability and neural differentiation of pluripotent cells.

In the brain tissue engineering, a 3D hydrogel encapsulated with therapeutic stem cells, which is injectable, is an ideal model. Another important issue is to increase the neuron differentiation of stem cells in the brain tissue regeneration because neurons growth is always inhibited in the damaged environment with the scar formation. To achieve this aim, the physical sonication

crosslinked silk fibroin hydrogel was chosen from our first step and then silk fibroin hydrogel was produced as a 3D injectable hydrogel which allows cells encapsulation by manipulating the sonication parameters. To improve the neuron differentiation, silk fibroin was chemically modified with IKAVA peptide which derived from laminin. To evaluate the unmodified and IKVAV-modified hydrogels, human neural stem cell were encapsulated in both hydrogels, the viability and neural differentiation were then evaluated.

The angiogenesis is also a critical aspect in the regeneration of brain tissue, especially when the damaged part is large. To understand whether the silk fibroin hydrogel can support the angiogenesis and if the conjugation of IKVAV peptide can increase angiogenesis, we prepared the silk fibroin unmodified and modified with IKVAV peptide, and scramble VVIAV peptide (control peptide). To evaluate the angiogenesis potential of different modified silk fibroin hydrogel, two systems were used. One is the mono-culture system in which the OEC are encapsulated inside hydrogels. VEGF could be added in the medium to induce the angiogenesis of OEC. Another system is to co-culture OEC with BM-MSCs. In this co-culture system, BM-MSCs could induce the angiogenesis without additional growth factors. By using these two systems, the angiogenesis structures formed inside hydrogels and the gene expression of different angiogenesis genes were evaluated.

Chapter 3: Different processing of silk fibroin-based hydrogel modulate the behavior of embryonic stem cells

3.1 Part I: Gelatin/silk fibroin hydrogel substrates by chemical genipin crosslinking *

*This part of work is based on the publication: Sun W, Incitti T, Migliaresi C, Quattrone A, Casarosa S, Motta A. 2014, Genipin-crosslinked gelatin–Silk fibroin hydrogels for modulating the behavior of pluripotent cells, Journal of Tissue Engineering and Regenerative Medicine. DOI: 10.1002/term.1868

3.1.1 Introduction

In stem cell-based tissue engineering, scaffolds are designed and fabricated as bioactive synthetic frameworks to promote interaction with host stem cells or with pre-seeded stem cells. The natural extracellular matrix (ECM) represents an appealing model to design bioactive scaffolds (*13*) and many reports have shown that ECM plays a critical role in modulating the behavior of stem cells (*131*). ECM mechanical properties and chemical cues can affect stem cells behavior by pulling cells against matrix or by interacting with cell surface integrins. Subsequently mechano-sensitive or integrin-mediated interactions convey these signals to intracellular downstream pathways that commit to specific cell differentiation fates or functions (*16, 132, 133*). By mimicking the ECM, biomaterials can be utilized to fabricate bioactive scaffolds to stimulate stem cells proliferation and differentiation by delivering intrinsic physical properties or incorporated chemical cues (*134*). Moreover, instead of common growth factor-induced differentiation system on tissue culture plate (TCP) *in vitro*, various biomaterials are constructed as 2D or 3D matrices to help guiding stem cells differentiation into specific cell types (*135*, *136*). The mechanical properties (*16*), chemical composition (*137*), and structure architecture (*138*) of scaffolds can all contribute to modulating the differentiation of stem cells. However so far, few reports have revealed the underlying mechanisms by which the scaffolds modulate the

differentiation of stem cells (*139, 140*). Therefore, looking for appropriate scaffolds to guide differentiation can benefit the successful application of stem cells in tissue engineering. Meanwhile, understanding the underlying mechanisms is becoming necessary in order to design more precise and adequate scaffolds.

To specifically study how artificial scaffolds can affect the proliferation and neural differentiation of pluripotent cells, hydrogels are mainly used, as they display similar mechanical properties to those of the central nervous system ECM (*46*). As one of the emerging and most physiologically relevant scaffolds, hydrogels are widely applied for 2D adhesion and 3D encapsulation systems to study stem cells differentiation behaviors (*141, 142*). Both types of culture are useful to elucidate the precise signaling cues for stem cells differentiation into specific cell types (*143*). Collagen is a major protein component in connective tissue and is most abundant in ECM of mammals. Gelatin is the denatured form of collagen, showing very low antigenicity (*144*). Gelatin-based scaffolds have been reported for cartilage (*145*) and bone (*146*)tissue engineering and for peripheral nerve guide conduits (*147*). Silk fibroin is a promising natural polymer that has been used for many years in tissue engineering and regenerative medicine due to its impressive biocompatibility and tunable mechanical properties (*97*). Various reprocessing formats of silk fibroin (films, fibers, sponges) have been explored for stem cell-based tissue engineering (*124*). Furthermore, silk fibroin-based materials have been shown to support cell adhesion, proliferation and osteogenic (*148*), chondrogenic (*149*) and neural differentiation (*111*). Blended scaffolds of gelatin and silk fibroin have been reported to enhance the degree of interconnection and to increase the surface area for cell attachment (*150*). Genipin, which is a natural crosslinker extracted from gardenia fruits (*151*), with very low cytotoxicity (*152*), has been used to crosslink chitosan, gelatin and other proteins containing residues with

primary amine groups (*153, 154*). Genipin-crosslinked gelatin has been successfully used for many biomedical applications in the past years (*147, 155*). However, few papers have reported data on the possible applications of genipin-crosslinked silk fibroin hydrogels and sonication-induced silk fibroin hydrogel (*156*).

In our research, the initial objective was to explore nature-derived hydrogels as active substrates to guide pluripotent cells proliferation and differentiation into the neural lineage by using mouse embryonic stem cells (mESCs). For this purpose, we prepared gelatin/silk fibroin hydrogels of different compositions and crosslinked by genipin. By changing the ratio between gelatin and silk fibroin, different morphologies, structures and mechanical properties of the hydrogel scaffolds were obtained and characterized. Neural differentiation was induced by culturing mESCs in Knockout Serum Replacement (KSR) supplemented medium for 15 days. This protocol shows that 50% of neurons are formed at day 15 on tissue culture plate (TCP) which was used as the control culture in our experiments (*157*). After seeding cells on TCP and hydrogel substrates, their viability and proliferation during differentiation were assessed through Live/Dead and DNA quantification assays. Moreover, the effects of substrates on mESCs differentiation were compared between hydrogel surfaces and TCP. Gene expression analyses were performed to analyze the differentiation fate by qRT-PCR at day 15.

3.1.2 Materials and Methods

3.1.2.1 Preparation of regenerated silk fibroin solution

Silk fibroin solutions were prepared according to the literature (*101*). *Bombyx mori* cocoons (Produced and kindly provided by Cooperativa Socio Lario, Como, Italy) (Fig 3.1.1) were peeled layer by layer. Then they were boiled for 30mins in 0.02M Na_2CO_3 (Merck, Germany) aqueous

solution to remove the sericin. After the de-gumming process, silk fibroin was cooling down by adding distilled water gradually. Then the obtained silk fibroin was thoroughly rinsed in distilled water. The dried obtained silk fibroin was dissolved in 9.3M LiBr (Sigma-Aldrich, U.S.A) (concentration at 20%) at 65°C for 4 hours followed by dialysis against distilled water for 3 days using Slide-A-Lyzer dialysis cassettes (MWCO3500, Pierce, U.S.A). Then the silk fibroin solution after dialysis was centrifuged to remove the impurities and silk aggregates formed during dialysis. The final concentration of the silk fibroin solution was calculated by Nanodrop spectrophotometer (ND-1000). Usually, the silk fibroin concentration was about 5.4%.

Fig 3.1.1 Cocoons kindly provided by Cooperativa Socio Lario, Como, Italy

3.1.2.2 Preparation of genipin-crosslinked gelatin/silk fibroin hydrogels

Gelatin (Type A, from porcine skin, Sigma-Aldrich, U.S.A) was prepared to 4wt % solution and genipin was dissolved to 2wt % solution in distilled water. The gelatin solution was blended with 5.4wt % silk fibroin solution and 2wt % genipin solution in 37°C under mild stirring. All solutions were sterilized by passing through 0.22um filters. The total solute concentration was 3% and genipin was 12% related to the total solute concentration (*154*). By changing the volume ratio between gelatin and silk fibroin solution, the final solutions were obtained in a mass ratio of gelatin: silk fibroin=100:0, 95:5, 80:20, 0:100 which were named G100, GS95, GS80, S100 respectively. S100 solutions were then incubated at 37◦C for 48 hours and G100, GS95, GS80

solutions were incubated for 18 hours to crosslink and to obtain hydrogels. The hydrogel composition and crosslinking time are shown in Table 3.1.1. The appearances of the hydrogels were shown in Fig 3.1.2.

Table3.1.1 The composition and crosslinking time of gelatin/silk fibroin hydrogels

Sample code	Gelatin	Silk fibroin	Total solute concen-tration	Genipin concentration (related to the total solute concentration)	Crosslinking time
G100	100	0	3%	12%	18h
GS95	95	5	3%	12%	18h
GS80	80	20	3%	12%	18h
S100	0	100	3%	12%	48h

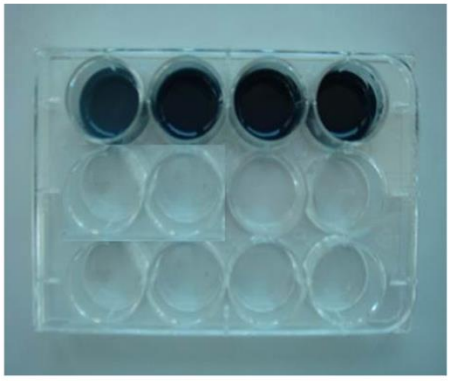

Fig3.1.2 The appearance of the genipin-crosslinked gelatin/silk fibroin hydrogels

3.1.2.3 Field Emission Scanning Electron Microscope (FE-SEM) characterization

To characterize the internal microstructures of genipin-crosslinked gelatin/silk fibroin scaffolds, hydrogel samples were frozen in liquid nitrogen to avoid the formation of large crystals and then were lyophilized at -50°C for 48 hours. The freeze-dried scaffolds were cut to expose the cross-sections and were coated with gold. The samples were observed using the FE-SEM (SUPRA 40/40VP ZEISS, Germany).

3.1.2.4 Fourier Transform Infrared - Attenuate Total Reflectance (FTIR-ATR) spectroscopy analysis

The lyophilized uncrosslinked and crosslinked samples were analyzed in FTIR-ATR (Fourier Transform Infrared - Attenuate Total Reflectance, Spectrum One Perkin-Elmer, U.S.A). Spectra region were collected from 600 cm^{-1} to 4000cm^{-1}. Spectra covering the amide I, II, III regions (1000–1800cm^{-1}) were performed by Graphpad Prism 5.0 software.

3.1.2.5 Rheological characterization of hydrogels

The rheological characterization of hydrogel samples was performed in Anton Paar Physica MCR Rheometer 301 fitted with a circulating environmental system for temperature control. The plate was equipped with a Peltier chamber to control temperature and to reduce evaporation during measurement. After the hydrogels were crosslinked in a mold (diameter 30mm), they were transferred to the plate to perform characterization. Oscillatory shear measurements were performed to evaluate the storage and loss modulus of hydrogels. Frequency sweeps were performed to determine values of the storage and loss modulus from 0.1 Hz to 10 Hz in a 25mm cone plate configuration at 37°C. A constant gap 0.7mm and strain 0.2% were used in the measurement. Triplicates of each hydrogel were tested.

3.1.2.6 Genipin crosslinking degree and reactive genipin content test

Ninhydrin assay was used to determine the crosslinking degree and reactive genipin content in crosslinked hydrogels (*104*). Ninhydrin can react with NH_2 groups (both primary and secondary) of proteins, producing a purple color which is detectable by spectrophotometer at 570 nm. By calculating the amount of NH_2 groups in the samples before and after crosslinking, the amount of NH_2 groups participating in the crosslinking process and the reactive genipin content in

crosslinked samples can be calculated. The genipin-crosslinked hydrogels and the corresponded solutions without crosslinking were frozen at -80°C overnight and then were lyophilized for 3 days. Samples before crosslinking and after crosslinking were equally weighed. Subsequently, the lyophilized samples were heated in 3ml ninhydrin (Sigma-Aldrich, U.S.A) solution (0.35% w/v) in ethanol (<96%, Sigma-Aldrich, U.S.A) at 90°C for 30mins under mild shaking. Each sample was made in triplicate. 3ml ninhydrin solution was treated under the same conditions as blank. After cooling down in cold water bath, the optical absorbance of the solution was measured with a microplate reader (Multiskan EX, Thermo Scientific, U.S.A) at a wavelength of 570 nm. Glycine solutions of various known concentrations were used as standards. Therefore, the number of free NH_2 group was calculated by the optical absorbance of the solution. Crosslinking degree and reactive genipin content can be calculated following the equation in which NH_2^{before} and NH_2^{after} are the mole fractions of free NH_2 remaining in the sample group before and after crosslinking, respectively. Here we assume that one genipin molecular reacts with two NH_2 groups (*158*).

$$\text{Crosslinking degree (\%)} = \frac{NH_2^{before} - NH_2^{after}}{NH_2^{before}} \times 100$$

$$\text{Reactive genipin content (\%)} = \frac{(NH_2^{before} - NH_2^{after}) \times MolecularWeight_{genipin}}{Weight_{sample} \times 2} \times 100$$

3.1.2.7 Embryonic stem cell culture and in vitro neuronal differentiation

The mouse embryonic stem cell line E14tg.2a **(**obtained from MMRRC, University of California, Davis) was maintained in self-renewal state by culturing on a 0.1% gelatin coated TCP in self-renewal medium (MMRRC guidelines). Cells used for differentiation were between Passage 25

to 30 and cultured as previously described (*157*). Before seeding cells, different hydrogel solutions were prepared as described above, and 500ul of each was used to cover the surface of one well in a 12 well-plate. After hydrogels gelated at 37°C, they were incubated in self-renewal medium at 37°C overnight to remove the excessive genipin. At day-1, cells were dissociated to a single-cell suspension and 1000 cells/cm^2 were plated on the hydrogel surfaces and on 0.1% gelatin coated TCP, and cultured in self-renewal medium for one day. Then at day 0 the medium was changed to differentiation medium (Knockout Dulbecco Minimal Essential Medium supplemented with 15% KSR, 2mM L-glutamine, 100U/ml penicillin/streptomycin, and 0.1mM β-mercaptoethanol) and cultured until day 15. The medium was replaced every two days during the differentiation process.

3.1.2.8 Cell viability and proliferation

The viability of the cells seeded on hydrogels was investigated by Live/Dead assay. Live and dead cells were stained by calcein AM and propidium iodide (PI) respectively. Briefly, cells/hydrogels were washed with PBS and then were incubated in GMEM medium/calcein AM (1μmol/ml) at 37°C for 15mins. Then cells were washed with PBS three times and were stained by GMEM medium/PI (20ng/ml) for 2mins at room temperature. After two more washes in PBS, they were observed by confocal microscopy (Nikon Eclipse Ti-E). To study cell proliferation, PicoGreen DNA assay was performed. Briefly, after washing with PBS, cells/hydrogels were collected and stored at -80°C. Following lyophilization, samples were cut into small pieces and lysed in PBE buffer (10mM EDTA in PBS) supplemented with 1mg/ml Proteinase K for 48 hours at 55°C. After centrifugation at 2000rpm for 10 min, the supernatants were collected for the assay. The DNA content was determined fluorometrically at excitation wavelength of 485nm and emission wavelength of 538nm using a fluorescent plate reader (Tecan Infinite M200).

Triplicates of each sample were tested. The amount of DNA was calculated by interpolation from a standard curve prepared using lambda DNA in TE buffer over a range of concentrations.

3.1.2.9 RNA isolation and QRT-PCR

Total RNA was isolated by Trizol (Sigma-Aldrich, U.S.A) and Qiagen RNeasy Mini Kit (*159*). Briefly, after phase separation using Trizol and chloroform, the upper aqueous phase was collected and mixed with 0.5 volume of ethanol (<96%, Sigma-Aldrich, U.S.A). The solution was transferred to the RNeasy spin columns and RNA purified according to the manufacturer's protocol. Reverse Transcription (RT)-PCR was performed using High-Capacity cDNA Reverse Transcription Kits (Applied Biosystems). Quantitative Real-Time (QRT)-PCR was performed in CFX96 Touch™ Real-Time PCR Detection System (Biorad). Three biological replicates of each sample and triplicate wells were performed. Sequences of specific primers and product length are listed in Table 3.1.2.

Table 3.1.2 Oligonucleotides sequences and product length in QRT-PCR

Oligonuc-leotides	Sequences(5'-3')	Product length (bp)
Oct4	Forward: 5'-TCAGCTTGGGCTAGAGAAGG-3' Reverse: 5'-GGCAGAGGAAAGGATACAGC-3'	191
Nanog	Forward: 5'-TGCTTACAAGGGTCTGCTACTGA-3' Reverse: 5'- TTGTTTGGGACTGGTAGAAGAATC-3'	113
Nestin	Forward: 5'-GATCGCTCAGATCCTGGAAG-3' Reverse: 5'- AGAGAAGGATGTTGGGCTGA-3'	241
βIIItubulin	Forward: 5'- TTCTGGTGGACTTGGAACCT-3' Reverse: 5'- ACTCTTTCCGCACGACATCT-3'	180
NCAM	Forward: 5'- AGGAGAAATCAGCGTTGGAG-3' Reverse: 5'- CGATGTTGGCGTTGTAGATG-3'	182
GFAP	Forward: 5'-GGAGAGGGACAACTTTGCAC-3' Reverse: 5'- CCAGCGATTCAACCTTTCTC-3'	164
Keratin 18	Forward: 5'-TTGTCACCACCAAGTCTGCC-3' Reverse: 5'- TTTGTGCCAGCTCTGACTCC-3'	213

GATA4	Forward: 5’-CACTATGGGCACAGCAGCTCC-3’ Reverse: 5’- TTGGAGCTGGCCTGCGATGTC-3’	146
Brachyury	Forward: 5’-GAACCTCGGATTCACATCGTGAGA-3’ Reverse: 5’- ATCAAGGAAGGCTTTAGCAAATGGG-3’	158
Sox 17	Forward: 5’- GCCAAAGACGAACGCAAGCGGT-3’ Reverse: 5’- TCATGCGCTTCACCTGCTTG-3’	211

3.1.2.10 statistics

All statistics were performed using Graphpad Prism 5. In the reactive genipin content test, data were analyzed by one-way analysis of variance (ANOVA) with Tukey’s post-hoc analysis. In DNA quantification test, one-way ANOVA with Tukey’s post hoc analysis and two-way ANOVA with Bonferroni post hoc test were performed. In QRT-PCR, ddCt method was used to analyze the data. Gene expression of cells on TCP (control) was set as 1 (no error bars). Other target gene expressions were calculated by the fold change related to the control. One-way ANOVA with Tukey’s post hoc analysis was performed for gene expression analysis.

3.1.3 Results

3.1.3.1 Hydrogel morphology characterization by SEM

SEM was used to examine the morphologies of freeze-dried hydrogels which are shown in Fig 3.1.3. The G100 hydrogel formed porous structure and polygonal pores, with size ranging from 10um to 20um (Fig 3.1.3a,b). The S100 hydrogel showed lamellar structures with small pores (Fig 3.1.3c,d). By adding silk fibroin to the gelatin, no significantly different structure was observed in blended samples GS95 (Fig 3.1.3e,f) and GS80 (Fig 3.1.3g,h) compared to G100. Both GS95 and GS80 kept the porous morphology like G100. Besides, the GS80 hydrogel showed a slight decrease of pore size.

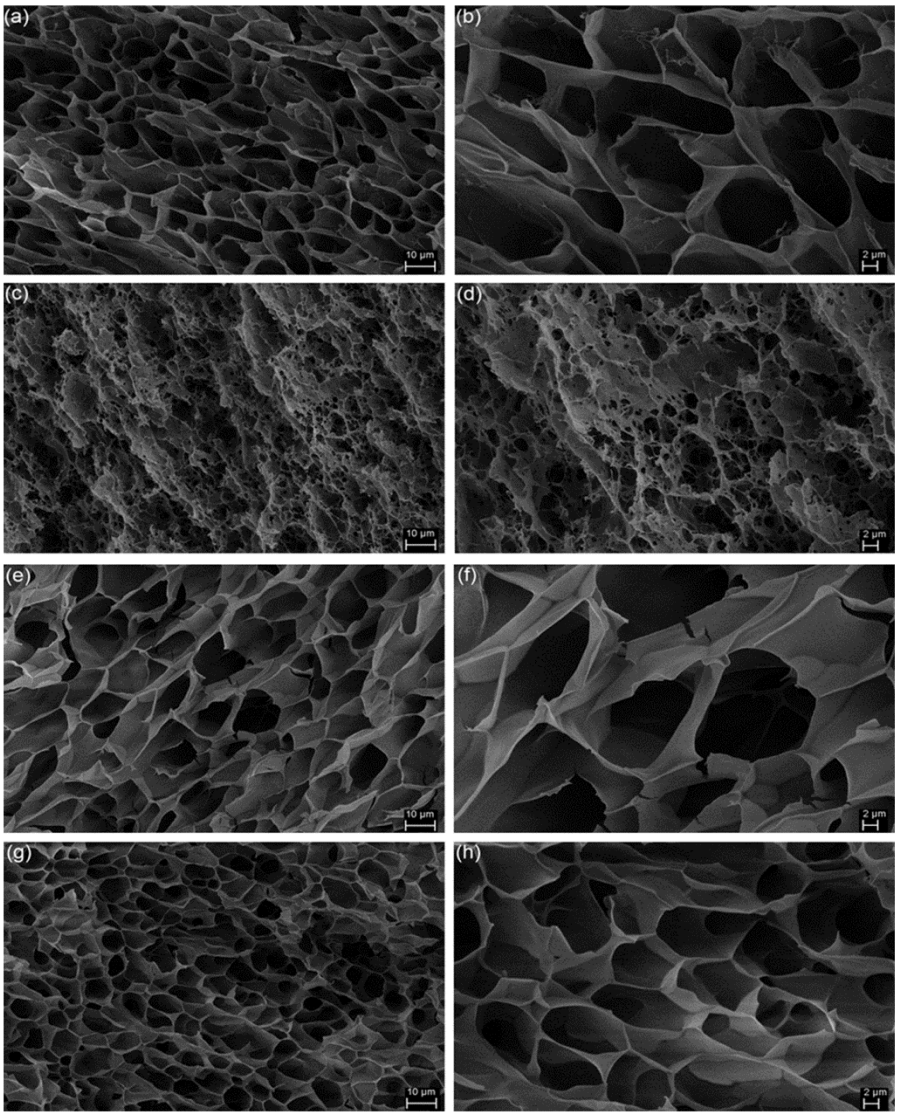

Fig3.1.3. Morphologies of genipin-crosslinked gelatin/silk fibroin hydrogels observed by SEM. (a,b) G100 (c,d) S100 (e,f) GS95 (g,h) GS80. Each sample was shown in 10µm and 2µm scales respectively.

3.1.3.2 Hydrogel protein conformation analysis by FTIR-ATR

Protein secondary structures of uncrosslinked and crosslinked samples were determined by FTIR-ATR (Fig 3.1.4). The spectrum of uncrosslinked S100 (Fig 3.1.4Aa) showed bands at 1644cm−1, 1514cm−1 and 1230cm−1 which corresponded to amide-I (1600-1690cm-1), amide-II (1480-1575cm-1) and amide-III (1229-1301 cm-1) conformation region (*160*). Compared to

the pure silk fibroin film (amide II at 1540cm−1) (*103*), the amide II at 1514cm−1 of uncrosslinked S100 indicated some of the molecular chains changed from random coil to β-sheet structure, which was probably due to the lyophilization process. After genipin crosslinking, S100 absorptions bands of amide I showed a shift from 1644cm−1 to 1621cm−1 (Fig 3.1.4Ba), indicating the further structure changes from random coil to β-sheet structure (*161*). It has been proven before that genipin could induce β-sheet structure formation of silk fibroin (*154*). Compared to the uncrosslinked G100 (Fig 3.1.4Ab), genipin-crosslinked G100 (Fig 3.1.4Bb) just showed a slightly shift in amide I and amide II region which indicated that the helical second structure of gelatin was not affected by genipin crosslinking, which was also reported by Chiono's and Xiao's papers (*155, 156*). In the crosslinked samples GS95 (Fig 3.1.4Bc), the amide I, II, III showed only slight variations with respect to the genipin-crosslinked G100 which were attributed to the low content of silk fibroin. The GS80 (Fig 3.1.4Bd) showed β-sheet structure formation after genipin crosslinking (amide II at 1516cm-1).

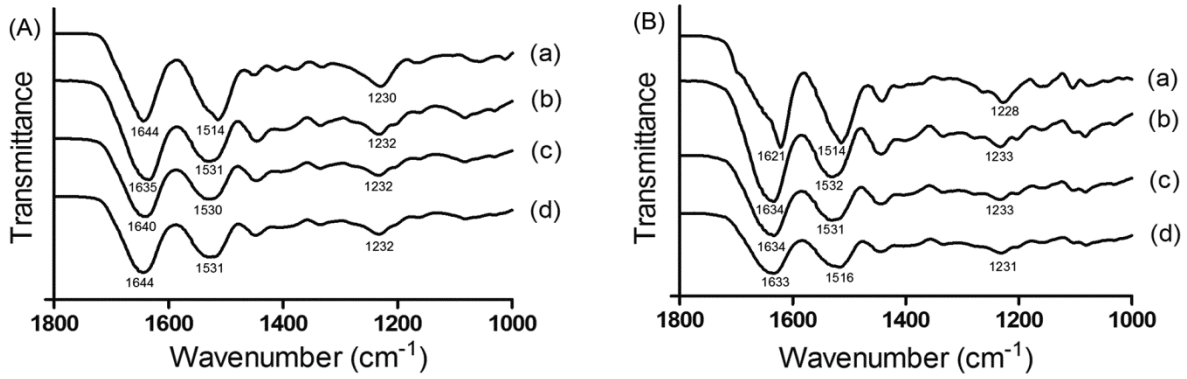

Fig 3.1.4 FTIR spectra of uncrosslinked (A) and crosslinked (B) gelatin/silk fibroin scaffolds: (a) S100 (b) G100 (c) GS95 (d) GS80.

3.1.3.3 Rheological test of hydrogels

Oscillatory shear measurements were performed to evaluate the storage and loss modulus of hydrogels. The typical moduli of microenvironment are E_{brain}=0.1-1KPa, E_{muscle}=8-17KPa and $E_{osteoid}$=25-40KPa (*16*) (Fig 3.1.5). Fig 3.1.6 showed the storage and loss modulus of the hydrogel samples in dynamic frequency sweep test. The storage modulus was significantly larger than loss modulus and was weakly dependent on frequency over the entire range which revealed these materials were typically gelled. G100 showed the lowest storage modulus (819.0±144.0Pa). In contrast, the S100 showed the highest storage modulus (46.1±1.4KPa). The storage modulus of blended hydrogels GS95 and GS80 had been improved by increasing silk fibroin content, reflecting possible increase of the intermolecular bonds and also the presence of higher amounts of crystalline β-sheet structures in the higher silk fibroin content hydrogels. The G100, GS95, GS80 hydrogel dynamic storage moduli were close to the elastic modulus of brain tissue.

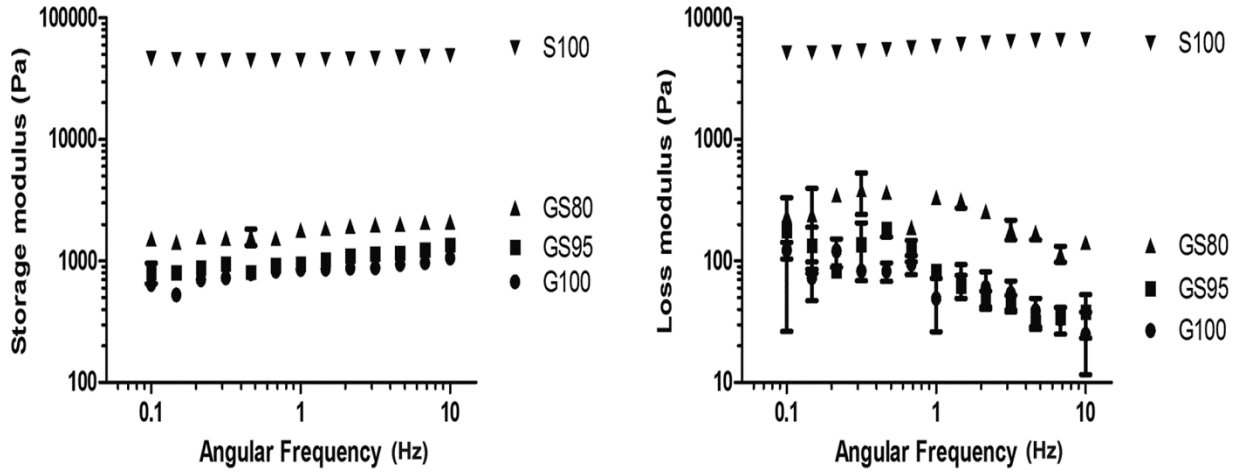

Fig 3.1.5 Characterization of storage and loss modulus of genipin-crosslinked gelatin/silk fibroin hydrogels by oscillatory shear measurements during frequency sweep analysis from 0.1Hz to 10Hz. Error bars represent Mean ± SEM (N=3).

3.1.3.4 Genipin crosslinking degree and reactive genipin content assay

To evaluate the crosslinking degree and reactive genipin content, ninhydrin assay was performed. Crosslinking degree is the relative crosslinking efficiency in each kind of sample. The G100, GS95, GS80, S100 showed the crosslink degree 70.1±2.1%, 61.3±2.7%, 62.6±2.5% and 93.7±0.8% respectively (Table 3.1.3). In the hydrogel formation process by genipin crosslinking, genipin preferentially reacts with the amino acids lysine and arginine of certain proteins. Gelatin contains high percentage of theses amino acids while silk fibroin chains contain a very low percentage of these amino acids (*154*). So the S100 hydrogel formation was a slow process and high crosslinking degree was needed to obtain the hydrogel. On the other hand, the G100, GS95, GS80 samples which had high gelatin content were able to form hydrogels in shorter time and at lower crosslinking degree.

In the meantime, the reactive genipin content of each crosslinked samples were shown in (Fig 3.1.6). The G100 (***$p<0.001$), GS95 (**$p<0.01$), GS80 (***$p<0.001$) showed significantly higher reactive genipin content than pure S100 which was due to the high percentage of reactive sites with genipin in gelatin. Besides, GS95 showed lower reactive genipin content than G100 ($^{\#}p<0.05$) because of the addition of silk fibroin, while GS80 showed similar reactive genipin content with G100 ($p>0.05$).

Table3.1.3 The crosslinking degree of genipin-crosslinked gelatin/silk fibroin hydrogels

Sample code	G100	GS95	GS80	S100
Crosslinking degree (%)	70.1±2.1%	61.3±2.7%	62.6±2.5%	93.7±0.8%

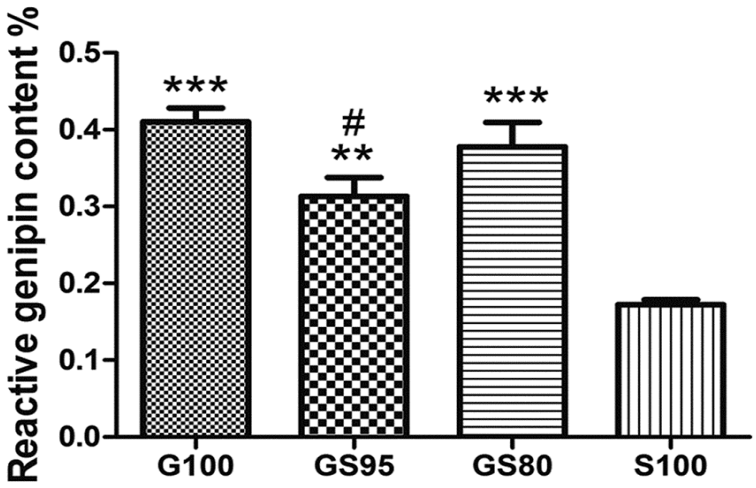

Fig 3.1.6 Reactive genipin content assay of Group A gelatin/silk fibroin hydrogels according to the amount of NH_2 groups which have participated the crosslinking reaction with genipin. (**p<0.01, ***p<0.001 correspond to S100, $^{\#}$p<0.05 corresponds to G100). Error bars represent Mean ± SEM (N=3).

3.1.3.5 Genipin-crosslinked gelatin/silk fibroin hydrogel maintain the viability and proliferation of ESCs

Cell viability was assessed by confocal microscopy using calcein AM/PI staining (Fig 3.1.7A). At day 0, cells showed good initial adhesion on all hydrogel substrates as cells on TCP. Subsequently cells survived and constantly proliferated on all the hydrogel substrates throughout the entire differentiation protocol, with very few dead cells observed in all conditions. In order to precisely evaluate the proliferation rate at different time points, cells proliferation was quantified by analyzing the DNA content at day 0, 3, 5, 7, 15 (Fig 3.1.7B). At day 0, the cells on all hydrogel substrates showed lower DNA content than TCP ($^{\#\#\#}$p<0.001). This was probably due to the fact that the cells started to proliferate at day 0 on TCP but not on the hydrogels, according to the observations made by confocal microscopy. However, cells on S100 showed better adhesion ($^{\$\$\$}$p<0.001) than on other hydrogels. At the initial stage from day 0 to day 5, the cells on all the hydrogel substrates showed lower proliferation speed and lower DNA content than TCP ($^{\#\#\#}$p<0.001). However, from day 5 to day 7, trends changed as cells on all hydrogels

exhibited a significant increase in proliferation (*$p<0.05$, ***$p<0.001$). At day 7, there were no significant differences ($p>0.05$) of DNA content between the cells on TCP and on hydrogel substrates. Moreover, the GS95 and GS80 showed higher DNA content than S100 ($^{\$}p<0.05$). From day 7 to day 15, cells on S100 were observed rapidly growing (***$p<0.001$). At day 15, the DNA content of cells cultured on the hydrogel substrates G100, GS95, GS80 showed no significant differences with TCP ($p>0.05$) while that on S100 showed higher DNA content ($^{\#\#}p<0.01$). These results were confirmed by confocal microscopy observations. Therefore, both gelatin and silk fibroin were compatible to promote ESCs growth and proliferation. At early stages (from day 0 to day 7), the high gelatin content in hydrogel promoted cells proliferation compared to silk fibroin. However, the silk fibroin played an important role in long term cell proliferation (from day 7 to day 15).

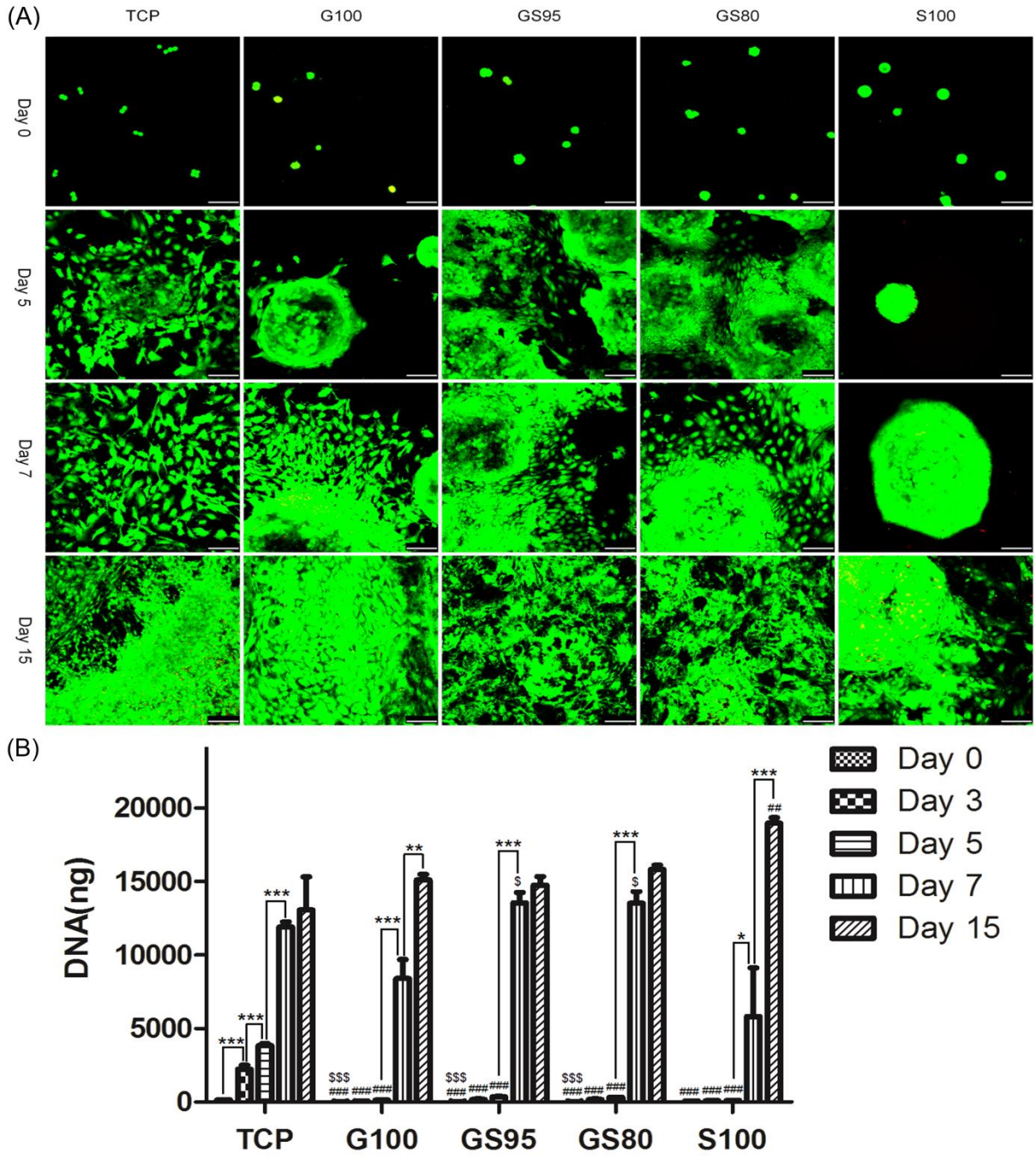

Fig3.1.7. (A) The viability of ESCs on gelatin/silk fibroin hydrogel substrates was observed by Live (green)/Dead (red) assay with confocal microscopy. Bar length: 100um (B) ESCs proliferation assessed by DNA quantification. Error bars represent Mean ± SEM (N=3).(*p<0.05, **p<0.01, ***p<0.001. $^{\#\#}$p<0.01 $^{\#\#\#}$p<0.001 correspond to TCP at the same time point, $^{\$}$p<0.05, $^{\$\$\$}$p<0.001 correspond to S100 at the same time point).

3.1.3.6 Genipin-crosslinked gelatin/silk fibroin hydrogels inhibit neural ectodermal differentiation of ESCs.

Our research goal was to evaluate whether these genipin-crosslinked gelatin/silk fibroin hydrogel substrates could support and guide ESCs neural differentiation by comparison with TCP. To evaluate this, ESCs were induced to neural differentiation in KSR supplemented medium on TCP and on different hydrogel substrates for 15 days. The morphologies of differentiating cells were shown by optical microscopy pictures (Fig 3.1.8A). In this differentiation protocol, mESCs were seeded at a very low density, allowing isolated single cell. The single cell started to proliferate to form a colony and then the progeny spread around it. At day 7, cells on G100, G95 and G80 formed colonies and also spread around them as cells on TCP, while the cells proliferated slower and just few cells spread around colonies on S100. At day 15, most cells on TCP showed typical morphology of differentiated neural cells (Fico et al., 2008). On the contrary, the cells grown on the hydrogel surfaces showed no obvious neural morphologies. To characterize the extent of neural differentiation, cells were collected at day 15 and RNA was extracted. Quantitative RT-PCR was performed to analyze different pluripotent and neural lineage gene markers. Oct4 and Nanog are crucial transcription factors necessary for efficient maintenance of ESCs pluripotency (*162*, *163*). At day 15, though Nanog expression levels in cells on the four hydrogel surfaces were similar ($p>0.05$) to undifferentiated ESCs, Oct4 expression levels greatly decreased ($^{\#\#}p<0.01$,$^{\#\#\#}p<0.001$). These expression profiles indicated that cells on hydrogel substrates and TCP were not capable to maintain pluripotency (Fig 3.1.8B). In order to characterize neural differentiation, the expression levels of mRNA for the neural precusor marker Nestin, the early neuronal marker βIII-tubulin, the late neuronal marker NCAM, and the glial marker GFAP were analyzed (Figure 3.1.8C). Cells on TCP showed highest expression levels of these four neural

differentiation markers which were consistent with the neural morphologies in the microscopy pictures. However, compared to TCP, cells on G100 and S100 showed greatly decreased expression levels of these neural markers (*$p<0.05$, ***$p<0.001$). Besides, GS95 and GS80 showed very low expression of neural markers (**$p<0.01$, ***$p<0.001$). These results indicated that GS95 and GS80 could totally block neural differentiation while G100 and S100 could inhibit neural differentiation to a certain extent.

3.1.3.7 Genipin-crosslinked gelatin/silk fibroin hydrogels GS95 and GS80 *enhance epithelial ectodermal differentiation of ESCs.*

Since neural ectodermal differentiation was inhibited on these hydrogel substrates, we checked the expression of all three germ layer genes in order to evaluate how ESCs differentiated (Fig 3.1.8D). Surprisingly, compared to both TCP and undifferentiated ESCs, differentiated cells on GS95 and GS80 showed significantly higher expression (*$p<0.05$, $^{\#\#}p<0.01$) of Keratin18, a marker of epithelial ectodermal differentiation. Furthermore, cells on G100, GS95, GS80 hydrogel substrates showed similar expression levels of Brachyury (mesodermal marker), GATA4 (meso-endodermal marker) and Sox17 (endodermal marker) compared to undifferentiated ESCs ($p>0.05$). However, cells on S100 exhibited higher expression of GATA4 and Sox17 compared to both TCP and undifferentiated ESCs (*$p<0.05$, **$p<0.01$, $^{\#\#}p<0.01$, $^{\#\#\#}p<0.001$). These results indicated that cells on S100 underwent uncertain differentiation events, giving rise to fates from all three germ layers. However, GS95 and GS80 could guide ESCs to epithelial ectodermal differentiation instead of neural ectodermal differentiation.

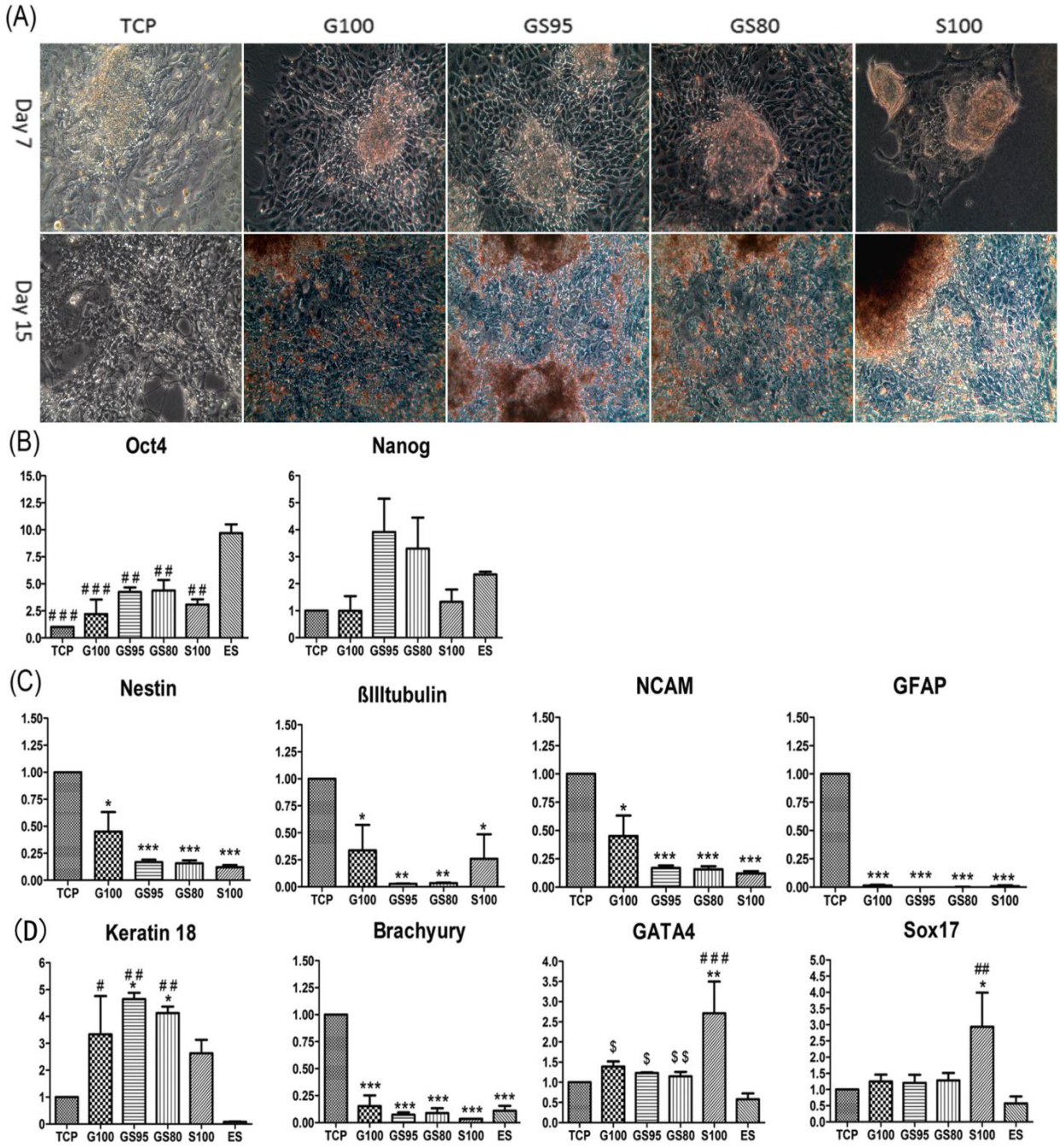

Fig 3.1.8. Optical Microscopy pictures and QRT-PCR of cells on TCP, G100, GS95, GS80, S100 and of undifferentiated ESCs (ES) at day 15: (A) Optical Microscopy pictures of cell morphologies at day7 and day15 (B) Expression levels of pluripotent gene markers of ESCs: Oct4, Nanog. (C) Expression levels of neural lineage markers: Nestin, βIII-tubulin, NCAM, GFAP. (D) Expression levels of three germ layer genes markers: Keratin 18, Brachyury, GATA4, Sox17. (*p<0.05, **p<0.01, ***p<0.001 correspond to TCP, $^{\#}$p<0.05, $^{\#\#}$p<0.01, $^{\#\#\#}$p<0.001 corresponds to ES, $^{\$}$P<0.05, $^{\$\$}$p<0.01 correspond to S100). Error bars represent Mean ± SEM (N=3).

3.1.4 Discussion

Stem cells give promising hope in the tissue engineering and regenerative medicine field because of their unlimited self-renewal capabilities and multilineage differentiation potential. However, one of the major concerns of stem cells is how to control their differentiation fates (*35*). *In vivo*, differentiating cells are embedded in ECM which not only provides structure support but also gives a dynamic environment to modulate their proliferation and differentiation (*164*). Therefore, to overcome this limitation when differentiating stem cells *in vitro*, biomaterials are designed to construct an artificial matrix in order to guide stem cells differentiation (*143*). However so far, no efficient general principles are known to predict how stem cells behave on a given biomaterial (*165*). Therefore, some stem cell researches focused on reconstructing 2D and 3D differentiation matrices prepared from natural and synthetic materials to study stem cells differentiation *in vitro(143).* In this study, mESCs were used as a model to study particularly how hydrogels influence their behaviors. We prepared different hydrogel substrates composed of gelatin and silk fibroin crosslinked by genipin to evaluate their influences on the proliferation and neural differentiation of mESCs. Gelatin, the denatured collagen, was chosen as main component of hydrogel because collagen is the abundant component of all ECM in animals. Moreover, gelatin is a commonly referenced addition for tissue engineering of brain and spinal cord to improve the biocompatibility and cell attachment (*166*). To increase the scaffold bioactive interaction with cells, silk fibroin was conjugated into the hydrogel (*150, 167*). To investigate the influence of chemical compositions and mechanical properties towards neural differentiation, we prepared different hydrogels with different ratios of gelatin and silk fibroin crosslinked by genipin. Since genipin preferentially reacts with gelatin, the gelation time of gelatin is much faster than silk fibroin. When the silk fibroin concentration was higher than 40% in the hydrogel, we observed

the phase separation under the microscopy. In order to reduce phase separation, we kept silk fibroin at a low content in the blended samples GS95 and GS80. By adding the silk fibroin to gelatin, the hydrogel morphologies slightly changed and the storage modulus was improved. In the crosslinking degree and reactive genipin content test, the GS95 showed lower reactive genipin content than G100, which was likely due to the molecular interaction between gelatin and silk fibroin. Through this interaction, the silk fibroin could hide some sites of gelatin to react with genipin. While in the GS80, some silk fibroin probably formed aggregates inside gelatin macromers during sol-gel transition, resulting from the phase separation. However, this phase separation was not visible in the microscopy. Therefore, there were comparable reactive sites with genipin compared to G100 which resulted in the similar reactive genipin content. When used to culture mESCs, the pure and blended gelatin/silk fibroin hydrogels were shown to maintain their viability and proliferation. In the early stage (from day 0 to day 7) of the differentiation process, the cells on G100, GS95 and GS80 showed higher proliferation speed and better cell spreading than S100. This was probably due to the larger pore size of G100, GS85 and GS95 that could increase the cell proliferation and spread. Moreover, silk fibroin has been reported to play important roles in long term cells proliferation (*168*). In addition, ESCs seeded on GS95 and GS80 hydrogel substrates displayed unexpected epithelial ectodermal differentiation fate instead of the neural ectodermal fate that cells showed on TCP using the same differentiation conditions (*157*). Although the storage moduli of G100, GS95 and GS80 were close to elastic modulus of brain tissue, neural differentiation was blocked on the hydrogels. However, an interesting and unexpected connection was that the relatively high reactive genipin content in GS95 and GS80 resulted in a more efficient epithelial differentiation than cells grown

on S100, which had lower reactive genipin content. These results suggest that the crosslinker genipin could be involved in the observed epithelial ectodermal differentiation.

In vertebrates, inhibition of the BMPs signaling pathway in the ectoderm is the hallmark of neural-fate acquisition, and forms the basis of the default model of neural induction. The default model proposes that neural induction happens as a result of the inhibition of BMPs signaling in the embryonic ectoderm (*169*). Kawasaki demonstrated that BMPs signaling was sufficient to block neurogenesis and to promote epithelial differentiation of mESCs (*170*). Interestingly, some papers reported that genipin was able to induce c-Jun NH_2-Terminal Kinase (JNK) expression (*171*). JNK is responsible for the phosphorylation of a variety of proteins including downstream kinases and transcription factors such as c-Jun. Other studies showed that in *Xenopus* embryos c-Jun could strongly activate BMP-4 transcription (*172*).

Consequently, due to the higher reactive genipin content, GS95 and GS80 may activate the BMP-4 signaling pathway in mESCs, resulting in increased epithelial ectodermal differentiation as compared to S100. Moreover, although the GS95 and GS80 had lower reactive genipin content than G100, cells on GS95 and GS80 showed higher k18 (epithelial differentiation marker) expression and further inhibited expression of neural differentiation markers. This could result from the addition of silk fibroin in GS95 and GS80 increases cell interaction with the hydrogel. However, on the sonication-induced hydrogel surfaces without genipin, the cells went to the neural differentiation. Based on these data, we hypothesize that our genipin-crosslinked hydrogels could increase the epithelial differentiation of mESCs to an extent depending on the reactive genipin content and hydrogel composition. Even though the mechanical properties are usually important in influencing stem cells differentiation, here we suggest that the crosslinker genipin and the combination of gelatin and silk fibroin in hydrogels could affect stem cells

differentiation, shifting their fate from neural ectodermal to epithelial ectodermal without the participation of additional growth factors. This hypothesis needs to be further investigated. However, it has some implications for designing scaffold to control the ectodermal differentiation fate of stem cells.

3.1.5 Conclusion

In this study, hydrogel substrates were prepared by gelatin and silk fibroin crosslinked with genipin. By adding the silk fibroin to the gelatin solution, the hydrogel pore size slightly decreased and the storage modulus increased. In addition, the crosslinking degree and reactive genipin content were altered. Although S100 showed higher crosslinking degree, the G100, GS95 and GS80 had higher reactive genipin content than S100. Furthermore, these gelatin/silk fibroin hydrogels could maintain ESCs viability and proliferation. Gelatin and silk fibroin played important roles in short term and long term proliferation during differentiation process respectively. By culturing ESCs on these hydrogel substrates in KSR supplemented medium for 15 days to induce neural differentiation, we found that the blended gelatin/silk fibroins GS95 and GS80 were able to change ESCs differentiation fate from neural ectodermal to epithelial ectodermal fate compared to TCP.

3.2 Part II: Silk fibroin/gelatin hydrogel substrates by physical sonication crosslinking

3.2.1 Introduction

The proliferation and differentiation of ESCs could be modulated by the culture substrates as we demonstrated in Part I. The structures and the chemical compositions of the hydrogel substrates both contribute to the proliferation and differentiation of ESCs. Interestingly, the genipin is suggested as a possible reason to inhibit the neural differentiation of ESC. Since our initial goal is to explore the hydrogel substrates for supporting the neural differentiation of ESCs. Therefore, the genipin crosslinking will be out of consideration in the next step.

Besides chemical crosslinking by genipin, silk fibroin hydrogels can also be produced by physical crosslinking like decreasing the PH (*103*). However, this gelation is a relatively long process for the future 3D encapsulating system with therapeutic cells for brain tissue regeneration. Recently, the novel technique has been developed to induce silk fibroin gelation by sonication. The sonication is a time controllable process from minutes to hours by changing the sonication parameters, including power output and time, as well as the silk fibroin concentration. These advantages could allow the cells addition before the gelation of silk fibroin (*129*). Moreover, other different natural polymers could be added to blend with silk fibroin and entrapped in the hydrogel (*168*).

In this study, silk fibroin hydrogel substrates were produced by sonication and physically blending with gelatin at different ratios. These hydrogels were characterized by FE-SEM, FTIR-ATR and rheological test. Then mESCs were seeded on these sonication-induced hydrogel substrates and kept in KSR supplemented medium for 15 days as described in Part I. The

immunocytochemistry and QRT-PCR were performed to characterize the neural differentiation of mESCs at Day 15.

3.2.2 Materials and methods

3.2.2.1 *Preparation of regenerated silk fibroin solution*

As described in Part I**.**

3.2.2.2 Preparation of sonication induced silk fibroin/gelatin hydrogels

For sonication-induced hydrogel group, it was prepared as a total solute concentration at 2%. The final solution was mixed in a mass ratio of silk fibroin: gelatin= 100:0, 95:5, 80:20 which named S100, SG95 and SG80 (Table 3.2.1). Then these solutions were sonicated at 20% amplitude for 20s by using sonicator Hiel scher UP400S (400W, 24kHz). The appearances of the hydrogels were shown in Fig 3.2.1.

Table3.2.1 The composition and crosslinking parameter of silk fibroin/gelatin hydrogels

Sample code	Silk fibroin	Gelatin	Total solute concen-tration	Amplitude	Sonication time
S100	100	0	2%	20%	20s
SG95	95	5	2%	20%	20s
SG80	80	20	2%	20%	20s

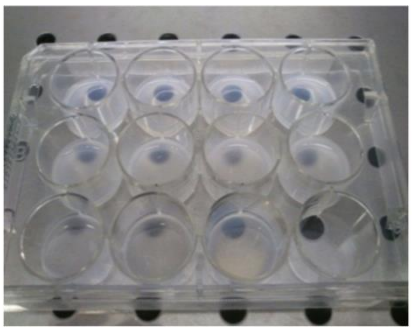

Fig 3.2.1 The appearance of the sonication induced silk fibroin/gelatin hydrogels

3.2.2.3 Field Emission Scanning Electron Microscope (FE-SEM) characterization

As described in Part I**.**

3.2.2.4 Fourier Transform Infrared - Attenuate Total Reflectance (FTIR-ATR) spectroscopy analysis

The lyophilized crosslinked S100, SG95 and SG80 were analyzed in FTIR-ATR as described in Part I**.**

3.2.2.5 Rheological characterization of hydrogels

As described in Part I**.**

3.2.2.6 Embryonic stem cell culture and in vitro neuronal differentiation

As described in Part I**.**

3.2.2.7 Immunocytochemistry

Immunocytochemistry was performed to analyze the neural differentiation of mESCs at day 15. The cells/hydrogel were rinsed in PBS and fixed in 10% formalin for one hour at room temperature. After washing in PBS at agitation for 20 minutes, the cells/hydrogel was incubated in blocking solution (5%BSA + 0.1%TritonX-100 in PBS) for 2 hours. Then they were reacted with primary antibody for 2 hours at room temperature and overnight at 4°C. After washing in

PBS for 45 minutes, they were reacted with secondary antibody for one hour and DAPI stainning for 20 mins. Primary antibodies are rabbit anti-βIII-tublin (Covance) as a neuron marker (1:1000) and mouse anti-MAP2 (Abcam) as a mature neuron marker (1:500). Secondary antibodies are Alexa Fluor 488 goat anti-mouse (Invitrogen) and Alexa Fluor 594 goat anti-rabbit (1:1000) (Invitrogen).

3.2.2.8 RNA isolation and QRT-PCR

As described in Part I**.**

3.1.2.9 Statistics

All statistics were performed using Graphpad Prism 5. In QRT-PCR, ddCt method was used to analyze the data. Gene expression of cells on TCP (control) was set as 1 (no error bars). Other target gene expressions were calculated by the fold change related to the control. One-way ANOVA with Tukey's post hoc analysis was performed for gene expression analysis.

3.2.3 Results

3.2.3.1 Hydrogel morphology characterization by FE-SEM

The sonication-induced S100 (Fig 3.2.2a,b) formed typically lamellar structures with some interconnected fibers in FE-SEM. The distance between the lamellar structures were around 10-20μm. By adding the gelatin in the silk fibroin, even with the low gelatin content at SG95 (Fig 3.2.2c,d), the typical lamellar structure decreased and more fibrous structures occurred. With the increasing gelatin content in SG80 (Fig 3.2.2e,f), it formed more open porous structures instead of lamellar structures.

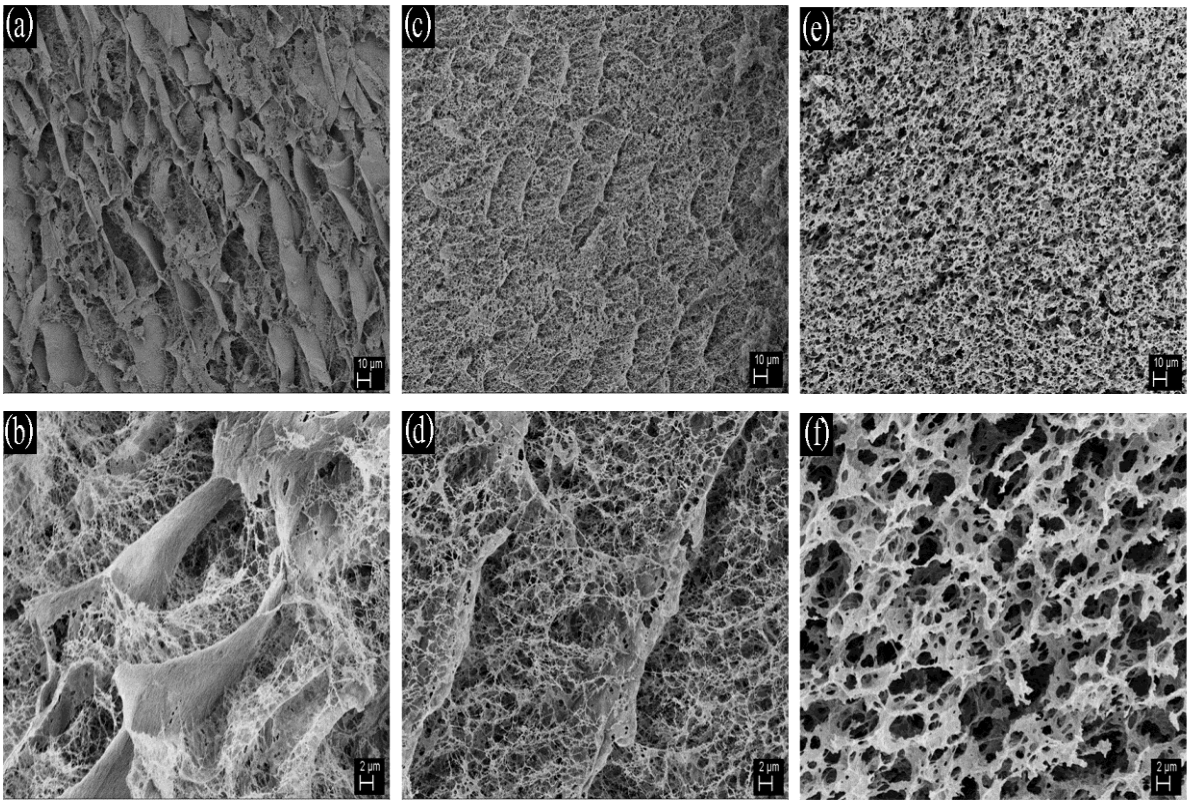

Fig 3.2.2 Morphologies of freeze-dried sonication-induced hydrogel scaffolds by FE-SEM. (a,b) S100 (c,d) SG95 (e,f) SG80

3.2.3.2 Hydrogel protein conformation analysis by FTIR-ATR

After sonication, the pure silk fibroin S100 showed typical β-sheet formation (bands at 1621cm^{-1} and 1514 cm^{-1}) (Fig 3.2.3a). Also SG95 (Fig 3.2.3b) and SG80 (Fig 3.2.3c) showed β-sheet formation (bands at 1621cm^{-1} and 1622cm^{-1}). In addition, the SG95 and SG80 changed slightly at the amide II band compare with S100, because of α-helix structure of the low content of gelatin.

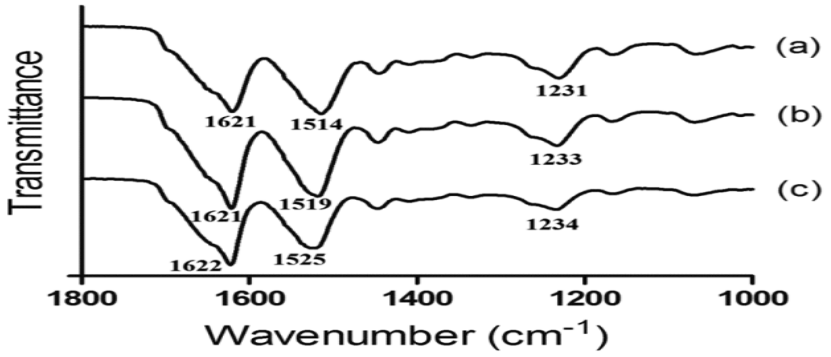

Fig 3.2.3 FTIR-ATR spectra of sonication-induced silk fibroin/gelatin hydrogels: (a) S100 (b) SG95 (c) SG80.

3.2.3.3 Rheological characterization of hydrogels

Fig 3.2.4 showed the storage and loss modulus of these three hydrogels in dynamic frequency sweep test. The storage modulus was significantly larger than loss modulus and was weakly dependent on frequency over the entire range which revealed these materials were typically gelled. The storage modulus of S100, SG95 and SG80 were 4245.0±178.7Pa, 3909.0±109.8Pa and 3182.0±63.1Pa respectively. The S100 had the highest storage modulus because of the crystalline β-sheet structures. However, the addition of gelatin reduced the storage modulus of blending hydrogels.

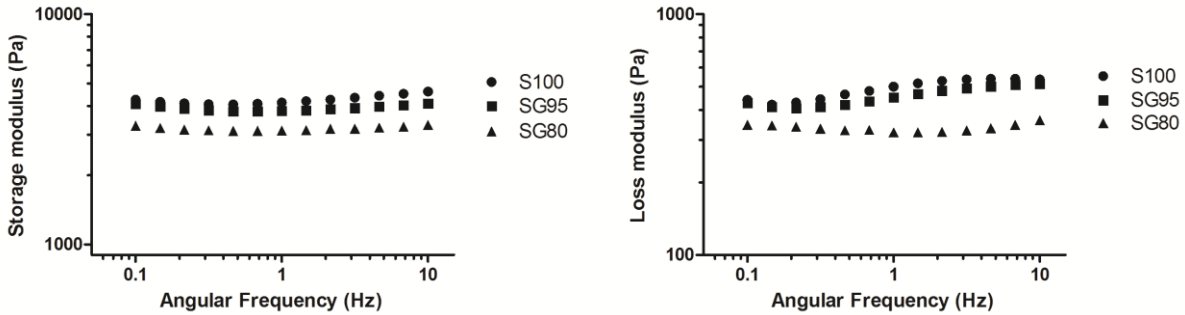

Figure 3.2.4. Characterization of storage and loss modulus of sonication-induced silk fibroin/gelatin hydrogels by oscillatory shear measurements during frequency sweep analysis from 0.1Hz to 10Hz. Error bars represent Mean ± SEM (N=3).

3.2.3.4 Immunocytochemistry of cells on sonication-induced hydrogels

On the sonication-induced silk fibroin/gelatin hydrogel surfaces, the cells also started to form colonies from single cells. Under optical microscopy, we observed the progeny from the colonies at day 9. Then at day15, in contrast to genipin-crosslinked gelatin/silk fibroin hydrogel substrates, we found typical morphologies of differentiated neural cells on the three hydrogel surfaces (Fig 3.2.5). In order to demonstrate the neural differentiation on these hydrogel substrates, we stained the cells on hydrogel surfaces and on TCP by neural markers βIII-tubulin and MAP2 at Day 15. Fig 3.2.6 showed that cells expressed both βIII-tubulin and MAP2 on these hydrogel surfaces and TCP. The cells differentiated not only in the colonies center, but also formed long projections around the colonies. This further indicated the neural differentiation of cells on sonication-induced hydrogel substrates.

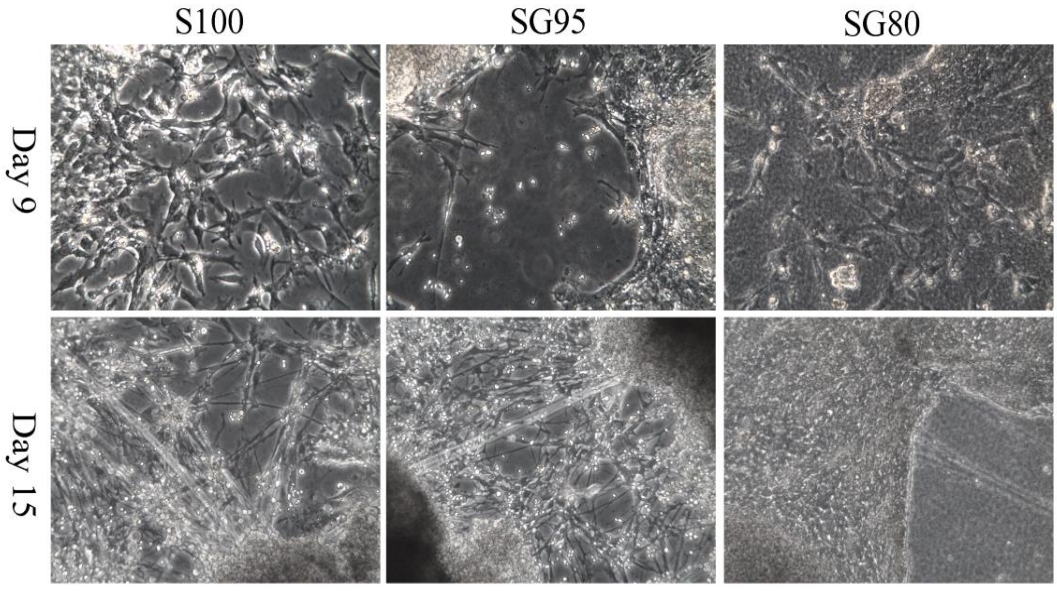

Fig3.2.5 Cell morphologies on sonication-induced hydrogel substrates under optical microscopy at Day 15.

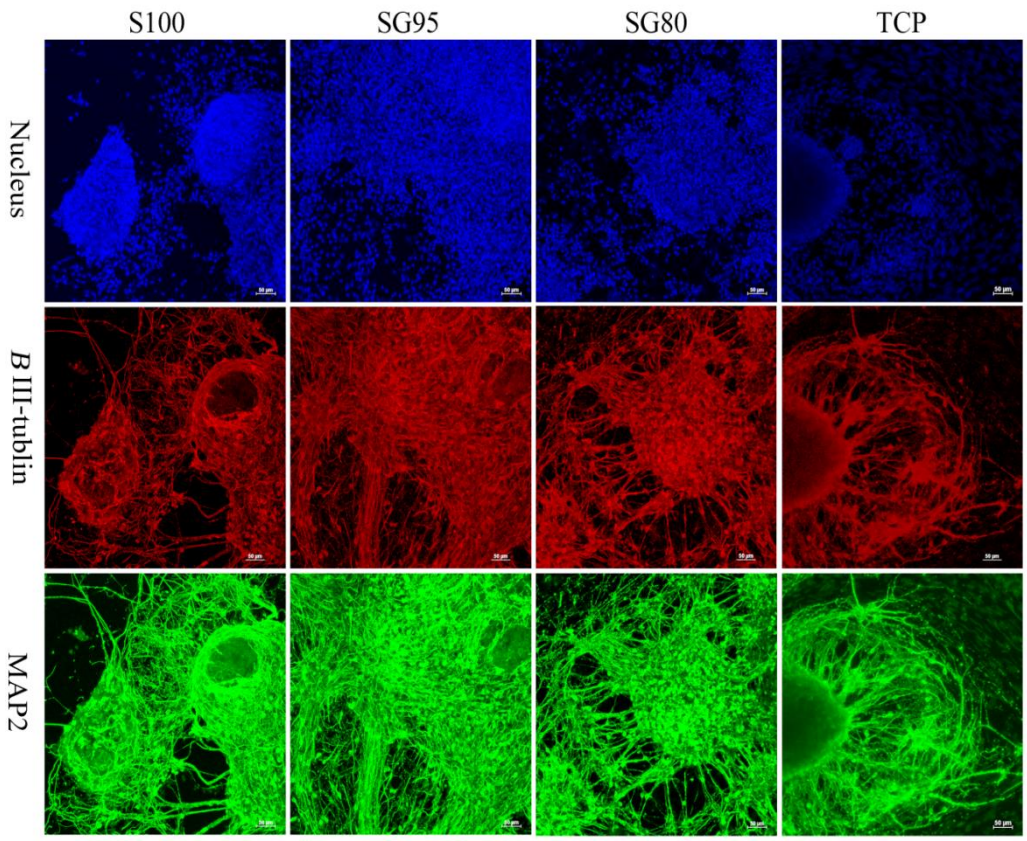

Fig3.2.6 Immunocytochemistry analysis on sonication-induced hydrogel substrates at Day 15

3.2.3.5 Sonication-induced silk fibroin/gelatin hydrogel support the neural differentiation of mESCs

Quantitative RT-PCR was performed to analyze different pluripotent and neural lineage gene markers (Fig 3.2.7). The cells on hydrogel surfaces showed similar Oct 4 and Nanog expression level as cells on TCP ($P>0.05$). However, compared to the undifferentiated ESC, they had significantly decreased Oct 4 and Nanog expression which indicated that these cells lost their pluripotency ($^{\#}p<0.05$, $^{\#\#}p<0.01$). In the meantime, they also showed the comparable expression levels of the neural lineage marker Nestin, βIII-tubulin, NCAM ($p>0.05$) and decreased levels of GFAP ($^{\star}p<0.05$) compared to TCP which indicated these sonication-induced hydrogel substrates supported the neuronal differentiation of ESCs as TCP but decreased astrocytes differentiation.

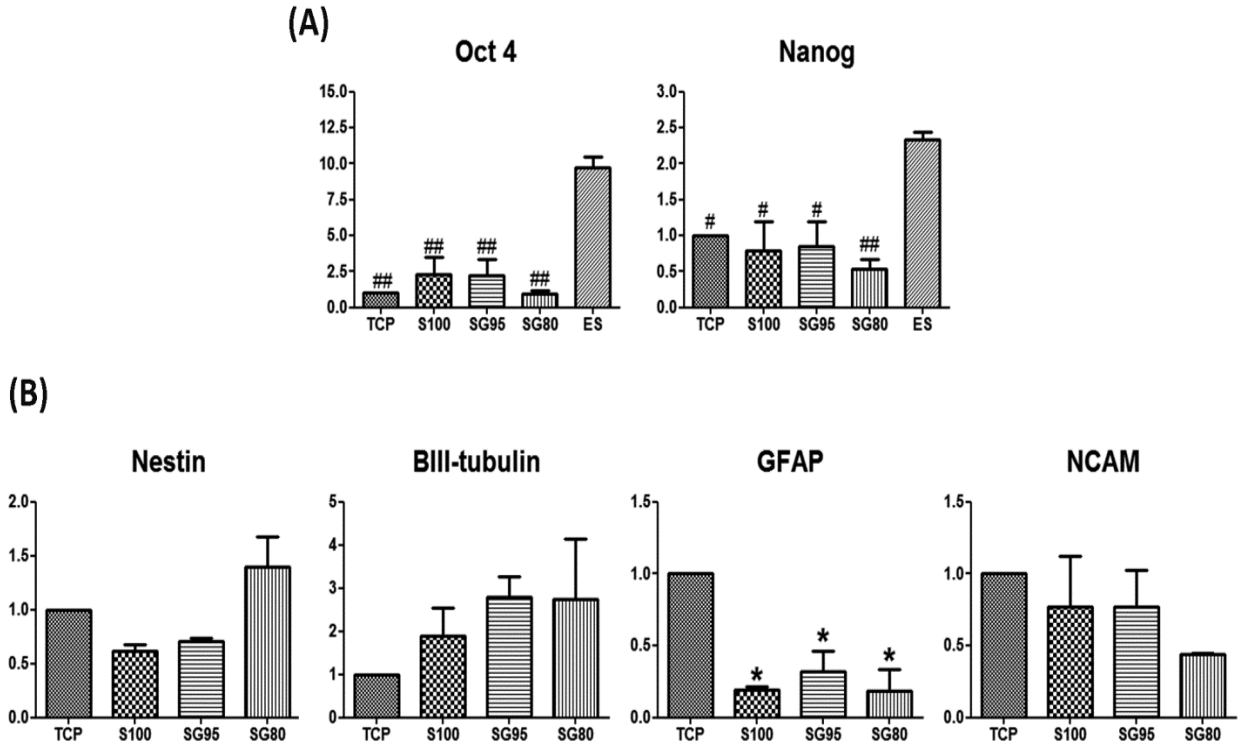

Fig3.2.7 QRT-PCR of mESCs on TCP and sonication induced hydrogel substrates S100, SG95, SG80 and on undifferentiated ESCs (ES) at day 15: (A) Expression levels of pluripotent gene markers of ESCs: Oct4, Nanog. (B) Expression levels of neural lineage markers: Nestin, βIII-tubulin, NCAM, GFAP. (*p<0.05, **p<0.01, ***p<0.001 correspond to TCP, $^{\#}$p<0.05, $^{\#\#}$p<0.01, $^{\#\#\#}$p<0.001 correspond to ES) Error bars represent Mean ± SEM (N=3).

3.2.4 Discussion

In the work before (part I), we found that genipin crosslinked gelatin/silk fibroin hydrogel substrates guide the ESCs differentiation into epithelial lineage instead of neural lineage. As we discussed, the genipin is possible to be one of the main issue involved in this phenomenon. Therefore, in part II work, the sonication physical crosslinking was used to produce the silk fibroin hydrogels. We chose 2% silk fibroin as a starting concentration because it had been demonstrated that it was a appropriate concentration for the cell adhesion and proliferation (*103*). In additon, the elastic moduli of 2% silk fibroin were close to the brain tissue although not

precisely in the range of brain tissue elastic moduli. Furthermore, the 2% was the lowest concentration which is still possible to blend with other materials and entrap them in the gelation process after sonication. The pure gelatin hydrogel was not used in the part of work because the gelatin can not be crosslinked and gelated by sonication. When blending gelatin with silk fibroin, gelatin should be kept at a low content (less than 20%) to be entrapped in 2% Silk fibroin. The gelatin chains were possibly trapped by the β-sheet crystal domains of silk fibroin, forming non-crystalline regions together with the crystallized regions of the silk fibroin chains which forming the homogeneous hydrogel (*168*). However, when the gelatin was more than 20%, we observed the precipitation in the silk fibroin which probably due to that the β-sheet crystal domains were not enough to entrap the gelatin chains and to form the stable hydrogel.

After seeding mESCs on the sonication-induced hydrogel surfaces, we observed the opposite behavior of cells on genipin-crosslinked hydrogel substrates. The cells showed typical neuron morphologies with long projections under the optical microscopy. In the meantime, the presence of neurons was demonstrated by the staining of βIII-tublin and MAP-2 on the sonication-induced hydrogel substrate. QRT-PCR was performed to evaluate the gene expression related to neural differentiation compared to TCP. The cells on the three hydrogels showed comparable pluripotent gene expression (Oct 4 and Nanog) with TCP. In addition, they also showed the comparable expression levels of Nestin, βIII-tublin and NCAM compared to TCP which indicated that these hydrogel substrates supported the neuron differentiation as TCP. Furthermore, the cells on these hydrogels all showed significantly decreased GFAP expression which indicated the decreased astrocytes differentiation. This was possibly because the harder substrates promote the glia cells differentiation (*173*). However, there were no significant differences between the pure silk fibroin S100 with SG95 and SG80 which were physically

blended with gelatin. One possible reason is that the gelatin could not interact with mESCs to increase the neural differentiation, while another reason could be due to the gelatin releasing from the silk fibroin in the medium during culturing process.

Consequently, these findings also supported our hypothesis that genipin could be possibly involved in guiding ESCs to epithelial differentiation. Sonication induced silk fibroin hydrogels could provide an interesting model to induce neural differentiation of ESCs. However, how to increase the neuron differentiation is still need to be further investigated.

3.2.5 Conclusion

Sonication-induced silk fibroin hydrogel were produced and physically blended with gelatin keeping at a low content. Then addition of gelatin could increase the porous structure and decrease the elastic moduli of silk fibroin hydrogel. By seeding ESCs on these hydrogel substrates, we found that ESCs went to neural differentiation as cells cultured on TCP. However, these hydrogel substrates have no significant difference compared to TCP in promoting neuron differentiation, but decreasing the astrocytes differentiation of mESC.

Acknowledgements

The authors acknowledge NHLBI-BayGenomics and NCRR-MMRRC (UC Davis) for the E14Tg2A cell line. The authors would like to thank Professor Riccardo Ceccato for help in the rheological test and Dr. Cristina Foss in the crosslinking degree analysis and discussion.

My Contribution

In this chapter, I prepared the materials and did the cell culturing. I conducted the materials characterization and biological evaluation: Live/Dead, DNA quantification, Immunocytochemistry and RT-PCR.

Chapter 4: Chemical modification of sonication induced silk fibroin hydrogels by IKVAV peptide *

*This part of work is based on the manuscript in preparation: Sun W, Migliaresi C, Quattrone A, Casarosa S, Motta A. Sonication induced silk fibroin hydrogel for brain tissue engineering.

4.1 Introduction

Damages to adult brain tissue can be caused by physical injuries like internal stroke or traumatic brain injury (TBI), resulting in death of neurons, axon disruptions and glial scar formation (*174-176*). However, the adult brain has the limited regenerative ability to replace the lost neurons and restore the tissue function in the damaged part. Neurons have a limited ability to proliferate and supplement the lost ones in the damaged environment that lacks neurotrophins and contains neuron growth inhibitors. In parallel, glial scars could further inhibit axons regeneration as a mechanical barrier or by producing inhibitory molecules in the injury part (*175*). Traditional treatments for these injuries rely on neuroprotective drugs to reduce further degeneration, though without tissue regeneration (*177*). Therefore, replacing the lost neurons and restoring functional tissues are vital to regenerate the damaged brain tissue. In this regard, neural stem cells (NSCs) are promising cell resources to replace the lost neurons and glial cells because they have the self-renewal capacity and ability to differentiate into different neural cells in the adult central nervous system (*52*). Endogenous NSCs can be found the hippocampus and the subventricular zone (SVZ) in the adult brain (*51*). However, self-repair from the endogenous NSCs is very limited (*178*). In the early reports of cell transplantation alone, cells viability was quite low after a few days after transplantation and the cells preferentially differentiated into glial cells. Therefore, how to increase cell survival and neuronal differentiation in the damaged inhibitory environment is still an obstacle. In brain tissue engineering, creating bioactive scaffolds combined with NSCs for transplantation therapy is an promising approach to regenerate tissue lost after brain injuries (*58*).

Hydrogels are attractive matrices to replace the damaged environment in stem cells transplantation for brain tissue engineering because of their mechanical properties comparable with brain tissue (*46, 166*). Especially injectable hydrogels, which can avoid further damage during the surgery procedures (*179*). Many hydrogel based scaffolds for brain tissue engineering have been reported as cell carriers or growth factor delivery vehicles (*58*). For this purpose, cell encapsulation in a hydrogel scaffold is believed to be a promising therapeutic approach (*23*). Encapsulation involves isolating a cell mass physically from an outside environment, aiming at maintaining normal cellular physiology within a desired permeability barrier (*180*). Then the encapsulated cells in the hydrogel scaffold can be cultured *in vitro* or transplanted *in vivo.*

In this study we explored the characteristics of a silk fibroin-based injectable hydrogel encapsulated with human neural stem cells (hNSC) as a potential strategy for brain tissue engineering. Silk fibroin is a natural fibrous polymer with low antigenicity and low inflammatory response (*97*). It has been used in many stem cells-based tissue engineering approaches, such as in bone and cartilage tissue regeneration (*129, 181*). Sonication is an efficient and time controllable way to gelate silk fibroin, which is a promising way to produce injectable hydrogels. Sonication initiates the formation of β-sheets structure in silk fibroin by alterations in hydrophobic hydration, thus accelerating the formation of physical crosslinks responsible for gel stabilization (*129*). By changing silk fibroin concentration and sonication parameters, such as power output and time, the gelation time could be controlled from minutes to hours. This fast sol-gel process allowed the addition of cells post-sonication as well as the injection into the target tissue before gelation.

In order to improve the bioactivity of silk fibroin with NSCs, silk fibroin was chemically immobilized with the laminin-derived peptide isoleucine-lysine-valine-alanine-valine (IKVAV).

Laminin is one of the important components of ECM and a basement membrane glycoprotein (*182*) which promotes neural stem cells growth by coating or in the medium (*183*), as well as promotes neuron survival and neurite outgrowth (*184*). IKVAV, the peptide derived from laminin, has been proven to be the active site of cell adhesion (*185*) and neurite outgrowth (*186*). Self-assembling hydrogels modified with IKVAV peptide have shown to improve the survival of encapsulated neural stem cells/embryonic stem cells survival and neuron differentiation (*58*) (*187*). Modification of silk fibroin with a cell-binding peptide has been reported (*118, 188*). RGD sequences covalently bound to silk fibroin were shown suitable in bone tissue engineering (*118*). However, to our knowledge, there are no reports about silk fibroin hydrogels potential application for brain tissue engineering, or for the IKVAV peptide covalently conjugated to silk fibroin hydrogels.

The purpose of this study is to evaluate silk-fibroin based hydrogels as potential 3D hydrogel scaffolds for brain tissue engineering and to understand the effects of chemical immobilization of IKVAV peptide for hNSCs viability and neuronal differentiation. First, we chose the concentration of silk fibroin according to the elastic moduli of brain tissue. The sonication induced silk fibroin hydrogels, unmodified and chemically modified with IKVAV peptide were prepared to encapsulate the hNSCs and to evaluate the cells viability and neural differentiation.

4.2 Materials and Method

4.2.1 Silk fibroin preparation and chemical modification

The unmodified silk fibroin solution was obtained as described in chapter 3 part I. For chemical modification, the silk fibroin was dissolved in 9.3M LiBr (dissolving concentration at 20%) at 65°C for 4 hours and was dialyzed in distilled water for one day. Then they were transfer into

MES buffer (0.1M MES, 0.5M NaCl, PH=6) and dialyzed for another day. Then silk fibroin-MES concentration was taken out and the concentration was measured around 5-6%. To reactive the carboxyl groups in silk fibroin, silk fibroin-MES solution was diluted to 3%. 0.4g EDC and 0.25g NHS per g silk fibroin were added into the 3% silk fibroin-MES solution. After 20mins reaction in mild stirring, 3.5ul β-mercaptoethanol per 1mg EDC were used to quench the EDC. Then 2mg IKVAV peptide per g of dry silk fibroin were added and mixed for two and half hour. 10mM hydroxylamine was used to stop the peptide conjugation reaction. Then the solution were dialysis for another one day against distilled water (*188*) (Fig 4.1). The final solution was around 1.5%. Unmodified silk fibroin was prepared in the same manner but without the addition of peptide.

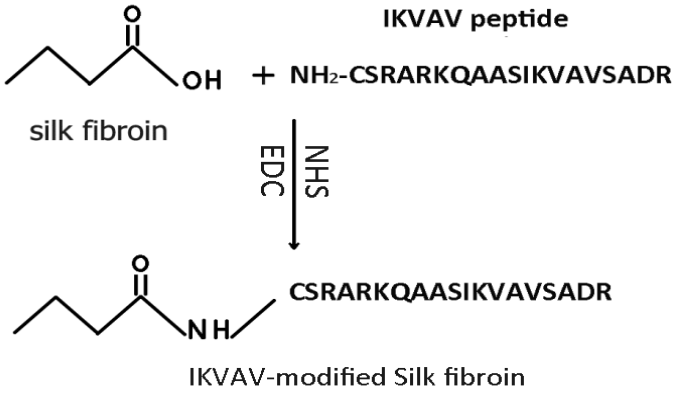

Fig 4.1 Silk fibroin modification with IKVAV peptide

4.2.2 Rheological characterization of hydrogels

As described in chapter 1.

4.2.3 Filed Emission Scanning Electron Microscope (FE-SEM) characterization

As described in chapter 1.

4.2.4 *Fourier Transform Infrared - Attenuate Total Reflectance (FTIR-ATR) spectroscopy analysis*

As described in chapter 1.

4.2.5Human neural stem cells culture and neural differentiation

Human neural stem cells were obtained from Gibco/Life Technologies as a commercially available product (N7800-200). The cells were derived from NIH approved H9 (WA09) human embryonic stem cells. The cells were expanded with cell-start coating plates in complete growth medium, which contained DMEM/F12 medium supplemented with 2% StemPro Neural Supplement and 2mM GlutaMAX, bFGF (20 ng/ml), EGF (20 ng/ml). After two days culture in complete growth medium, neural differentiation medium (Neurobasal medium supplement with 2% B27 serum-free supplement) was placed for 7 days and changed every two days.

4.2.6 Sonication induced silk fibroin gelation and cells encapsulation

The 1% unmodified, IKVAV-modified silk fibroin solutions were supplemented with DMEM/F12 powder and sodium bicarbonate at a concentration of 0.0135 g/mL and 0.0037 g/mL, respectively. Then all the solutions were filtered by 0.22um filter. 0.5ml of each solution was loaded in 1.5ml eppendorf tube and was sonicated with the Hielscher UP400S (400W, 24kHz) (Fig 4.2). Each solution was sonicated at 50% amplitude for 15 seconds. After five minutes of sonication, the solutions were mixed with hNSC pellet ($4x10^6$cells/ml hydrogel). Then 50ul of each sample were aliquoted to one well of 96 well plates and gelated in 37°C for 1 hour. After gelation, 200ul complete growth medium were added in each well. After two days, the medium was changed to neural differentiation medium at day 0 and cells were kept differentiating for 7 days by changing medium every two days.

Fig 4.2 Sonicator Hielscher UP400S (400W, 24kHz).

4.2.7 Cell viability assay

The viability of the hNSCs encapsulated in hydrogels was investigated by Live/Dead assay. Live and dead cells were stained by calcein AM and propidium iodide (PI) respectively. Cells/hydrogel were washed with PBS and then were incubated in calcein AM/PBS (2µmol/ml) at 37°C for 30mins. Then cells were washed with PBS three times and were stained by PI/PBS (20ng/ml) for 5mins at 37°C. After two more washes in PBS, they were observed by confocal microscopy (Nikon Eclipse Ti-E).

4.2.8 Cell proliferation

The proliferation of hNSCs in hydrogels was assessed by Alamar Blue assay on day 0, 3 and 7 after encapsulation according to the manufacturer's instructions. The assay was performed in 96-well plates. 50ul of cells/hydrogel were added in each well with triplicates of each sample. Each well was incubated with 200ul 10% Alamar Blue reagent in culture medium for 4 hours in humidified, 95% air/5% CO_2 atmosphere at 37°C. At the end of incubation, 100ul of the supernatant were then transferred to a 96-well plate and fluorescence intensity was determined

with a microplate reader (Tecan Infinite M200) (excitation/emission: 565 nm/595 nm). The same media incubated with hydrogel without cells were used as controls and their fluorescence value was subtracted from corresponding hydrogels encapsulated with cells.

4.2.9 Immunocytochemistry analysis

Immunocytochemistry was performed to analyze the neural differentiation of hNSCs at day 0 and day 7. Primary antibodies used are mouse anti-Nestin (Abcam) as a neural precusor marker (1:200), rabbit anti-βIII-tublin (Covance) as a neuronal marker(1:1000), mouse anti-MAP2 (Abcam) as a mature neuronal marker (1:500) and rabbit anti-GFAP (Abcam) as an astrocyte marker (1:500). Secondary antibodies used are Alexa Fluor 488 goat anti-mouse and Alexa Fluor 594 goat anti-rabbit (Invitrogen) (1:1000).

4.2.10 Quantification of neuron percentage and neurite outgrowth length

Nikon Eclipse Ti-E confocal microscopy was used to capture fluorescence images. The neuron percentage and neurite length of these images were quantified by Columbus system (PerkinElmer). At least three independent pictures were taken from three different samples. Quantification of neurons was calculated by counting βIII-tublin positive cells and MAP-2 positive cells and divided by DAPI-stained nuclei number. Neurite length was also normalized by neurons number.

4.2.11 Statistics

Statistics were performed using Graphpad Prism 5. In Alamar Blue assay, one-way ANOVA with Tukey's post hoc analysis and two-way ANOVA with Bonferroni post hoc test were

performed. In the quantification of neuron percentage and neurite outgrowth, t-test was performed.

4.3 Results

4.3.1 Rheology of silk fibroin hydrogel unmodified and IKVAV-modified

The stiffness of the silk fibroin hydrogels was characterized by the oscillatory shear measurements. Fig 4.3 shows the storage and loss modulus of dynamic frequency sweep tests of silk fibroin hydrogels unmodified and modified with IKVAV peptide. The storage modulus was weekly dependent on the frequency and higher than loss modulus significantly which indicated the formation of silk fibroin gel after sonication crosslinking. The storage modulus of IKVAV-modified silk fibroin hydrogel (2902±96Pa) was higher than the unmodified silk fibroin hydrogel (1366±37Pa). In the two hydrogels, the elastic moduli of unmodified silk fibroin hydrogel were closer to the range of brain tissue elastic moduli (100–1000 Pa) (*189*).

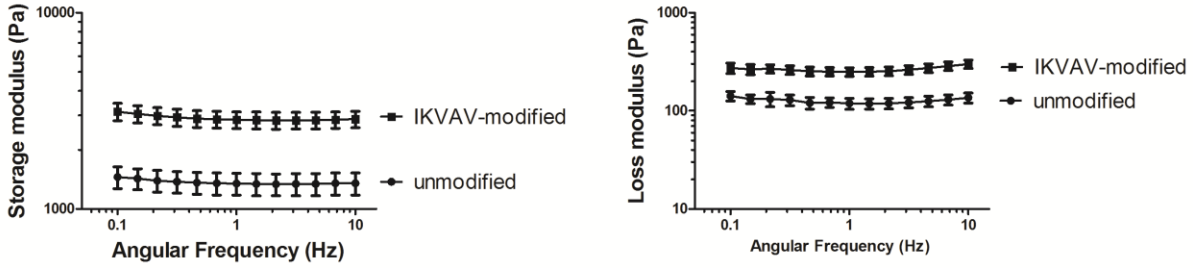

Fig4.3 Characterization of storage and loss modulus of ummodified and IKVAV-modifed silk fibroin hydrogel by oscillatory shear measurements during frequency sweep analysis from 0.1Hz to 10Hz. Error bars represent Mean ± SEM (N=3).

4.3.2 Hydrogel morphology characterization by FE-SEM

The hydrogel internal structure morphologies were characterized by FE-SEM (Fig 4.4). Unmodified silk fibroin hydrogel formed flake-like structures with some holes inside. However, after peptide conjugation, the modified silk fibroin hydrogels formed an interconnected porous structure with the pore size ranging from 10um to 20um.

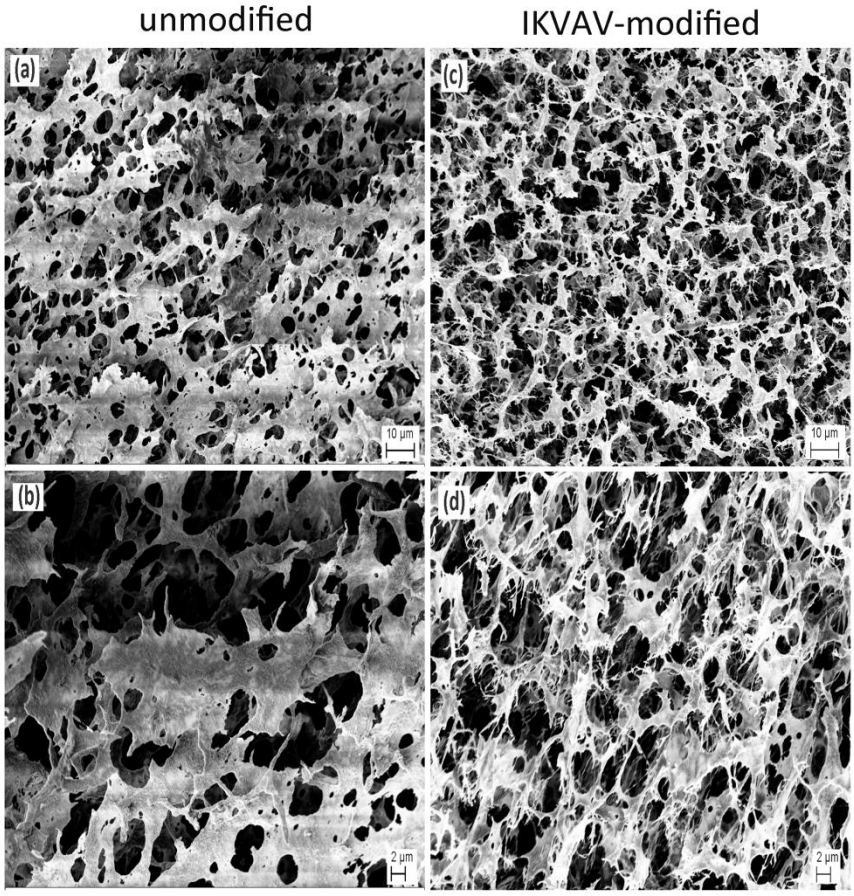

Fig4.4 Morphologies of freeze-dried hydrogels observed by FE-SEM. (a,b) unmodified (c,d) IKVAV-modified silk fibroin hydrogel. Each sample was shown in 10µm and 2µm scales respectively.

4.3.3 Hydrogel protein conformation analysis by FTIR-ATR

FTIR-ATR was performed to monitor the protein conformation changes of the unmodified and IKVAV-modified hydrogels before and after sonication crosslinking. Fig4.5 shows the FTIR

spectra in the special range of 1800-1000 cm^{-1}. According to the previous study, the absorption bands observed for silk fibroin at 1655±5 cm^{-1} (amide I), 1540±5 cm^{-1} (amide II) and 1235± 5 cm^{-1} (amide III) are assigned to the random coil structure and the absorption bands at 1625±5 cm^{-1} (amide I), 1525±5 cm^{-1} (amide II) and 1265±5 cm^{-1} (amide III) are assigned to characteristic of β-sheet structure (*103, 190*). Before crosslinking, the unmodified and IKVAV-modified silk fibroin showed bands at 1640-1650 cm^{-1} and 1230-1240 cm^{-1} region, which indicated the presence of a random coil or intermediate structure (*103*). However, the amide II bands at 1510-1520 cm^{-1} might be due to the lyophilization process (*127*). After sonication crosslinking, the bands at amide I and amide II were shifted to the 1625±5 cm^{-1}, 1525±5 cm^{-1} range which indicated the characteristic of β-sheet structure. Furthermore, the amide III bands of both crosslinked samples at 1233 cm^{-1} and 1272 cm^{-1} also indicated the β-sheet structure (*103*).

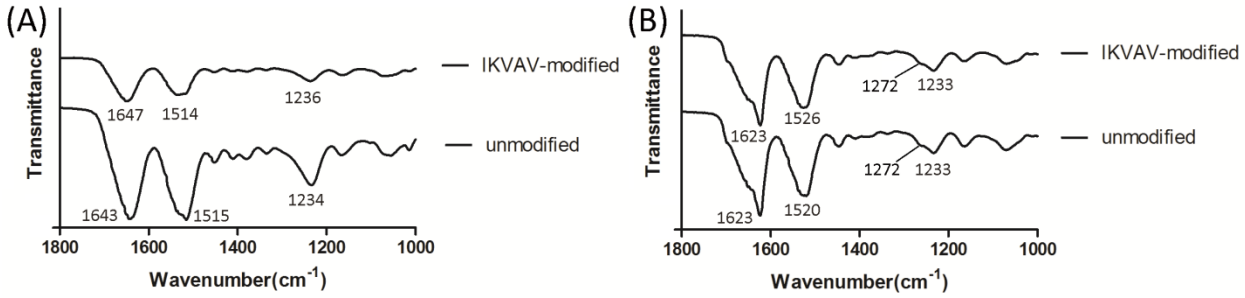

Fig 4.5 FT-IR spectra of unmodified and IKVAV-modified silk fibroin hydrogel before (A) and after (B) sonication crosslinking.

4.3.4 Cell viability assay

The viability of cells encapsulated in the hydrogels was assessed by confocal microscopy with Calcium AM/PI staining at day 0 and day 7 (Fig 4.6). After encapsulation, most of hNSCs cultured in complete medium for two days were viable in both hydrogels at day 0. At day 7,

some single cells grew to aggregates and projections from cells were observed. Cells encapsulated in both hydrogels showed increased cell death at day 7 compared to day 0. In the unmodified silk fibroin hydrogels, a large amount of the cells were dead. However, the IKVAV-modified hydrogel showed higher cell viability and better distribution in comparison to unmodified silk fibroin.

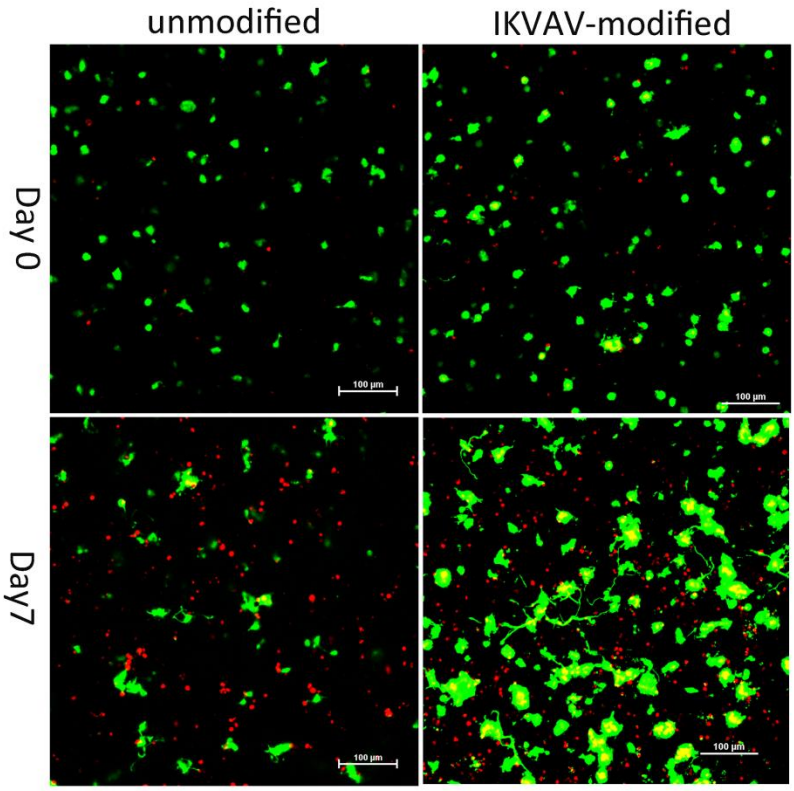

Fig4.6 The viability of hNSCs encapsulated in unmodified and IKVAV-modified silk fibroin hydrogels analyzed by Live (green)/Dead (red) assay with confocal microscopy at day 0 and day 7. Bar length: 100um

4.3.5 Cell proliferation assay

Alamar Blue assay was performed to test cells proliferation during the neural differentiation process. In Fig 4.7, the resulting fluorescence is proportional to the number of viable cells in the sample, thus proliferation of hNSCs could be assessed. At day 0, the IKVAV-modified group

showed higher fluorescence intensity (**p<0.01) which indicates that from day -2 to day 0, the cells in IKVAV-modified hydrogels proliferated faster than in the unmodified hydrogels. From day 0 to day 3 and from day 3 to day 7, the cells in both hydrogel groups showed significant cell death (***p<0.001,$^{###}$p<0.001, $^{\$\$\$}$p<0.001). However, the cells in IKVAV-modified silk fibroin hydrogels showed higher fluorescence intensity at each time point (**p<0.01, ***p<0.001) which indicates that IKVAV-modified silk fibroin hydrogels could increase the proliferation of cells in the differentiation process compared to the unmodified silk fibroin hydrogels.

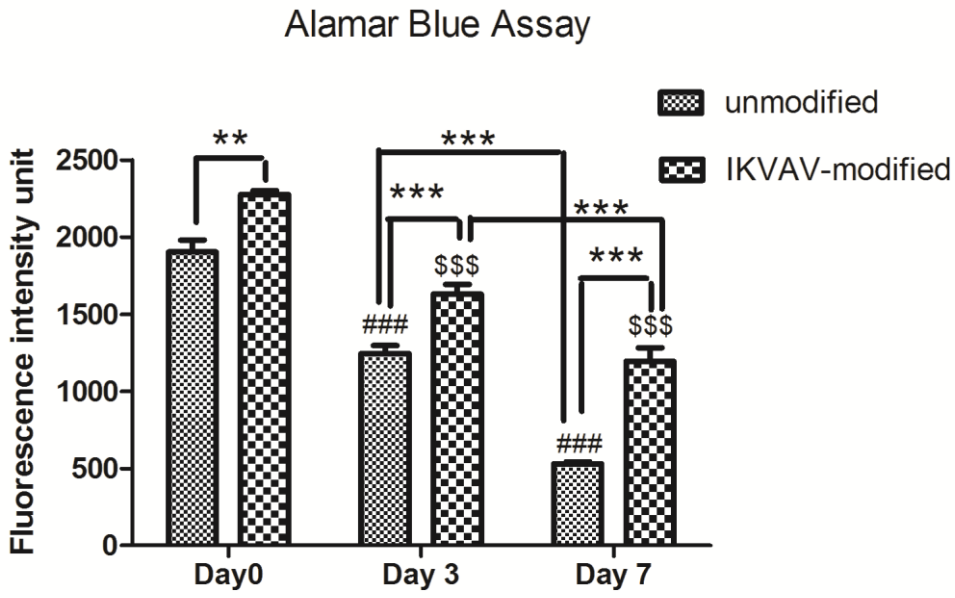

Fig 4.7 Cell proliferation of hNSCs in unmodified and IKVAV-modified silk fibroin hydrogels at different time points analyzed by Alamar Blue assay (*p<0.05, **p<0.01, ***p<0.001. ###p<0.001 correspond to unmodified silk fibroin at day 0, $$$p<0.001 correspond to IKVAV-modified silk fibroin at day 0).

.

4.3.6 Immunocytochemistry for neuron percentage and neurite length quantification.

Immunocytochemistry was performed to characterize the differentiated cells in the differentiation process at day 0 and day 7 (Fig 4.8). At day 0, cells showed positive staining of

nestin, which indicated their undifferentiated state after two days in culture in the self-renewal medium. After one week of differentiation culture, the cells were tested with Nestin, βIII-tublin, MAP-2 and GFAP antibodies. In both hydrogels, the cells were induced to neural differentiation and showed Nestin, βIII-tublin and MAP-2 positive signals, without GFAP expression. At day 7, the cells encapsulated in IKVAV-modified silk fibroin hydrogel showed more βIII-tublin positive cells compared to unmodified silk fibroin hydrogels (Fig 4.9) which indicated that more early neurons were differentiated. In the meantime, more MAP-2 positive cells occurred in the IKVAV-modified hydrogels than in the unmodified hydrogels. Furthermore, the image quantification showed that βIII-tublin positive cells and MAP-2 positive cells percentage in IKVAV-modified silk fibroin hydrogels were significantly higher than in unmodified silk fibroin hydrogels, revealing that the IKVAV peptide modification could increase neuron differentiation and neuron maturation. However, there was no significant difference of the neurite outgrowth length of neurons between each other.

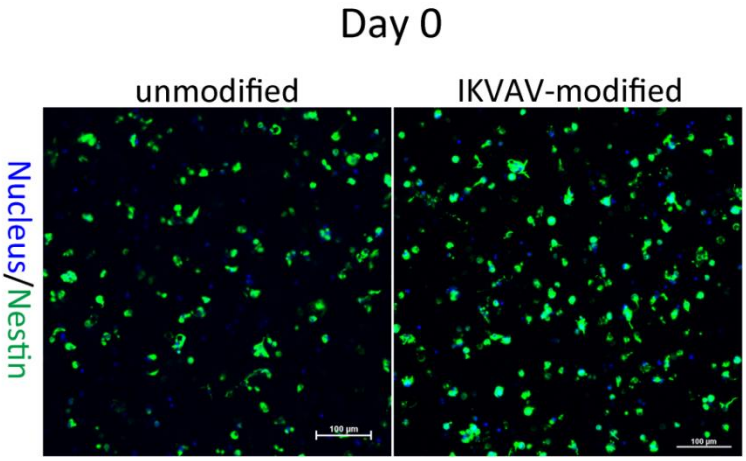

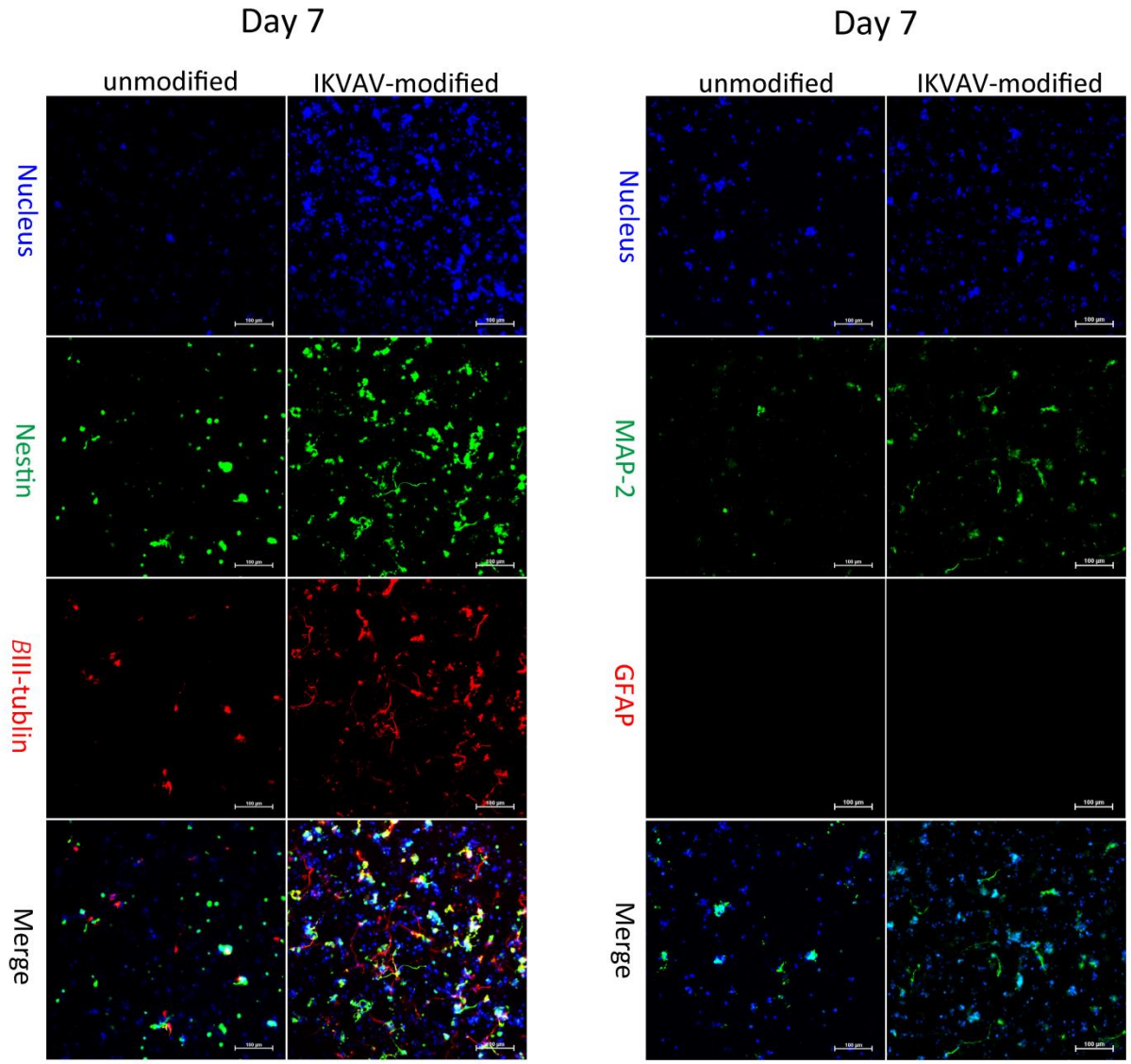

Fig4.8 Immunohistochemistry analysis of hNSCs encapsulated in unmodified and IKVAV-modified hydrogesl at Day 0 and Day 7. Cells were stained with Nestin (green), βIII-tublin (red), MAP-2 (green), GFAP (red). Scan bar=100um.

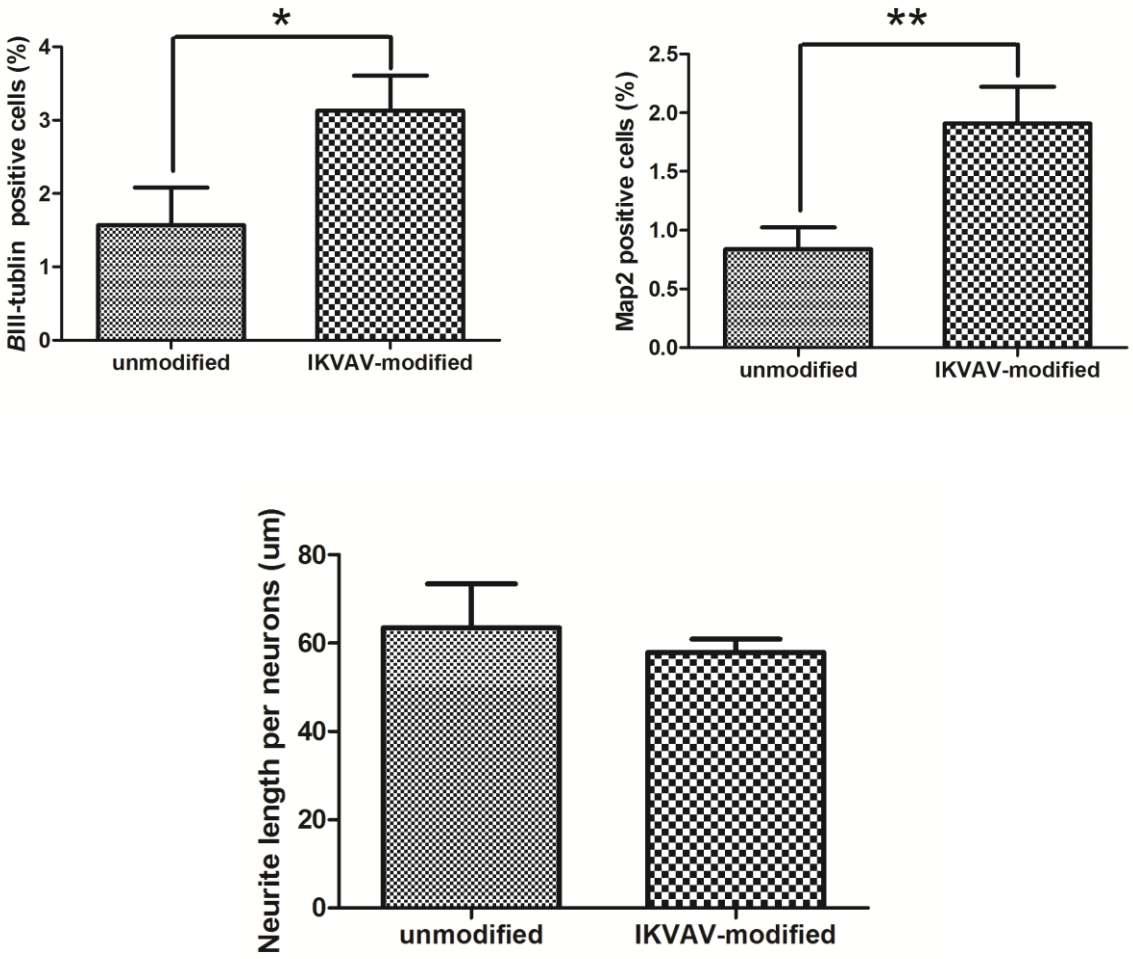

Fig 4.9 Quantification of the βIII-tublin and MAP-2 positive cells percentage and neurite length.

4.4 Discussion

Silk fibroin, the natural polymer, has been investigated for many years because of their low inflammatory and low immunogenic properties (*191, 192*). By processing aqueous silk fibroin solution into various kinds of materials such as films, sponges and electrospun nets can meet the needs of different applications such as cartilage and bone tissue engineering. Compared to these applications, silk fibroin hydrogel application in soft tissue engineering has been rarely reported (*193*). Recently, sonication has been developed to assemble the silk fibroin into hydrogel in a controlled way. The gelation time can be controlled from minutes to hours, this fast gelation

process can benefit the brain tissue engineering as hydrogels can then be used as injectable materials. In the meantime, there are no reports about sonication-induced silk fibroin applications for brain regeneration yet. To our knowledge, this is the first time to modify the silk fibroin by IKVAV peptide and to produce the IKVAV-modified silk fibroin hydrogel by sonication.

It is notable that the stiffness of the hydrogel is very important to neural stem cells behavior according to many data which show it can affect neural differentiation and neurite outgrowth. In this experiment, we chose the most comparable elastic moduli of the silk fibroin hydrogel at 1% (258±16 Pa). However, the unmodified silk fibroin hydrogel storage modulus increased in the modification process even without the addition of peptide. This could probably due to the EDC/NHS addition in the modification, which could increase the β-sheet structure in the silk fibroin (*194*), which in turn results in the stiffness increase. To increase the bioactivity of hydrogels to neural cells, laminin-derived IKVAV peptide was preferentially selected because its applications for neural tissue engineering were reported (*70, 195*). Therefore, we hypothesize that the bioactivity and interaction of silk fibroin to NSCs could be increased by chemically modifying with laminin-derived peptide IKVAV.

After encapsulation, cells in IKVAV-modified hydrogels showed better cell viability and higher proliferation than those encapsulated in the unmodified hydrogels, as shown by the Live/Dead and Alamar Blue analysis. One possible explanation is that the structure of IKVAV-modified silk fibroin hydrogel changes after the addition of peptide, compared to unmodified SF, resulting in more open porous structure which could benefit the cells proliferation and migration. Another explanation could be the IKVAV provide adhesion sequence which resulted the increase of the cell adhesion and thus increased the viability. In some previous work, it has been shown that bio-adhesive sequences such as RGD and IKVAV can increase cell attachment and growth through

integrin-mediated pathway (*196, 197*). However, the viable cells kept decreasing in both hydrogels in this differentiation process. One reason could be that in the differentiation process, many cells would turn to the apoptosis fate, which was also observed in stem cells differentiation on 2D differentiation process (*157*). Another reason could be that the IKVAV peptide conjugation was not enough to support the hNSC attachment and neuronal differentiation. Therefore, other ECM components may be needed to add in this hydrogel system.

In this differentiation process, the IKVAV peptide could increase neuron differentiation and the maturation of the neurons which was probably due to the fact that it mimics laminin structure supports of the neural ECM. This IKVAV peptide positively improved the neuron differentiation fate, thus it could potentially accelerate brain tissue regeneration. In this study, there were no GFAP positive cells found in the differentiation process, which could due to the fact that glial differentiation of hNSCs takes longer time. Sun Y et al reported that the differentiation of GFAP positive cells took more than one month (*198*). Interestingly, higher ratios of neurons occurred in the IKVAV-modified compared to unmodified silk fibroin hydrogel after one week differentiation, while the IKVAV didn't improve the length of neurite outgrowth. This could probably due to the hydrogel structure limitation, the pore size may be not large enough for the cells migration and neurite outgrowth. It was also possibly due to the relatively low concentration of IKVAV.

However, this work suggested the new potential application of IKVAV-modified silk fibroin hydrogel in brain tissue engineering. To further improve the hydrogels, the silk fibroin hydrogel pore size could be optimized and increased IKVAV peptide concentration could be used to increase the neuron differentiation and neurite outgrowth. Another approach could involve

immobilizing different kinds of peptide to the silk fibroin to further increase the cell adhesion and neurite outgrowth.

4.5 Conclusion

In this study, the silk fibroin hydrogels by sonication crosslinking were prepared for brain tissue regeneration. By chemically immobilizing with IKVAV peptide, the morphologies of hydrogel scaffolds were more porous and the stiffness increased. HNSCs could be successfully encapsulated in hydrogels. By inducing neural differentiation of hNSCs for one week, cells in IKVAV-modified silk fibroin hydrogel showed better viability, proliferation, increased neuron differentiation and maturation compared to cells in unmodified silk fibroin hydrogel. Therefore, the IKVAV-modified silk fibroin hydrogel could be possibly used as potential 3D scaffolds for brain tissue engineering.

Acknowledgements

We thank Professor Riccardo Ceccato for help in the rheological test. We also thank to Valentina Adami and Pamela Gatto for their help with Columbus software.

Chapter 5: Angiogenesis evaluation in sonication induced silk fibroin hydrogels*

*This part of work was performed at: Experimental Trauma Surgery, University Medical Center Schleswig-Holstein, Kiel 24105, Germany, under the supervision of prof. Sabine Fuchs

5.1 Introduction

Although significant success has been achieved by combing polymers and cells in tissue engineering, a particular challenge still need to be solved is the loss of tissue viability after the implantation of larger tissue constructs. The limit of effective diffusive transport of oxygen has been suggested to be only 150-200 µm (*199*). Thus larger implanted constructs require the formation of the blood vessels which mediates gas and nutrient exchange, metabolic processes, and waste expulsion (*200*). Angiogenesis is the process of new blood vessels formation from the pre-existing vasculature (*201*) which plays an important role in wound healing and tissue repair (*202*). Vasculogenesis is the neovessel formation through the assembly of endothelial cells into a tube, followed by stabilization and maturation into blood vessels (*203*). During the vasculogenesis, the differentiation and functional integration of endothelial progenitor cells into the vasculature are induced (*204*). Hematopoietic stem cell populations and endothelial progenitor cells can increase neovascularization of tissue after ischemia and contributes to angiogenesis, thereby, providing a ideal therapeutic option (*205*). OEC (Outgrowth endothelial cells), also called late EPC, are defined as a specific class of endothelial cells, one type of cells that were isolated from the mononuclear cells fraction of human peripheral blood (*83*). The key function of EPC includes the formation of vascular structures in pro-angiogenic matrices *in vitro*, as well as the potential to contribute to the vascularization *in vivo* (*77*). Successful neovascularization is a critical factor for the therapeutic outcomes in organs and tissues deprived of an adequate, stable vasculature. Furthermore, vascularization is critical to create complex and

3D bioengineered tissues. To achieve neovascularization, several strategies have been reported. Angiogenic growth factors such as VEGF and FGF-2 were used in the delivery systems to induce potent angiogenic responses. Furthermore, pre-vascularized constructs based on endothelial cells (ECs) or EPC integrated into scaffolds and were developed for tissue engineering (*206, 207*). This strategy would allow accelerating the vascularization process after the implantation.

The process of angiogenesis is controlled by the interaction of EC with angiogenic growth factors such as vascular endothelial growth factor (VEGF) (*208*), but also the ECM is very important factor in the development of functional blood vessels. At the initial stage of angiogenesis, ECs at their normal quiescent states can be activated by VEGF inducing ECs proliferation and sprouting of blood vessels. As angiogenesis proceeds, ECM has essential functions in regulating ECs migration, invasion, proliferation, and survival by providing key signaling events. In addition, the activated ECs proliferate and secrete various proteases, such as membrane-type matrix metalloproteinases (MT-MMPs) to degrade the basement membrane and ECM (*209*). The stabilization of nascent vessels is mediated by recruitment of mural cells. Human mesenchymal stem cells (MSCs) have been shown to efficiently stabilize nascent blood vessels in vivo by differentiating into perivascular precursor cells and depositing new ECM proteins to promote vessel formation and maturation (*210*). Therefore, co-cultures of EC and MSC have been used as a model of studying vasculogenesis (*203, 211*). In addition, MSC provide a series of growth factors such as VEGF triggering the process of neovascularization (*212*).

As described in the chapter 3, sonication induced silk fibroin hydrogels conjugated with IKVAV peptide could be a candidate 3D hydrogel for brain tissue engineering. In addition, induction of

angiogenesis is supposed to stimulate endogenous recovery mechanisms, including neurogenesis, synaptogenesis, neuronal and synaptic plasticity (*213*). Until now, no reports have evaluated the pro-angiogenic potential of the sonication-induced silk fibroin hydrogel. In addition to the role of the IKVAV as factor to induce neurite outgrowth, this peptide has also been reported to induce angiogenesis (*214*).

In this study, unmodified silk fibroin hydrogels, IKVAV-modified and control peptide VVIAK-modified hydrogels were evaluated in terms of their angiogenic potential using human OECs in a mono-culture system or in co-culture with human bone marrow MSC. In these different approaches the cells were encapsulated in 3D silk fibroin based hydrogels at the concentration of 1million cells/ml hydrogel. The structures and morphological appearances of the three hydrogels as well as encapsulated cells were evaluated by FE-SEM. In addition, the endothelial and angiogenic response was evaluated by confocal microscopy after staining for endothelial marker CD31. The proliferation of cells in hydrogels was evaluated by DNA quantification. QRT-PCR was performed to assess the expression of angiogenesis and endothelial marker related genes.

5.2 Materials and Method

5.2.1 Silk fibroin solution preparation and chemical modification

The silk fibroin preparation and modification were the same as described by chapter 3 part I and chapter 4, the H_2O, IKVAV and VVIAK peptide were added in modification process as described in chapter 4, the samples were named unmodified, IKVAV-modified and VVIAK-modified respectively. The final concentration of the three solutions was 1%.

5.2.2 Isolation and expansion of OEC

The OEC were isolated and cultured according to protocols as described previously (*215*). Mononuclear cells were isolated from peripheral blood buffy coats. 25ml peripheral blood was diluted with 25ml PBS in 50ml tube. Then 35ml of this mixture that was carefully added to 15 ml of Biocoll followed by centrifugating for 35 minutes at 400g without break, according to Biocoll gradient centrifugation (Fig 5.1). The mononuclear cells were cultured in endothelial cell growth medium-2 (EGM-2) with full supplements from the kit (10 ml FBS, 0.2 ml Hydrocortisone, 2 ml hFGF, 0.5 ml VEGF, 0.5 ml IFG-1, 0.5 ml ascorbic acid, 0.5 ml hEGF, 0.5 ml Heparin), 5% FBS, and 1% penicillin/streptomycin, on collagen coated well plates. $5x10^6$ mononuclear cells/well were seeded on 24 culture-well plates and then fed with fresh medium every two days. After 1 week of culture, adherent cells were collected and reseeded in a density of $0.5x10^6$cells/well to collect OEC. Then colonies of OEC with cobble-stone-like morphology appearing after 2-3 weeks in culture were trypsinized and expanded. The appearance of OEC was shown in Fig 5.2.

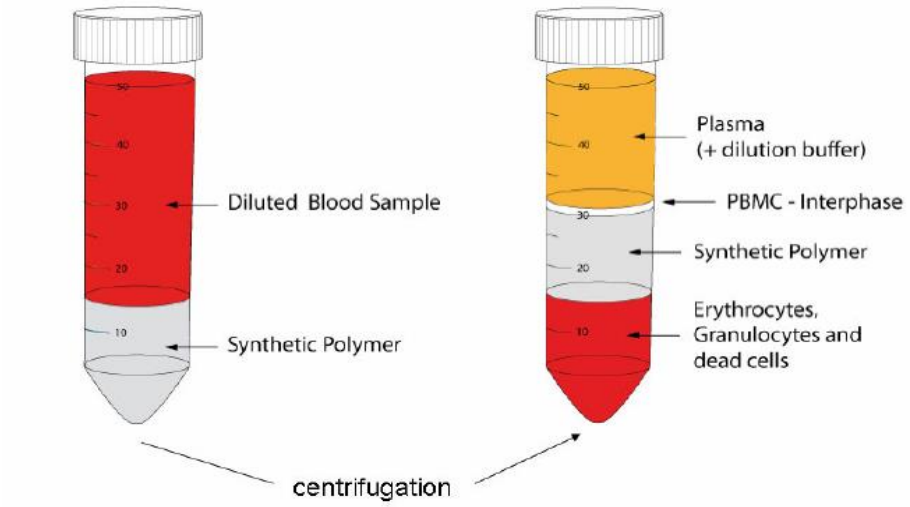

Figure 5.1 Isolation of mononuclear cells from peripheral blood buffy coat. According http://pluriselect.com/buffy-coat.html

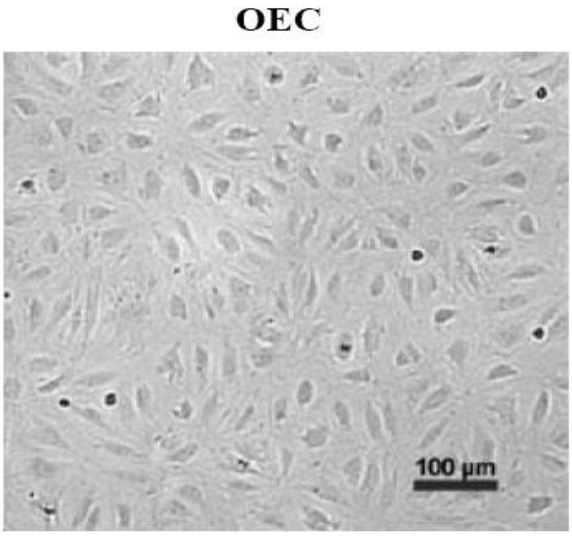

Figure 5.2 The morphology of OEC

5.2.3 Isolation and expansion of human bone-marrow mesenchymal stem cells (BM-MSCs)

Human BM-MSCs were isolated from bone marrow of human cancellous bone fragments of adult donors. Bone fragments were washed several times with phosphate buffered saline to collect the loosely associated cell fractions. The washing solution containing bone marrow residues was filtered by cell strainer and centrifuged for 10 minutes at 400g, and the cell pellet was re-suspended in DMEM/Ham F-12 supplemented with 20% FBS and 1% Penicillin/Streptomycin. Cells were seeded at a density of 2×10^6 cells/cm^2 on collagen-coated flasks (T75). MSC-like colonies appearing after 7-10 days were expanded using a splitting ratio of 1:3 and were cultivated in DMEM-Ham F12 supplemented with 20% FBS and 1% Penicillin/Streptomycin.

5.2.4 Cells encapsulation

500ul of each 1% unmodified, IKVAV-modified and VVIAK-modified solutions were sonicated at 10% amplitude for 25s by sonicator (SONOPULS HD 2070, 70W, 20kHz). After 5 minutes, the cell pellets were mixed with the silk fibroin solution. Then the cells/solution were added in 8-well chamber slides (200ul in each well for confocal microscopy), in 96-well plates (50ul in each well for DNA quantification), in 48-well plates (200ul in each well for RNA extraction) and in 24 well-plate (400ul in each well on coverslip for SEM). For mono-culture, 1million OEC were mixed with 1ml hydrogel solution. For co-culture, half million of OEC and half million of BM-MSC were mixed with 1ml hydrogel solution. After incubation in 37°C for one hour, then EGM-2 medium plus VEGF (50ng/ml) were added in the mono-culture system, and EGM-2 medium were added in co-culture system.

5.2.5 Preparation of samples for FE-SEM

The hydrogel samples without cells for characterization were dried by freeze-drying and critical point drying. Freeze-drying samples were frozen the liquid nitrogen and then were transfer to the freeze-drier immediately. After one day lyophilization, samples were taken out and coated with gold, then they were observed under FE-SEM (SUPRA 40/40VP ZEISS). The critical point drying samples were dehydrated with increasing concentrations of ethanol from 50% (v/v) to 100% (v/v) at 10% per step and 15 minutes for each step. The ethanol was then removed by a critical point dryer. Then they were coated with Au/Pt (80/20) and were observed under FE-SEM (TM300, HITACHI).

The hydrogel samples with cells were fixed in 4% formalin and 1% glutaraldehyde mixture for 30 minutes, followed by dehydrated with increasing concentrations of ethanol from 50% (v/v) to

100% (v/v) at 10% per step and 15 minutes for each step, as well as critical point drying. Then they were coated with Au/Pt (80/20) and were observed under FE-SEM (S4800, HITACHI).

5.2.6 Immunofluorescence staining

At day4 and day10 after encapsulation, the hydrogel/cell samples were fixed with 4% paraformaldehyde, samples were washed three times with PBS and permeabilized using 0.5% Triton X-100 for 20 minutes. After washing in PBS for 3 times (15 minutes each time), cells were incubated with the following primary antibodies CD31 (Dako, 1:50) diluted in 1% bovine serum albumin (BSA) in PBS for 2 hour at room temperature. After washing 3 times with PBS (15 minutes each time), cells were incubated with the secondary Alexa Fluor 488 goat anti-mouse antibody (Invitrogen) diluted 1:1000 in 1% BSA in PBS for 1 hour at room temperature. For nuclear counterstaining, cells were treated with 4',6-diamidino-2-phenylindole (DAPI). Samples were then observed using Zeiss LSM 510 Meta confocal laser scanning microscope.

5.2.7 DNA quantification

To quantify the cells proliferation, 50ul of hydrogel/cells solution were put in one well of 96-well plate after encapsulation, triplicate samples were prepared in three different hydrogels of each donor at each time point. Briefly, after washing with PBS, cells/hydrogels were collected and stored at -80°C. Following lyophilization, the sample in each well were lysed in 250ul PBE buffer (10mM EDTA in PBS) supplemented with 1mg/ml Proteinase K for 24 hours at 55°C. Then DNA quantification procedure was same as described in chapter 3 part I.

5.2.8 RNA isolation and reverse transcription

The RNA isolation and reverse transcription was the same as described in chapter 3 part I.

5.2.9 QRT-PCR

To assess the expression of endothelial markers, as well as the expression of angiogenic factors, QRT-PCR was performed using Glycerin-Aldehyde-3-phosphate (GAPDH) as a internal control. All the primers were from QuantiTect Primer Assay-Qiagen. QRT-PCR was performed using Rotor Gene (Quiagen) System. Primers are listed in Table 5.1.

Table 5.1 Primers for QRT-PCR

Gene name	**Sequence**	**Company**
CD31	F 5'-CCGGATCTATGACTCAGGGACCAT-3' R 5'-GGATGGCCTCTTTCTTGTCCAG-3'	Eurofins
Gene name	**Primer assay name**	**Catalogue number**
SM-Actin	Hs_ACTA _1_SG QuantiTect Primer Assay	QT00088102
VE-Cadherin	Hs_CDH5_1_SG QuantiTect Primer Assay	QT00013244
Integrin α5	Hs_ITGA5_1_SG QuantiTect Primer Assay	QT00080871
Integrin β1	Hs_ITGB1_1_SG QuantiTect Primer Assay	QT00068124
Collagen type IV	Hs_COL4A1_1_SG QuantiTect Primer Assay	QT00005250
MMP9	Hs_MMP9_1_SG QuantiTect Primer Assay	QT00040040
GAPDH	Hs_GAPDH_1_SG QuantiTect Primer Assay	QT00079247

5.2.10 Statistics

All statistics were performed using Graphpad Prism 5. In QRT-PCR, ddCt method was used to analyze the data. Gene expression of cells on TCP (control) was set as 1 (no error bars). Other target gene expressions were calculated by the fold change related to the control. In DNA quantification test, one-way ANOVA with Tukey's post hoc analysis and two-way ANOVA with Bonferroni post hoc test were performed. One-way ANOVA with Tukey's post hoc analysis was performed for gene expression analysis.

5.3 Results

5.3.1 Hydrogel morphologies by FE-SEM

The inner structures of these three hydrogels were examined in FE-SEM by freeze-drying and critical point drying (Fig 5.3). In the freeze-dried samples, unmodified silk fibroin hydrogel formed flake-like structure with many holes on that. The IKVAV-modified and VVIAK-modified hydrogel formed porous and fibrous structures. In contrast, these three hydrogels formed condense and compact structures after critical point drying and no obvious differences were observed between each other.

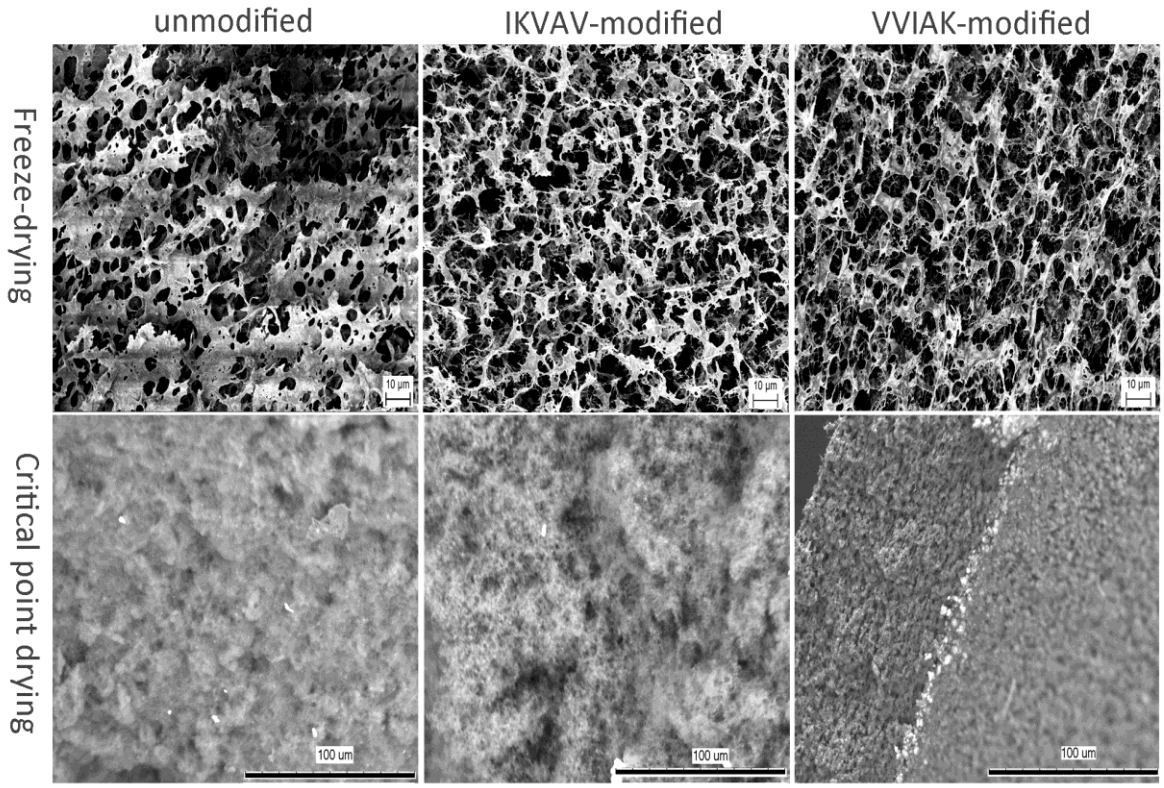

Fig 5.3 FE-SEM morphologies of silk fibroin hydrogels unmodified, IKVAV-modified and VVIAK-modified by freeze-drying and critical point drying.

5.3.2 Immunofluorescence staining of mono-culture from donor 1 in silk fibroin hydrogels unmodified and IKVAV-modified.

The mono-culture system were incubated in EGM-2 medium plus VEGF (50ng/ml) to induce angiogenesis. At different time points the cells were staining with endothelial cells marker CD31 and detected by immunofluorescence. At day 4 after encapsulation (Fig 5.4), the OEC in both unmodified and IKVAV-modified showed a round shape without angiogenic elongation in the hydrogel. At day 10, the cells still kept the round shape which indicated that angiogenic structures were not formed.

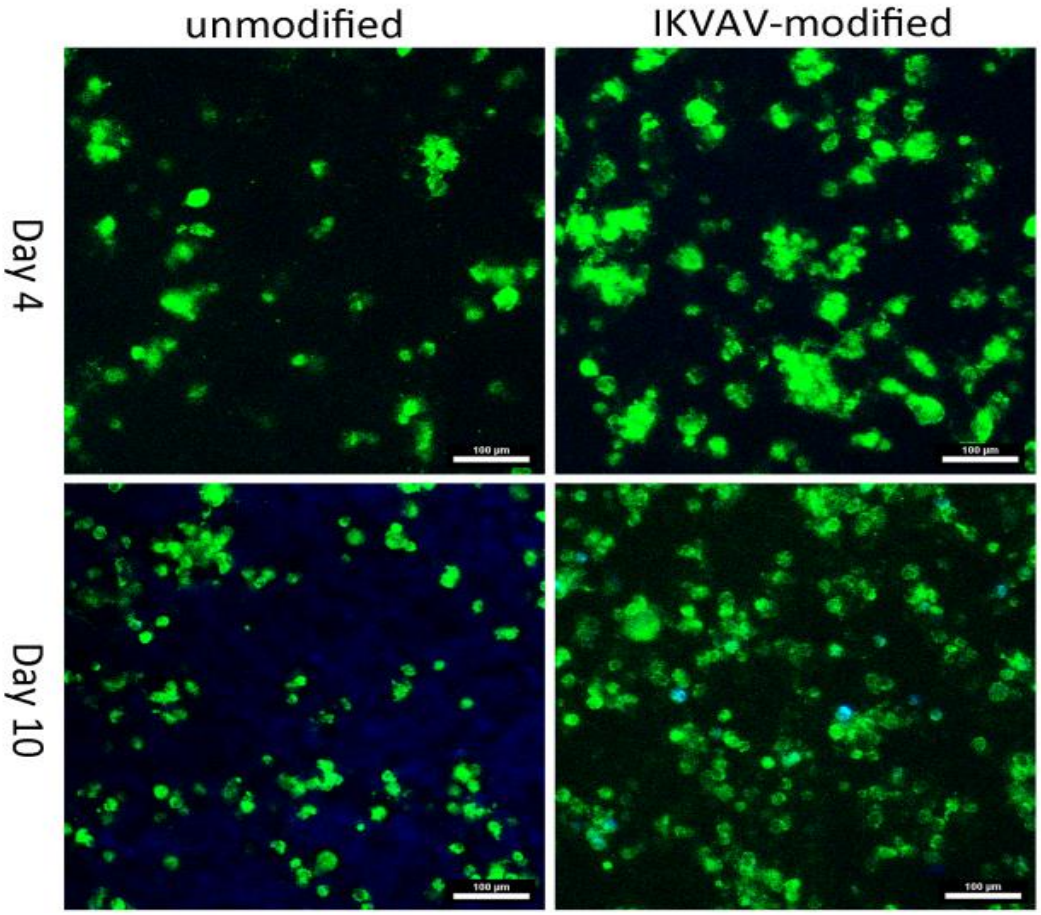

Fig 5.4 Immunofluorescence staining of mono-culture in unmodified and IKVAV-modified hydrogels at day 4 and day 10. The cells were stained by the endothelial cells marker CD31 (green), bar=100um.

5.3.3 FE-SEM of OEC mono-culture from donor 1 in silk fibroin hydrogels unmodified and IKVAV-modified.

At day 10, OEC mono-culture in silk fibroin hydrogels unmodified and IKVAV-modified was observed by FE-SEM (Fig 5.5). From the picture, some small round shape OECs can be found in the both hydrogels (Fig5.5 arrows). This morphology was consistent to the morphology we observed by confocal microscopy, indicating that these OEC showed a small round shape, however, without angiogenic elongation of cells.

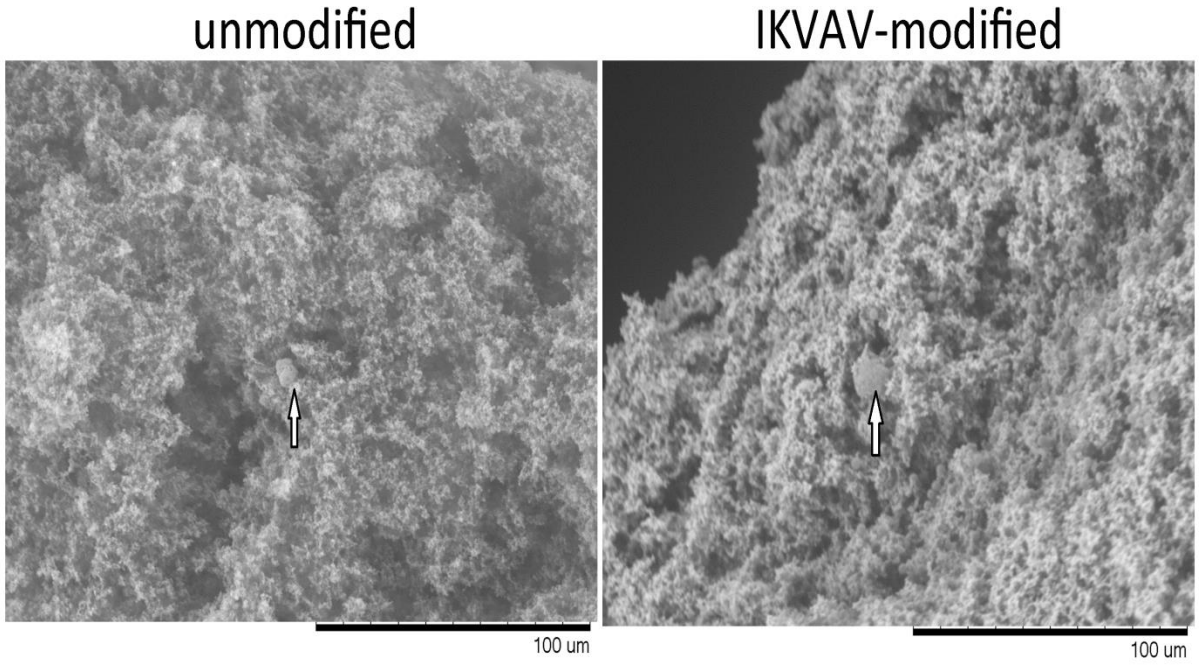

Fig 5.5 FE-SEM of OEC mono-culture in unmodified and IKVAV-modified hydrogels at day 10.

5.3.4 Immunofluorescence staining of co-cultures from three donors of OEC in silk fibroin hydrogels unmodified, IKVAV-modified and VVIAK-modified.

In the co-culture systems which were incubated in EGM-2 without VEGF stimulation, the OEC start to form elongated structures at day4 which indicated the angiogenesis in all three hydrogels

(Fig 5.6). In donor 1 and donor 2, there seemed to be more elongated CD31 positive cells compared to donor 3. In donor 3, more round CD31 positive cells were shown at day 4, which could be due to the different growth status of OEC from different donors. At day10, we observed the typically connected and tubular angiogenic structure for samples of donor 1 in all three hydrogels. However, compared to donor 1, the cells from donor 2 and donor 3 just formed some single located angiogenic structures in hydrogels which resulted from the different angiogenic activity of OEC from different donors.

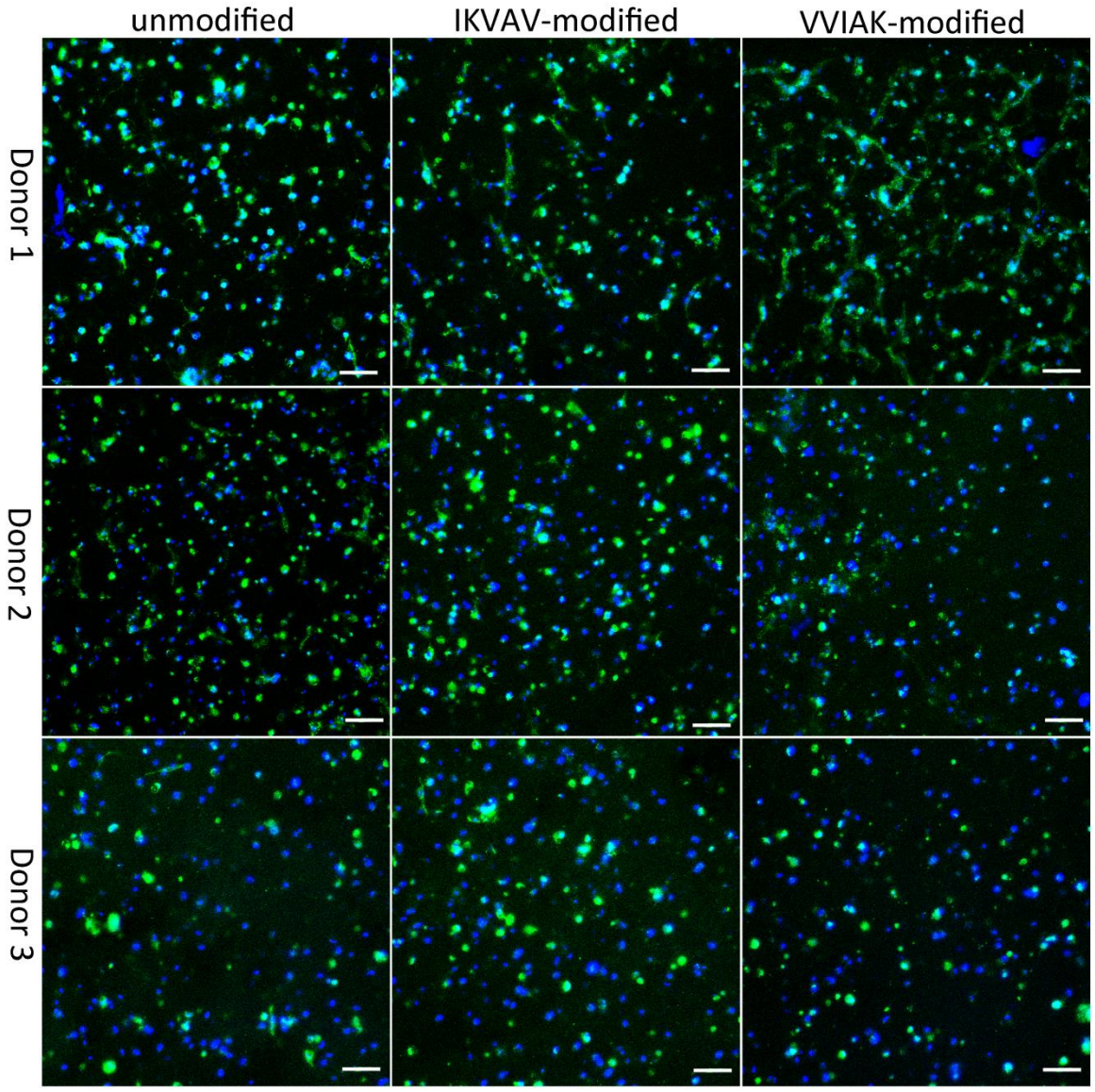
Day 4
unmodified
IKVAV-modified
VVIAK-modified
Donor 1
Donor 2
Donor 3

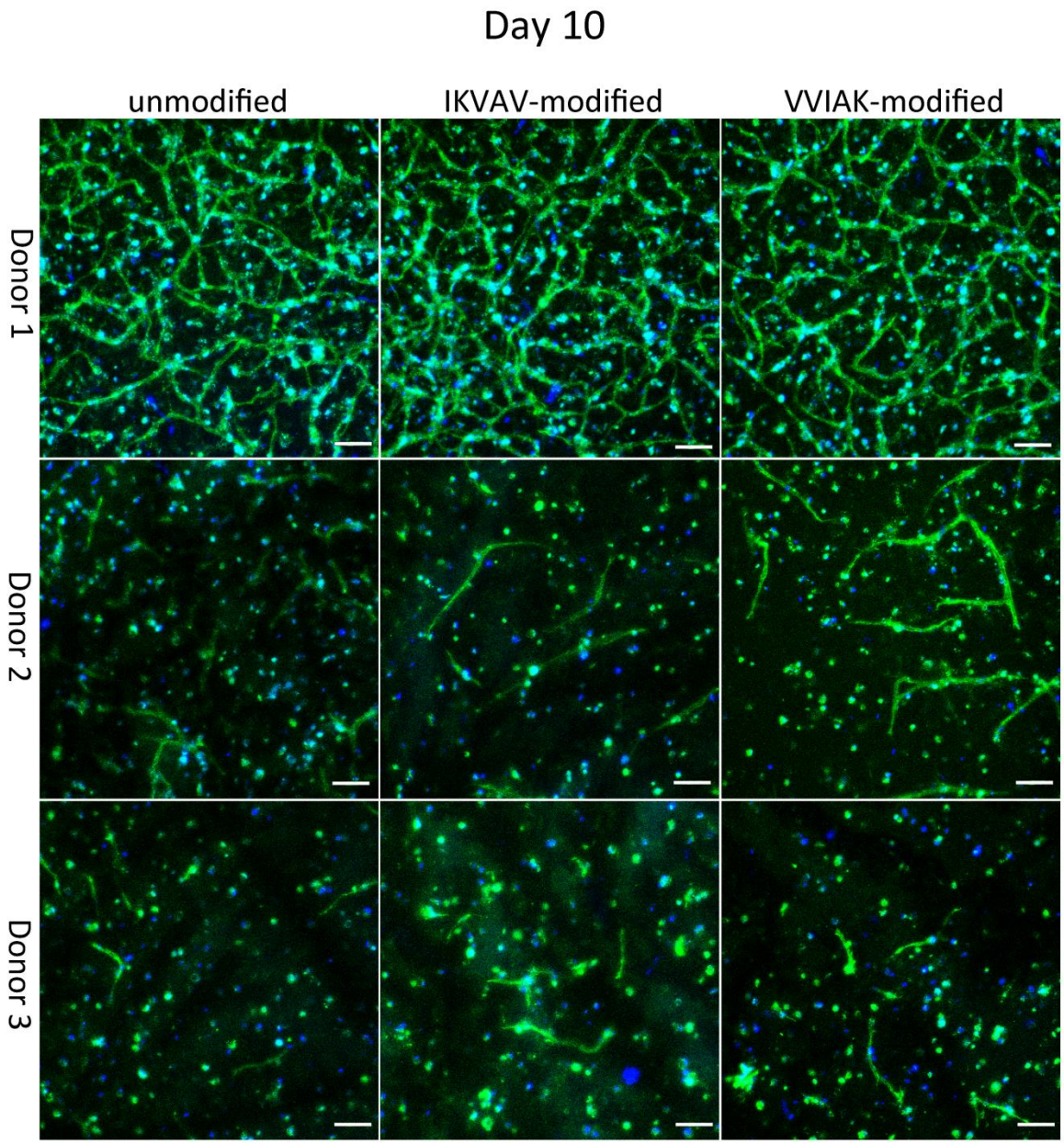

Fig5.6 Immunofluorescence staining of co-culture from three donors of OEC staining CD31 in unmodified, IKVAV-modified and VVIAK-modified silk fibroin hydrogels at Day 4 and Day 10. The cells were stained by the endothelial cells marker CD31 (green) and DAPI (blue) Bar=50um.

5.3.5 Cell proliferation.

DNA quantification was performed to detect the proliferation of OEC/MSC during 10 days (Fig 5.7). DNA contents were evaluated at day 0, day 4 and day 10. At day 0, there were no significant differences between the different hydrogels, which indicated the equal cell number

encapsulated in different hydrogels. Although there was a slight decrease of the DNA content at day 4 and slight increase of DNA content at day 10, there were no significant differences at different time points in the different group. This was probably due to a comparable cell growth , resulting in similar DNA content at different time points. Moreover, cells in three hydrogel also showed comparable DNA content at each time point which revealed that the cell proliferation speed was similar in each kind of hydrogel.

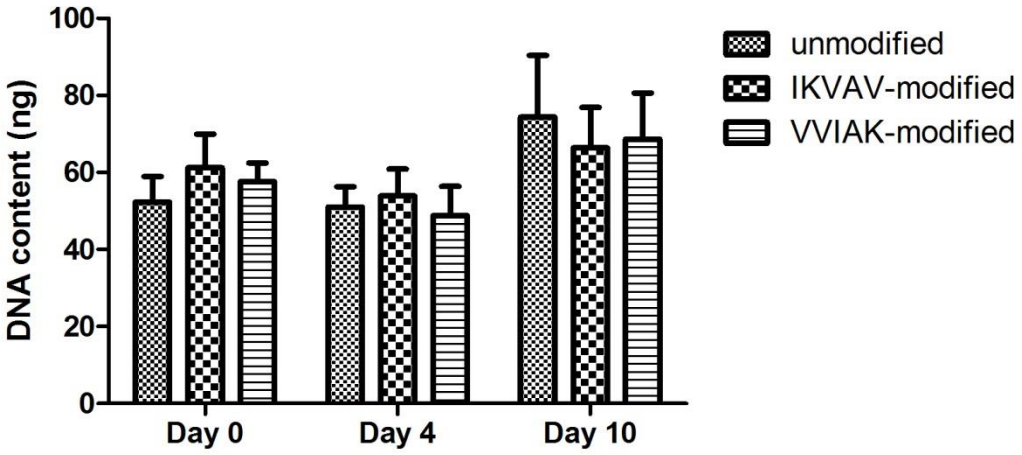

Fig 5.7 The OEC/MSC proliferation assessed by DNA quantification. Error bars represent Mean ± SEM (N=3 donors).

5.3.6 QRT-PCR of co-culture from three donors of OEC in unmodified, IKVAV-modified and VVIAK-modified silk fibroin hydrogel.

In order to compare the angiogenesis related gene expression in unmodified, IKVAV-modified and VVIAK-modified hydrogels, QRT-PCR was performed from three donors at day 10 (Fig 5.8). We analyzed the endothelial markers CD31 and vascular endothelial-cadherin (VE-cadherin), as well as the vascular stabilization involved marker smooth muscle actin (SM-actin). In addition we assessed Integrin α5 and MMP9 expressions which are associated with angiogenic activation of endothelial cells, as well as integrin β1 expression which is related to the EC homing, invasion and differentiation, and the collagen type IV expression which is related to the

basal membrane in functional blood vessels. There are no significant differences inCD31 and VE-cadherin expression which indicated comparable angiogenic structures in the different hydrogel angiogenesis from three donors. Moreover, the similar expression at integrin α5, MMP9 and Integrin β1 gene revealed that the angiogenic progress including EC adhesion, invasion and differentiation is comparable in different hydrogels (Fig 5.6). In addition, the collagen type IV expression resulted from the comparable production of this matrix protein in these different hydrogels.

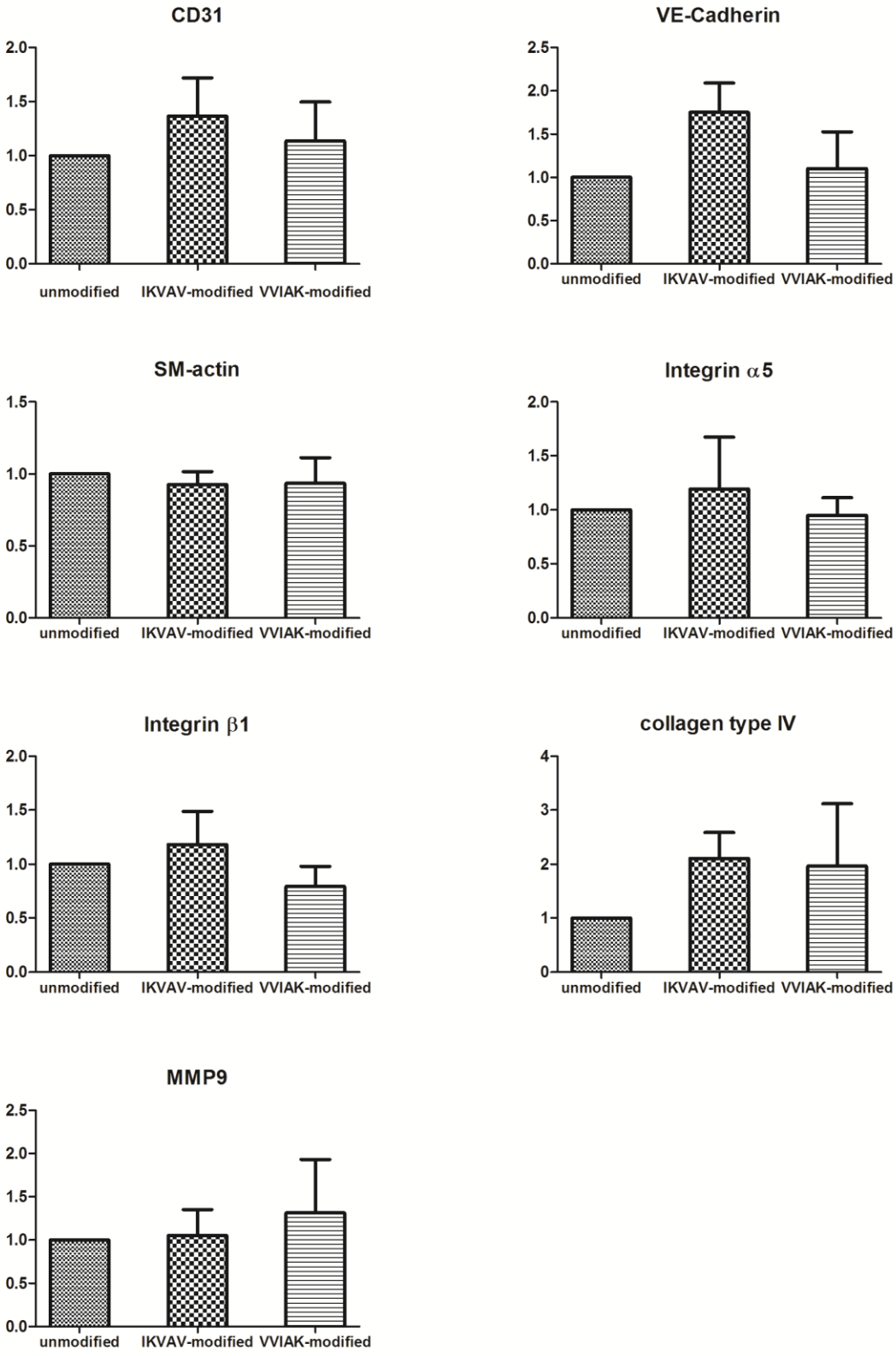

Fig5.8 QRT-PCR analysis of OEC/MSC co-culture from three donors of OEC. Error bars represent Mean ± SEM (N=3 donors)

5.*3.7FE-SEM morphologies of co-culture in silk fibroin hydrogels unmodified, IKVAV-modified and VVIAK modified at day 10.*

In order to assess the morphology of the OEC/MSC co-cultures inside the hydrogel scaffold, FE-SEM was performed (Fig 5.9). In the different hydrogel, obvious angiogenic structures were observed characterized by the smooth, tubular and elongating structures. The EC appear as very smooth cells adhered inside the hydrogel scaffold (Fig 5.9.g arrow 1) forming tubular and interconnected structures (Fig 5.9.g arrow 2). From the picture, very clear angiogenesis structures were observed (Fig 5.9.c). Smooth and flat endothelial cells with protruding cell nuclei were wrapped outside the tubular structure (Fig 5.9.c arrow). At the end of the tubular angiogenic structures, a series of branches were found which revealed the ongoing angiogenic progress (Fig 5.9.e arrow). Moreover, typically vascular lumen-like structure was shown in picture (Fig 5.9.i arrow), which indicated the maturation of the angiogenic structure. Although the MSCs are difficult to distinguish, some rough cells around the angiogenesis structure or beneath the EC are probably the MSC or differentiated MSC acting as mural cells.

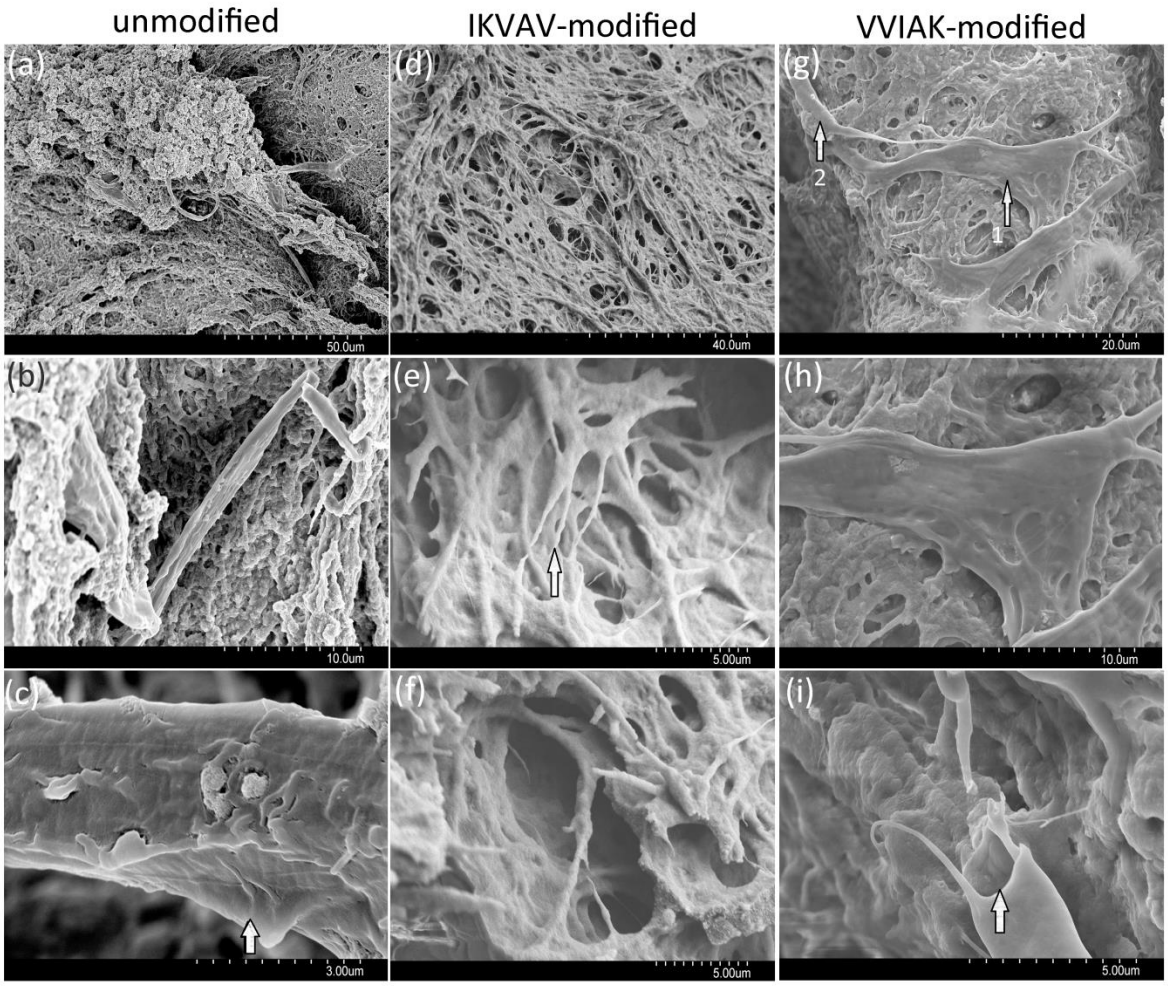

Fig5.9 FE-SEM morphologies of OEC/MSC co-culture in the three different hydrogels at day 10.

5.4 Discussion

According to the chapter 4, the sonication-induced silk fibroin conjugated with IKVAV peptide could be a candidate hydrogel for brain tissue engineering. In this part of the thesis, we evaluated the potential of unmodified, IKVAV-modified and VVIAK-modified silk fibroin hydrogels to support the formation of angiogenic structures. Compared to chapter 4, we set up the VVIAK-modified silk fibroin hydrogel as another control of scramble peptide, in order to confirm the function of IKVAV sequences.

The first experiment was performed in order to investigate if unmodified or IKVAV-modified hydrogels can induce the angiogenesis of encapsulated OEC. However, even after the addition of VEGF (50ng/ml) into the EGM-2 medium, the OEC still kept the round shape inside the hydrogel without elongated structures. In the FE-SEM pictures of hydrogel scaffolds, hydrogels showed a small pore size in freeze-drying samples and very condense structures after critical point drying. Therefore the OEC behavior could result from the condense structure of the hydrogel that inhibits the cells' moving and elongation when encapsulated inside the hydrogel. If the cells can not move and elongate, this could cause the cell apoptosis and death. However, another possibility could be that the silk fibroin unmodified and IKVAV-modified could not support the OEC adhesion and migration which may require other factor derived from natural ECM.

Interestingly, in the co-culture system, the OEC could move and elongate to form angiogenic structures after 4 days. Then after 10 days they form capillary connected tubular vascular structures in all three different hydrogels. In the angiogenic process, the VEGF plays an important role in endothelial cells survival, proliferation and migration. However, the ECM is another important regulator of angiogenesis. In the silk fibroin hydrogels, the condense structure or the surface topography possibly impedes the elongation and movement of the OEC, which blocks the angiogenesis. However, the addition of BM-MSC seems to reverse this effect, resulting in angiogenesis and the formation of capillary network formation. In the co-culture system, BM-MSCs secret many angiogenic factors such as (VEGF and Ang-1) (*216, 217*). Upon contact with endothelial cells, BM-MSC could also differentiate into pericytes and smooth muscle cells that help to stabilize the nascent vessels. Furthermore, MSC produce various ECM components, such as collagen type I, collagen type IV, fibronectin and laminin (*218*). All of

these factors contribute to the angiogenic activation of endothelial cells and to the maturation of vascular structures. In the co-culture system, no significant differences in the angiogenesis potential among unmodified, IKVAV-modified and VVIAK-modified hydrogels were observed. Nevertheless potential proangiogenic effects of the IKVAV peptide might be covered by the strong impact of the MSC in the co-culture system. Many diverse matrix (such as collagen type I, collagen type IV, fibronectin and laminin) and growth factors (such as VEGF, Ang-1) produced by MSC may deposit in the hydrogels that obviously increasing the angiogenesis of OEC, while the peptide function and contribution may be much weaker than the factors produced by MSC. In order to demonstrate the function of IKVAV peptide in the future, another kind of model should be set up based on a mono-culture system where angiogenesis in OEC could be induced by growth factors such as VEGF.

Consequently, the unmodified and modified silk fibroin hydrogels both support the angiogenesis but also need the assistance in the angiogenic process by MSC. Silk fibroin hydrogels thus provide a promising model of an injectable soft hydrogel system for vascularization applications in the field of brain ischemia, wound healing, soft tissue regeneration, cardiovascular regeneration and so on.

5.5 Conclusion

In this study, we prepared sonication-induced unmodified, IKVAV-modified and VVIAK-modified silk fibroin hydrogels. The OEC mono-culture in unmodified and IKVAV-modified failed to form angiogenic structures even after the supplementation with VEGF, which might be due to the dense structure of the hydrogels. However, in the co-culture system, all three different hydrogels could support angiogenesis even although the angiogenic ability of individual donors

was slightly different. However, the quantity of angiogenic structures and morphologies were similar in the individual donors in three different hydrogels. This was further supported by the semiQRT-PCR. All these hydrogels could support the formation of angiogenesis structure which resulted in pre-vascularization in the hydrogel but need the assistance of co-implanted MSCs or other cells which might penetrate into the wound healing area after the implantation.

Acknowledgements

We would like to thank Prof. Gorb and Joachim Oesert from the Zoology Department in Kiel University for the excellent help in FE-SEM. We would like to thank Prof. Andreas Tholey for the designing of VVIAK peptide and also thank Katrin Lange and Gabriele Nessenius for the technician support.

6 Directions for future work

Brain tissue engineering is still facing a series of scientific challenges although researchers have already achieved great success in this field. In this thesis, we performed studies focusing on the design and evaluation of silk fibroin based hydrogels for the encapsulation of hNSC for brain tissue regeneration. In addition, we assessed the encapsulation of OEC/MSC in different variants of silk fibroin hydrogels to induce neovascularization after ischemic brain injury.

By using 3D silk fibroin hydrogels formed after sonication, we found that the conjugation of the IKVAV peptide could increase the cell viability and neuronal differentiation. These data indicated that the silk fibroin conjugated with IKVAV peptide could be applied as a candidate material for brain tissue engineering. However, although the viability and neuronal differentiation of human neural stem cells were improved by the silk fibroin hydrogel modified with IKVAV peptide, they are still far away from the needs for a successful implantation because of the relatively low viability and ratio of neuronal differentiation. In order to improve the hNSC viability and neuronal differentiation, other ECM components should be considered to be added to the system mimicking the ECM composition in the brain. Besides, some growth factors (such as neurotrophins) are necessary to be loaded in the hydrogel, which could improve the survival, growth and function of neurons.

Although OEC in mono-culture did not form angiogenic structures in silk fibroin hydrogels, they can form angiogenic structures with the assistance of MSC. However, potential effects by IKVAV peptide conjugation were probably covered by the strong angiogenic effects of MSC. In order to further demonstrate the IKVAV peptide function in angiogenesis, another hydrogel

model should be set up in which the OEC are able to form angiogenesis structure in mono-culture under growth factor stimulation, such as VEGF.

In brain tissue engineering, the sonication induced silk fibroin hydrogel encapsulated with OEC and MSC could be potentially applied in treating brain injury caused by ischemia. Moreover, these soft silk fibroin hydrogel encapsulated with OEC/MSC are also promising in other applications for tissues regeneration where neovascularization is an essential element. This could include dermal wound healing, myocardial ischemia or soft tissue regeneration. Although MSCs are able to differentiate into chondroblasts, adipocytes, neurons, glia, cardiomyocytes, or osteoblasts, the potential of MSC usage in cell therapy of bone defects is widely discussed at present. It has been demonstrated that application of MSC increased angiogenesis and osteogenesis in the damaged bone (*219*). However, for brain tissue engineering, BM-MSCs are not well characterized as a cell source to differentiate into neural cells or to support neural regeneration. To solve the problem of neural cell loss and ischemia in the brain injury, some interesting strategies could be investigated in the future, such as the co-culture of NSCs with OECs or even triple culture by adding MSC in hydrogel, aiming at restoring the functional brain tissue.

7 Acknowledgments

I am grateful to the three years' funding from Bridging the Gap Erasmus Mundus project. I really appreciate that Prof. Claudio Migliaresi accepted me as a PhD student and give me this opportunity to study in Biotech and Biomolecular Science PhD School at the University of Trento. I also would like to thank Prof. Alessandro Quattrone and Prof. Antonella Motta as my tutor and advisor in my three years work. I would like to thank Prof. Claudio Migliaresi, Prof. Alessandro Quattrone and Prof. Antonella Motta all for designing the whole project for my PhD study. I am deeply grateful to Prof. Antonella Motta for her constant encouragement and great guidance in the detailed work as my advisor. I am also greatly indebted to Prof. Simona Casarosa and Prof. Sabine Fuchs who kindly supervised me and greatly helped me in the collaboration work. I would like to thank Prof. Paolo Macchi for the kind help in my experiments and study in the Biomolecular Science PhD school. I also would like thank for the help of Prof Andreas Tholey and Prof. Stanislav N. Gorb and Joachim Oesert during my study in university of Kiel. I also want to thank Betty Balduin for her great help during my study in the Biomolecular Science PhD school.

I also would like to thank the colleagues who I worked with and who help me a lot in the three years. Thanks to Tania Incitti and Cristina Foss help me design experiment and analyze the data. Thanks to Devid Maniglio, Cristian Lorendi, Luca Gasperini, Walter Bonani, Matteo Stoppato, Lorenzo Moschini, Eleonora Carletti, and Mariangela Fedel offered greatly kind help in the experiments.

I also would like to thank colleagues in Experimental Trauma Surgery of Kiel University. Thanks to Yang Shi and Jana Schlenk for their help in the experiment. Thanks to the technicians Katrin Lange and Gabriele Nessenius for culturing cells and help in experiments.

8 References

1. Ikada, Y. (2006) Challenges in tissue engineering, *Journal of The Royal Society Interface 3*, 589-601.
2. Williams, D. F. (2006) To engineer is to create: the link between engineering and regeneration, *Trends in Biotechnology 24*, 4-8.
3. Langer, R., and Vacanti, J. (1993) Tissue engineering, *Science 260*, 920-926.
4. Ko, I. K., Lee, S. J., Atala, A., and Yoo, J. J. (2013) In situ tissue regeneration through host stem cell recruitment, *Exp Mol Med 45*, e57.
5. Erggelet, C., Endres, M., Neumann, K., Morawietz, L., Ringe, J., Haberstroh, K., Sittinger, M., and Kaps, C. (2009) Formation of cartilage repair tissue in articular cartilage defects pretreated with microfracture and covered with cell-free polymer-based implants, *Journal of Orthopaedic Research 27*, 1353-1360.
6. Service, R. F. (2000) Tissue Engineers Build New Bone, *Science 289*, 1498-1500.
7. Ma, P. X., and Langer, R. (1999) Morphology and mechanical function of long-term in vitro engineered cartilage, *Journal of Biomedical Materials Research 44*, 217-221.
8. Davis, M. W., and Vacanti, J. P. (1996) Toward development of an implantable tissue engineered liver, *Biomaterials 17*, 365-372.
9. Richardson, T. P., Peters, M. C., Ennett, A. B., and Mooney, D. J. (2001) Polymeric system for dual growth factor delivery, *Nat Biotech 19*, 1029-1034.
10. Schense, J. C., Bloch, J., Aebischer, P., and Hubbell, J. A. (2000) Enzymatic incorporation of bioactive peptides into fibrin matrices enhances neurite extension, *Nat Biotech 18*, 415-419.
11. Howard, D., Buttery, L. D., Shakesheff, K. M., and Roberts, S. J. (2008) Tissue engineering: strategies, stem cells and scaffolds, *Journal of Anatomy 213*, 66-72.
12. Chan, B. P., and Leong, K. W. (2008) Scaffolding in tissue engineering: general approaches and tissue-specific considerations, *Eur Spine J 17*, 467-479.
13. Owen, S. C., and Shoichet, M. S. (2010) Design of three-dimensional biomimetic scaffolds, *Journal of Biomedical Materials Research Part A 94A*, 1321-1331.
14. O'Brien, F. J. (2011) Biomaterials & scaffolds for tissue engineering, *Materials Today 14*, 88-95.
15. Discher, D. E., Janmey, P., and Wang, Y.-l. (2005) Tissue Cells Feel and Respond to the Stiffness of Their Substrate, *Science 310*, 1139-1143.
16. Engler, A. J., Sen, S., Sweeney, H. L., and Discher, D. E. (2006) Matrix Elasticity Directs Stem Cell Lineage Specification, *Cell 126*, 677-689.
17. Brahatheeswaran Dhandayuthapani, Y. Y., Toru Maekawa, and D. Sakthi Kumar. (2011) Polymeric Scaffolds in Tissue Engineering Application: A Review, *International Journal of Polymer Science 2011*.
18. Ramakrishna, S., Mayer, J., Wintermantel, E., and Leong, K. W. (2001) Biomedical applications of polymer-composite materials: a review, *Composites Science and Technology 61*, 1189-1224.
19. Yang, F., Murugan, R., Wang, S., and Ramakrishna, S. (2005) Electrospinning of nano/micro scale poly(l-lactic acid) aligned fibers and their potential in neural tissue engineering, *Biomaterials 26*, 2603-2610.
20. Li, W.-J., Danielson, K. G., Alexander, P. G., and Tuan, R. S. (2003) Biological response of chondrocytes cultured in three-dimensional nanofibrous poly(ϵ-caprolactone) scaffolds, *Journal of Biomedical Materials Research Part A 67A*, 1105-1114.

21. Uematsu, K., Hattori, K., Ishimoto, Y., Yamauchi, J., Habata, T., Takakura, Y., Ohgushi, H., Fukuchi, T., and Sato, M. (2005) Cartilage regeneration using mesenchymal stem cells and a three-dimensional poly-lactic-glycolic acid (PLGA) scaffold, *Biomaterials 26*, 4273-4279.
22. Kenawy, E.-R., Bowlin, G. L., Mansfield, K., Layman, J., Simpson, D. G., Sanders, E. H., and Wnek, G. E. (2002) Release of tetracycline hydrochloride from electrospun poly(ethylene-co-vinylacetate), poly(lactic acid), and a blend, *Journal of Controlled Release 81*, 57-64.
23. Malafaya, P. B., Silva, G. A., and Reis, R. L. (2007) Natural–origin polymers as carriers and scaffolds for biomolecules and cell delivery in tissue engineering applications, *Advanced Drug Delivery Reviews 59*, 207-233.
24. Chevallay, B., and Herbage, D. (2000) Collagen-based biomaterials as 3D scaffold for cell cultures: applications for tissue engineering and gene therapy, *Med. Biol. Eng. Comput. 38*, 211-218.
25. Yang, C., Hillas, P., Báez, J., Nokelainen, M., Balan, J., Tang, J., Spiro, R., and Polarek, J. (2004) The Application of Recombinant Human Collagen in Tissue Engineering, *BioDrugs 18*, 103-119.
26. Tabata, Y., and Ikada, Y. (1998) Protein release from gelatin matrices, *Advanced Drug Delivery Reviews 31*, 287-301.
27. Young, S., Wong, M., Tabata, Y., and Mikos, A. G. (2005) Gelatin as a delivery vehicle for the controlled release of bioactive molecules, *Journal of Controlled Release 109*, 256-274.
28. Nishinari, K., and Takahashi, R. (2003) Interaction in polysaccharide solutions and gels, *Current Opinion in Colloid & Interface Science 8*, 396-400.
29. Cascone, M. G., Barbani, N., P.Giusti, C. C., Ciardelli, G., and Lazzeri, L. (2001) Bioartificial polymeric materials based on polysaccharides, *Journal of Biomaterials Science, Polymer Edition 12*, 267-281.
30. Venugopal, J., and Ramakrishna, S. (2005) Applications of polymer nanofibers in biomedicine and biotechnology, *Appl Biochem Biotechnol 125*, 147-157.
31. Yu, L., Dean, K., and Li, L. (2006) Polymer blends and composites from renewable resources, *Progress in Polymer Science 31*, 576-602.
32. Lutolf, M. P., Gilbert, P. M., and Blau, H. M. (2009) Designing materials to direct stem-cell fate, *Nature 462*, 433-441.
33. Koh, C. J., and Atala, A. (2004) Tissue Engineering, Stem Cells, and Cloning: Opportunities for Regenerative Medicine, *Journal of the American Society of Nephrology 15*, 1113-1125.
34. Thomson, J. A., Itskovitz-Eldor, J., Shapiro, S. S., Waknitz, M. A., Swiergiel, J. J., Marshall, V. S., and Jones, J. M. (1998) Embryonic Stem Cell Lines Derived from Human Blastocysts, *Science 282*, 1145-1147.
35. Korin, N., and Levenberg, S. (2007) Engineering human embryonic stem cell differentiation, *Biotechnology & genetic engineering reviews 24*, 243-261.
36. Tatyana A.Prokhorova, L. M. H., UlrikFrandsen, NicholasDitzel, Henrik D.Schrøder, Jorge S.Burns, and MoustaphaKassem. . (2009) Teratoma Formation by Human Embryonic Stem Cells Is Site Dependent and Enhanced by the Presence of Matrigel, *Stem Cells and Development. 18*, 47-54.
37. Shieh, S.-J., and Vacanti, J. P. (2005) State-of-the-art tissue engineering: From tissue engineering to organ building, *Surgery 137*, 1-7.
38. Pittenger, M. F., Mackay, A. M., Beck, S. C., Jaiswal, R. K., Douglas, R., Mosca, J. D., Moorman, M. A., Simonetti, D. W., Craig, S., and Marshak, D. R. (1999) Multilineage Potential of Adult Human Mesenchymal Stem Cells, *Science 284*, 143-147.
39. Romanov, Y. A., Svintsitskaya, V. A., and Smirnov, V. N. (2003) Searching for Alternative Sources of Postnatal Human Mesenchymal Stem Cells: Candidate MSC-Like Cells from Umbilical Cord, *STEM CELLS 21*, 105-110.
40. Cross, M., and Dexter, T. M. (1991) Growth factors in development, transformation, and tumorigenesis, *Cell 64*, 271-280.

41. Lee, K., Silva, E. A., and Mooney, D. J. (2011) Growth factor delivery-based tissue engineering: general approaches and a review of recent developments, *Journal of The Royal Society Interface 8*, 153-170.
42. Cohen, G. B., Ren, R., and Baltimore, D. Modular binding domains in signal transduction proteins, *Cell 80*, 237-248.
43. Risau, W. (1997) Mechanisms of angiogenesis, *Nature 386*, 671-674.
44. Simmons, C. A., Alsberg, E., Hsiong, S., Kim, W. J., and Mooney, D. J. (2004) Dual growth factor delivery and controlled scaffold degradation enhance in vivo bone formation by transplanted bone marrow stromal cells, *Bone 35*, 562-569.
45. Patel, Z. S., Young, S., Tabata, Y., Jansen, J. A., Wong, M. E. K., and Mikos, A. G. (2008) Dual delivery of an angiogenic and an osteogenic growth factor for bone regeneration in a critical size defect model, *Bone 43*, 931-940.
46. Li, X., Katsanevakis, E., Liu, X., Zhang, N., and Wen, X. (2012) Engineering neural stem cell fates with hydrogel design for central nervous system regeneration, *Progress in Polymer Science 37*, 1105-1129.
47. Stein, D. G., and Wright, D. W. (2010) Progesterone in the clinical treatment of acute traumatic brain injury, *Expert Opinion on Investigational Drugs 19*, 847-857.
48. Ai, J., Kiasat-Dolatabadi, A., Ebrahimi-Barough, S., Ai, A., Lotfibakhshaiesh, N., Norouzi-Javidan, A., Saberi, H., Arjmand, B., and Aghayan, H. R. (2013) Polymeric Scaffolds in Neural Tissue Engineering: A Review, *Arch Neurosci 1*, 15-20.
49. Cullen, D. K., Stabenfeldt, S. E., Simon, C. M., Tate, C. C., and LaPlaca, M. C. (2007) In vitro neural injury model for optimization of tissue-engineered constructs, *Journal of Neuroscience Research 85*, 3642-3651.
50. Cui, F. Z., Tian, W. M., Hou, S. P., Xu, Q. Y., and Lee, I. S. (2006) Hyaluronic acid hydrogel immobilized with RGD peptides for brain tissue engineering, *J Mater Sci: Mater Med 17*, 1393-1401.
51. Temple, S. (2001) The development of neural stem cells, *Nature 414*, 112-117.
52. Gage, F. H. (2000) Mammalian Neural Stem Cells, *Science 287*, 1433-1438.
53. Pagano, S. F., Impagnatiello, F., Girelli, M., Cova, L., Grioni, E., Onofri, M., Cavallaro, M., Etteri, S., Vitello, F., Giombini, S., Solero, C. L., and Parati, E. A. (2000) Isolation and Characterization of Neural Stem Cells from the Adult Human Olfactory Bulb, *STEM CELLS 18*, 295-300.
54. Miller, F. D., and Gauthier-Fisher, A. (2009) Home at Last: Neural Stem Cell Niches Defined, *Cell Stem Cell 4*, 507-510.
55. Chen, S., Lewallen, M., and Xie, T. (2013) Adhesion in the stem cell niche: biological roles and regulation, *Development 140*, 255-265.
56. Ruoslahti, E. (1996) Brain extracellular matrix, *Glycobiology 6*, 489-492.
57. Guo, J., Leung, K. K. G., Su, H., Yuan, Q., Wang, L., Chu, T.-H., Zhang, W., Pu, J. K. S., Ng, G. K. P., Wong, W. M., Dai, X., and Wu, W. (2009) Self-assembling peptide nanofiber scaffold promotes the reconstruction of acutely injured brain, *Nanomedicine : nanotechnology, biology, and medicine 5*, 345-351.
58. Cheng, T.-Y., Chen, M.-H., Chang, W.-H., Huang, M.-Y., and Wang, T.-W. (2013) Neural stem cells encapsulated in a functionalized self-assembling peptide hydrogel for brain tissue engineering, *Biomaterials 34*, 2005-2016.
59. Lin, H. J., O'Shaughnessy, T. J., Kelly, J., and Ma, W. (2004) Neural stem cell differentiation in a cell–collagen–bioreactor culture system, *Developmental Brain Research 153*, 163-173.
60. Hou, S., Tian, W., Xu, Q., Cui, F., Zhang, J., Lu, Q., and Zhao, C. (2006) The enhancement of cell adherence and inducement of neurite outgrowth of dorsal root ganglia co-cultured with

hyaluronic acid hydrogels modified with Nogo-66 receptor antagonist in vitro, *Neuroscience 137*, 519-529.

61. Banerjee, A., Arha, M., Choudhary, S., Ashton, R. S., Bhatia, S. R., Schaffer, D. V., and Kane, R. S. (2009) The influence of hydrogel modulus on the proliferation and differentiation of encapsulated neural stem cells, *Biomaterials 30*, 4695-4699.
62. Leipzig, N. D., and Shoichet, M. S. (2009) The effect of substrate stiffness on adult neural stem cell behavior, *Biomaterials 30*, 6867-6878.
63. Hynes, S. R., Rauch, M. F., Bertram, J. P., and Lavik, E. B. (2009) A library of tunable poly(ethylene glycol)/poly(L-lysine) hydrogels to investigate the material cues that influence neural stem cell differentiation, *Journal of Biomedical Materials Research Part A 89A*, 499-509.
64. Slaughter, B. V., Khurshid, S. S., Fisher, O. Z., Khademhosseini, A., and Peppas, N. A. (2009) Hydrogels in Regenerative Medicine, *Advanced Materials 21*, 3307-3329.
65. Namba, R. M., Cole, A. A., Bjugstad, K. B., and Mahoney, M. J. (2009) Development of porous PEG hydrogels that enable efficient, uniform cell-seeding and permit early neural process extension, *Acta Biomaterialia 5*, 1884-1897.
66. Engler, A. J., Sen, S., Sweeney, H. L., and Discher, D. E. Matrix Elasticity Directs Stem Cell Lineage Specification, *Cell 126*, 677-689.
67. Li, H., Wijekoon, A., and Leipzig, N. D. (2012) 3D Differentiation of Neural Stem Cells in Macroporous Photopolymerizable Hydrogel Scaffolds, *PLoS ONE 7*, e48824.
68. Baron-Van Evercooren, A., Kleinman, H. K., Ohno, S., Marangos, P., Schwartz, J. P., and Dubois-Dalcq, M. E. (1982) Nerve growth factor, laminin, and fibronectin promote neurite growth in human fetal sensory ganglia cultures, *Journal of Neuroscience Research 8*, 179-193.
69. Tashiro, K.-I., Sephel, G. C., Greatorex, D., Sasaki, M., Shirashi, N., Martin, G. R., Kleinman, H. K., and Yamada, Y. (1991) The RGD containing site of the mouse laminin A chain is active for cell attachment, spreading, migration and neurite outgrowth, *Journal of Cellular Physiology 146*, 451-459.
70. Koh, H. S., Yong, T., Chan, C. K., and Ramakrishna, S. (2008) Enhancement of neurite outgrowth using nano-structured scaffolds coupled with laminin, *Biomaterials 29*, 3574-3582.
71. Hersel, U., Dahmen, C., and Kessler, H. (2003) RGD modified polymers: biomaterials for stimulated cell adhesion and beyond, *Biomaterials 24*, 4385-4415.
72. Tashiro, K., Monji, A., Yoshida, I., Hayashi, Y., Matsuda, K., Tashiro, N., and Mitsuyama, Y. (1999) An IKLLI-containing peptide derived from the laminin alpha1 chain mediating heparin-binding, cell adhesion, neurite outgrowth and proliferation, represents a binding site for integrin alpha3beta1 and heparan sulphate proteoglycan, *Biochem. J. 340*, 119-126.
73. Gunn, J. W., Turner, S. D., and Mann, B. K. (2005) Adhesive and mechanical properties of hydrogels influence neurite extension, *Journal of Biomedical Materials Research Part A 72A*, 91-97.
74. Pettikiriarachchi, J. T. S., Parish, C. L., Shoichet, M. S., Forsythe, J. S., and Nisbet, D. R. (2010) Biomaterials for Brain Tissue Engineering, *Australian Journal of Chemistry 63*, 1143-1154.
75. Ohab, J. J., Fleming, S., Blesch, A., and Carmichael, S. T. (2006) A Neurovascular Niche for Neurogenesis after Stroke, *The Journal of Neuroscience 26*, 13007-13016.
76. Carmichael, S. T., Ohab, J., and Nguyen, J. (0000) Post-stroke neurogenesis and the neurovascular niche: Newly born neuroblasts localize to peri-infarct cortex in close association with the vascular endothelium, *J Cereb Blood Flow Metab 25*, S214-S214.
77. Fuchs, S., Dohle, E., Kolbe, M., and Kirkpatrick, C. (2010) Outgrowth Endothelial Cells: Sources, Characteristics and Potential Applications in Tissue Engineering and Regenerative Medicine, In *Bioreactor Systems for Tissue Engineering II* (Kasper, C., Griensven, M., and Pörtner, R., Eds.), pp 201-217, Springer Berlin Heidelberg.

78. Asahara, T., Murohara, T., Sullivan, A., Silver, M., van der Zee, R., Li, T., Witzenbichler, B., Schatteman, G., and Isner, J. M. (1997) Isolation of Putative Progenitor Endothelial Cells for Angiogenesis, *Science 275*, 964-966.
79. Salven, P., Mustjoki, S., Alitalo, R., Alitalo, K., and Rafii, S. (2003) VEGFR-3 and CD133 identify a population of CD34+ lymphatic/vascular endothelial precursor cells, *Blood 101*, 168-172.
80. Shi, Q., Rafii, S., Wu, M. H.-D., Wijelath, E. S., Yu, C., Ishida, A., Fujita, Y., Kothari, S., Mohle, R., Sauvage, L. R., Moore, M. A. S., Storb, R. F., and Hammond, W. P. (1998) Evidence for Circulating Bone Marrow-Derived Endothelial Cells, *Blood 92*, 362-367.
81. Kalka, C., Masuda, H., Takahashi, T., Kalka-Moll, W. M., Silver, M., Kearney, M., Li, T., Isner, J. M., and Asahara, T. (2000) Transplantation of ex vivo expanded endothelial progenitor cells for therapeutic neovascularization, *Proceedings of the National Academy of Sciences 97*, 3422-3427.
82. Fan, Y., and Yang, G.-Y. (2007) Therapeutic Angiogenesis for Brain Ischemia: A Brief Review, *Jrnl Neuroimmune Pharm 2*, 284-289.
83. Hur, J., Yoon, C.-H., Kim, H.-S., Choi, J.-H., Kang, H.-J., Hwang, K.-K., Oh, B.-H., Lee, M.-M., and Park, Y.-B. (2004) Characterization of Two Types of Endothelial Progenitor Cells and Their Different Contributions to Neovasculogenesis, *Arteriosclerosis, Thrombosis, and Vascular Biology 24*, 288-293.
84. del Zoppo, G. J., and Mabuchi, T. (2003) Cerebral Microvessel Responses to Focal Ischemia, *J Cereb Blood Flow Metab 23*, 879-894.
85. Fukuda, S., Fini, C. A., Mabuchi, T., Koziol, J. A., Eggleston, L. L., and del Zoppo, G. J. (2004) Focal Cerebral Ischemia Induces Active Proteases That Degrade Microvascular Matrix, *Stroke 35*, 998-1004.
86. Shen, F., Su, H., Fan, Y., Chen, Y., Zhu, Y., Liu, W., Young, W. L., and Yang, G.-Y. (2006) Adeno-Associated Viral Vector-Mediated Hypoxia-Inducible Vascular Endothelial Growth Factor Gene Expression Attenuates Ischemic Brain Injury After Focal Cerebral Ischemia in Mice, *Stroke 37*, 2601-2606.
87. Hayashi, T., Noshita, N., Sugawara, T., and Chan, P. H. (2003) Temporal Profile of Angiogenesis and Expression of Related Genes in the Brain After Ischemia, *J Cereb Blood Flow Metab 23*, 166-180.
88. Fadini, G. P., Agostini, C., and Avogaro, A. (2005) Endothelial Progenitor Cells in Cerebrovascular Disease, *Stroke 36*, 1112-1113.
89. Ohta, T., Kikuta, K.-i., Imamura, H., Takagi, Y., Nishimura, M., Arakawa, Y., Hashimoto, N., and Nozaki, K. (2006) Administration of Ex Vivo-expanded Bone Marrow-derived Endothelial Progenitor Cells Attenuates Focal Cerebral Ischemia-reperfusion Injury in Rats, *Neurosurgery 59*, 679-686 610.1227/1201.NEU.0000229058.0000208706.0000229088.
90. Taguchi, A., Soma, T., Tanaka, H., Kanda, T., Nishimura, H., Yoshikawa, H., Tsukamoto, Y., Iso, H., Fujimori, Y., Stern, D. M., Naritomi, H., and Matsuyama, T. (2004) Administration of CD34+ cells after stroke enhances neurogenesis via angiogenesisin a mouse model, *The Journal of Clinical Investigation 114*, 330-338.
91. Altman, G. H., Diaz, F., Jakuba, C., Calabro, T., Horan, R. L., Chen, J., Lu, H., Richmond, J., and Kaplan, D. L. (2003) Silk-based biomaterials, *Biomaterials 24*, 401-416.
92. Rossitch, E., Jr., Bullard, D., and Oakes, W. J. (1987) Delayed foreign-body reaction to silk sutures in pediatric neurosurgical patients, *Child's Nerv Syst 3*, 375-378.
93. Yin, J., Chen, E., Porter, D., and Shao, Z. (2010) Enhancing the Toughness of Regenerated Silk Fibroin Film through Uniaxial Extension, *Biomacromolecules 11*, 2890-2895.
94. Fuchs, S., Motta, A., Migliaresi, C., and Kirkpatrick, C. J. (2006) Outgrowth endothelial cells isolated and expanded from human peripheral blood progenitor cells as a potential source of autologous cells for endothelialization of silk fibroin biomaterials, *Biomaterials 27*, 5399-5408.

95. Hu, K., Lv, Q., Cui, F. Z., Feng, Q. L., Kong, X. D., Wang, H. L., Huang, L. Y., and Li, T. (2006) Biocompatible Fibroin Blended Films with Recombinant Human-like Collagen for Hepatic Tissue Engineering, *Journal of Bioactive and Compatible Polymers 21*, 23-37.
96. Horan, R. L., Antle, K., Collette, A. L., Wang, Y., Huang, J., Moreau, J. E., Volloch, V., Kaplan, D. L., and Altman, G. H. (2005) In vitro degradation of silk fibroin, *Biomaterials 26*, 3385-3393.
97. Vepari, C., and Kaplan, D. L. (2007) Silk as a biomaterial, *Progress in Polymer Science 32*, 991-1007.
98. Zhou, C.-Z., Confalonieri, F., Jacquet, M., Perasso, R., Li, Z.-G., and Janin, J. (2001) Silk fibroin: Structural implications of a remarkable amino acid sequence, *Proteins: Structure, Function, and Bioinformatics 44*, 119-122.
99. Sashina, E. S., Bochek, A. M., Novoselov, N. P., and Kirichenko, D. A. (2006) Structure and solubility of natural silk fibroin, *Russ J Appl Chem 79*, 869-876.
100. Yamada, H., Igarashi, Y., Takasu, Y., Saito, H., and Tsubouchi, K. (2004) Identification of fibroin-derived peptides enhancing the proliferation of cultured human skin fibroblasts, *Biomaterials 25*, 467-472.
101. Rockwood, D. N., Preda, R. C., Yucel, T., Wang, X., Lovett, M. L., and Kaplan, D. L. (2011) Materials fabrication from Bombyx mori silk fibroin, *Nat. Protocols 6*, 1612-1631.
102. Motta, A., Maniglio, D., Migliaresi, C., Kim, H.-J., Wan, X., Hu, X., and Kaplan, D. L. (2009) Silk Fibroin Processing and Thrombogenic Responses, *Journal of Biomaterials Science, Polymer Edition 20*, 1875-1897.
103. Motta, A., Migliaresi, C., Faccioni, F., Torricelli, P., Fini, M., and Giardino, R. (2004) Fibroin hydrogels for biomedical applications: preparation, characterization and in vitro cell culture studies, *Journal of Biomaterials Science, Polymer Edition 15*, 851-864.
104. Foss, C., Merzari, E., Migliaresi, C., and Motta, A. (2013) Silk Fibroin/Hyaluronic Acid 3D Matrices for Cartilage Tissue Engineering, *Biomacromolecules 14*, 38-47.
105. Sugihara, A., Sugiura, K., Morita, H., Ninagawa, T., Tubouchi, K., Tobe, R., Izumiya, M., Horio, T., Abraham, N. G., and Ikehara, S. (2000) Promotive Effects of a Silk Film on Epidermal Recovery from Full-Thickness Skin Wounds, *Experimental Biology and Medicine 225*, 58-64.
106. Roh, D.-H., Kang, S.-Y., Kim, J.-Y., Kwon, Y.-B., Young Kweon, H., Lee, K.-G., Park, Y.-H., Baek, R.-M., Heo, C.-Y., Choe, J., and Lee, J.-H. (2006) Wound healing effect of silk fibroin/alginate-blended sponge in full thickness skin defect of rat, *J Mater Sci: Mater Med 17*, 547-552.
107. Min, B.-M., Lee, G., Kim, S. H., Nam, Y. S., Lee, T. S., and Park, W. H. (2004) Electrospinning of silk fibroin nanofibers and its effect on the adhesion and spreading of normal human keratinocytes and fibroblasts in vitro, *Biomaterials 25*, 1289-1297.
108. Ma, X., Cao, C., and Zhu, H. (2006) The biocompatibility of silk fibroin films containing sulfonated silk fibroin, *Journal of Biomedical Materials Research Part B: Applied Biomaterials 78B*, 89-96.
109. Bonani, W., Maniglio, D., Motta, A., Tan, W., and Migliaresi, C. (2011) Biohybrid nanofiber constructs with anisotropic biomechanical properties, *Journal of Biomedical Materials Research Part B: Applied Biomaterials 96B*, 276-286.
110. Yang, Y., Chen, X., Ding, F., Zhang, P., Liu, J., and Gu, X. (2007) Biocompatibility evaluation of silk fibroin with peripheral nerve tissues and cells in vitro, *Biomaterials 28*, 1643-1652.
111. Chen, C.-S., Soni, S., Le, C., Biasca, M., Farr, E., Chen, E.-T., and Chin, W.-C. (2012) Human stem cell neuronal differentiation on silk-carbon nanotube composite, *Nanoscale Res Lett 7*, 1-7.
112. Sofia, S., McCarthy, M. B., Gronowicz, G., and Kaplan, D. L. (2001) Functionalized silk-based biomaterials for bone formation, *Journal of Biomedical Materials Research 54*, 139-148.
113. Li, C., Vepari, C., Jin, H.-J., Kim, H. J., and Kaplan, D. L. (2006) Electrospun silk-BMP-2 scaffolds for bone tissue engineering, *Biomaterials 27*, 3115-3124.

114. Hofmann, S., Hagenmüller, H., Koch, A. M., Müller, R., Vunjak-Novakovic, G., Kaplan, D. L., Merkle, H. P., and Meinel, L. (2007) Control of in vitro tissue-engineered bone-like structures using human mesenchymal stem cells and porous silk scaffolds, *Biomaterials 28*, 1152-1162.
115. Fini, M., Motta, A., Torricelli, P., Giavaresi, G., Nicoli Aldini, N., Tschon, M., Giardino, R., and Migliaresi, C. (2005) The healing of confined critical size cancellous defects in the presence of silk fibroin hydrogel, *Biomaterials 26*, 3527-3536.
116. Kim, K.-H., Jeong, L., Park, H.-N., Shin, S.-Y., Park, W.-H., Lee, S.-C., Kim, T.-I., Park, Y.-J., Seol, Y.-J., Lee, Y.-M., Ku, Y., Rhyu, I.-C., Han, S.-B., and Chung, C.-P. (2005) Biological efficacy of silk fibroin nanofiber membranes for guided bone regeneration, *Journal of Biotechnology 120*, 327-339.
117. Meinel, L., Fajardo, R., Hofmann, S., Langer, R., Chen, J., Snyder, B., Vunjak-Novakovic, G., and Kaplan, D. (2005) Silk implants for the healing of critical size bone defects, *Bone 37*, 688-698.
118. Meinel, L., Karageorgiou, V., Hofmann, S., Fajardo, R., Snyder, B., Li, C., Zichner, L., Langer, R., Vunjak-Novakovic, G., and Kaplan, D. L. (2004) Engineering bone-like tissue in vitro using human bone marrow stem cells and silk scaffolds, *Journal of Biomedical Materials Research Part A 71A*, 25-34.
119. Kundu, B., Rajkhowa, R., Kundu, S. C., and Wang, X. (2013) Silk fibroin biomaterials for tissue regenerations, *Advanced Drug Delivery Reviews 65*, 457-470.
120. Kim, U.-J., Park, J., Li, C., Jin, H.-J., Valluzzi, R., and Kaplan, D. L. (2004) Structure and Properties of Silk Hydrogels, *Biomacromolecules 5*, 786-792.
121. Matsumoto, A., Chen, J., Collette, A. L., Kim, U.-J., Altman, G. H., Cebe, P., and Kaplan, D. L. (2006) Mechanisms of Silk Fibroin Sol−Gel Transitions, *The Journal of Physical Chemistry B 110*, 21630-21638.
122. Chen, X., Li, W., Zhong, W., Lu, Y., and Yu, T. (1997) pH sensitivity and ion sensitivity of hydrogels based on complex-forming chitosan/silk fibroin interpenetrating polymer network, *Journal of Applied Polymer Science 65*, 2257-2262.
123. Ayub Haider, Z., Arai, M., and Hirabayashi, K. (1993) Mechanism of the Gelation of Fibroin Solution, *Bioscience, biotechnology, and biochemistry 57*, 1910-1912.
124. Wang, Y., Kim, H.-J., Vunjak-Novakovic, G., and Kaplan, D. L. (2006) Stem cell-based tissue engineering with silk biomaterials, *Biomaterials 27*, 6064-6082.
125. L. Wang, Y. W., J. Qu, Y. Hu, R. You and M. Li. (2013) The Cytocompatibility of Genipin-Crosslinked Silk Fibroin Films, *Journal of Biomaterials and Nanobiotechnology 4*, 213-221.
126. Silva, S. S., Motta, A., Rodrigues, M. T., Pinheiro, A. F. M., Gomes, M. E., Mano, J. F., Reis, R. L., and Migliaresi, C. (2008) Novel Genipin-Cross-Linked Chitosan/Silk Fibroin Sponges for Cartilage Engineering Strategies, *Biomacromolecules 9*, 2764-2774.
127. Sun, W., Incitti, T., Migliaresi, C., Quattrone, A., Casarosa, S., and Motta, A. (2014) Genipin-crosslinked gelatin–silk fibroin hydrogels for modulating the behaviour of pluripotent cells, *Journal of Tissue Engineering and Regenerative Medicine*, n/a-n/a.
128. L. Wang, Y. W., J. Qu, Y. Hu, R. You and M. Li. (2013) The Cytocompatibility of Genipin-Crosslinked Silk Fibroin Films, In *Journal of Biomaterials and Nanobiotechnology*, pp 213-221.
129. Wang, X., Kluge, J. A., Leisk, G. G., and Kaplan, D. L. (2008) Sonication-induced gelation of silk fibroin for cell encapsulation, *Biomaterials 29*, 1054-1064.
130. Yucel, T., Cebe, P., and Kaplan, D. L. (2009) Vortex-Induced Injectable Silk Fibroin Hydrogels, *Biophysical journal 97*, 2044-2050.
131. Votteler, M., Kluger, P. J., Walles, H., and Schenke-Layland, K. (2010) Stem Cell Microenvironments - Unveiling the Secret of How Stem Cell Fate is Defined, *Macromolecular Bioscience 10*, 1302-1315.
132. Reilly, G. C., and Engler, A. J. (2010) Intrinsic extracellular matrix properties regulate stem cell differentiation, *Journal of Biomechanics 43*, 55-62.

133. Jaramillo, M., Singh, S. S., Velankar, S., Kumta, P. N., and Banerjee, I. (2012) Inducing endoderm differentiation by modulating mechanical properties of soft substrates, *Journal of Tissue Engineering and Regenerative Medicine*, n/a-n/a.
134. Dawson, E., Mapili, G., Erickson, K., Taqvi, S., and Roy, K. (2008) Biomaterials for stem cell differentiation, *Advanced Drug Delivery Reviews 60*, 215-228.
135. Haque, A., Yue, X.-S., Motazedian, A., Tagawa, Y.-i., and Akaike, T. (2012) Characterization and neural differentiation of mouse embryonic and induced pluripotent stem cells on cadherin-based substrata, *Biomaterials 33*, 5094-5106.
136. Li, L., Davidovich, A. E., Schloss, J. M., Chippada, U., Schloss, R. R., Langrana, N. A., and Yarmush, M. L. (2011) Neural lineage differentiation of embryonic stem cells within alginate microbeads, *Biomaterials 32*, 4489-4497.
137. Yang, F., Cho, S.-W., Son, S. M., Hudson, S. P., Bogatyrev, S., Keung, L., Kohane, D. S., Langer, R., and Anderson, D. G. (2010) Combinatorial Extracellular Matrices for Human Embryonic Stem Cell Differentiation in 3D, *Biomacromolecules 11*, 1909-1914.
138. Xie, J., Willerth, S. M., Li, X., Macewan, M. R., Rader, A., Sakiyama-Elbert, S. E., and Xia, Y. (2009) The differentiation of embryonic stem cells seeded on electrospun nanofibers into neural lineages, *Biomaterials 30*, 354-362.
139. Park, J. S., Chu, J. S., Tsou, A. D., Diop, R., Tang, Z., Wang, A., and Li, S. (2011) The effect of matrix stiffness on the differentiation of mesenchymal stem cells in response to TGF-β, *Biomaterials 32*, 3921-3930.
140. Keselowsky, B. G., Collard, D. M., and Garcia, A. J. (2005) Integrin binding specificity regulates biomaterial surface chemistry effects on cell differentiation, *PNAS 102*, 5953-5957.
141. Sasaki, D., Shimizu, T., Masuda, S., Kobayashi, J., Itoga, K., Tsuda, Y., Yamashita, J. K., Yamato, M., and Okano, T. (2009) Mass preparation of size-controlled mouse embryonic stem cell aggregates and induction of cardiac differentiation by cell patterning method, *Biomaterials 30*, 4384-4389.
142. Popa, E. G., Caridade, S. G., Mano, J. F., Reis, R. L., and Gomes, M. E. (2013) Chondrogenic potential of injectable κ-carrageenan hydrogel with encapsulated adipose stem cells for cartilage tissue-engineering applications, *Journal of Tissue Engineering and Regenerative Medicine*, n/a-n/a.
143. Dickinson, L. E., Kusuma, S., and Gerecht, S. (2011) Reconstructing the Differentiation Niche of Embryonic Stem Cells Using Biomaterials, *Macromolecular Bioscience 11*, 36-49.
144. Yao, C.-H., Liu, B.-S., Chang, C.-J., Hsu, S.-H., and Chen, Y.-S. (2004) Preparation of networks of gelatin and genipin as degradable biomaterials, *Materials Chemistry and Physics 83*, 204-208.
145. Lien, S.-M., Ko, L.-Y., and Huang, T.-J. (2009) Effect of pore size on ECM secretion and cell growth in gelatin scaffold for articular cartilage tissue engineering, *Acta Biomaterialia 5*, 670-679.
146. Park, J.-B. (2011) The use of hydrogels in bone-tissue engineering, *Medicina Oral Patologia Oral Y Cirugia Bucal 16*, E115-E118.
147. Chen, Y.-S., Chang, J.-Y., Cheng, C.-Y., Tsai, F.-J., Yao, C.-H., and Liu, B.-S. (2005) An in vivo evaluation of a biodegradable genipin-cross-linked gelatin peripheral nerve guide conduit material, *Biomaterials 26*, 3911-3918.
148. Wang, J., Yang, Q., Mao, C., and Zhang, S. (2012) Osteogenic differentiation of bone marrow mesenchymal stem cells on the collagen/silk fibroin bi-template-induced biomimetic bone substitutes, *Journal of Biomedical Materials Research Part A 100A*, 2929-2938.
149. Bhardwaj, N., and Kundu, S. C. (2012) Chondrogenic differentiation of rat MSCs on porous scaffolds of silk fibroin/chitosan blends, *Biomaterials 33*, 2848-2857.
150. Lu, Q., Zhang, X., Hu, X., and Kaplan, D. L. (2010) Green Process to Prepare Silk Fibroin/Gelatin Biomaterial Scaffolds, *Macromolecular Bioscience 10*, 289-298.

151. Akao, T., Kobashi, K., and Aburada, M. (1994) ENZYMATIC STUDIES ON THE ANIMAL AND INTESTINAL BACTERIAL METABOLISM OF GENIPOSIDE, *Biological & Pharmaceutical Bulletin 17*, 1573-1576.
152. Sung, H.-W., Liang, I. L., Chen, C.-N., Huang, R.-N., and Liang, H.-F. (2001) Stability of a biological tissue fixed with a naturally occurring crosslinking agent (genipin), *Journal of Biomedical Materials Research 55*, 538-546.
153. Motta, A., Barbato, B., Foss, C., Torricelli, P., and Migliaresi, C. (2011) Stabilization of Bombyx mori silk fibroin/sericin films by crosslinking with PEG-DE 600 and genipin, *Journal of Bioactive and Compatible Polymers 26*, 130-143.
154. Silva, S. S., Motta, A., Rodrigues, M. r. T., Pinheiro, A. F. M., Gomes, M. E., Mano, J. o. F., Reis, R. L., and Migliaresi, C. (2008) Novel Genipin-Cross-Linked Chitosan/Silk Fibroin Sponges for Cartilage Engineering Strategies, *Biomacromolecules 9*, 2764-2774.
155. Chiono, V., Pulieri, E., Vozzi, G., Ciardelli, G., Ahluwalia, A., and Giusti, P. (2008) Genipin-crosslinked chitosan/gelatin blends for biomedical applications, *Journal of Materials Science: Materials in Medicine 19*, 889-898.
156. Xiao, W., Liu, W., Sun, J., Dan, X., Wei, D., and Fan, H. (2012) Ultrasonication and Genipin Cross-Linking to Prepare Novel Silk Fibroin–Gelatin Composite Hydrogel, *Journal of Bioactive and Compatible Polymers 27*, 327-341.
157. Fico, A., Manganelli, G., Simeone, M., Guido, S., Minchiotti, G., and Filosa, S. (2008) High-throughput screening-compatible single-step protocol to differentiate embryonic stem cells in neurons, *Stem Cells and Development 17*, 573-584.
158. Muzzarelli, R. A. A. (2009) Genipin-crosslinked chitosan hydrogels as biomedical and pharmaceutical aids, *Carbohydrate Polymers 77*, 1-9.
159. Wang, C., Hao, J., Zhang, F., Su, K., and Wang, D.-A. (2008) RNA extraction from polysaccharide-based cell-laden hydrogel scaffolds, *Analytical Biochemistry 380*, 333-334.
160. Kong, J., and Yu, S. (2007) Fourier Transform Infrared Spectroscopic Analysis of Protein Secondary Structures, *Acta Biochimica et Biophysica Sinica 39*, 549-559.
161. Shao, J., Zheng, J., Liu, J., and Carr, C. M. (2005) Fourier transform Raman and Fourier transform infrared spectroscopy studies of silk fibroin, *Journal of Applied Polymer Science 96*, 1999-2004.
162. Niwa, H., Miyazaki, J.-i., and Smith, A. G. (2000) Quantitative expression of Oct-3/4 defines differentiation, dedifferentiation or self-renewal of ES cells, *Nat Genet 24*, 372-376.
163. Chambers, I., Silva, J., Colby, D., Nichols, J., Nijmeijer, B., Robertson, M., Vrana, J., Jones, K., Grotewold, L., and Smith, A. (2007) Nanog safeguards pluripotency and mediates germline development, *Nature 450*, 1230-1234.
164. Daley, W. P., Peters, S. B., and Larsen, M. (2008) Extracellular matrix dynamics in development and regenerative medicine, *Journal of Cell Science 121*, 255-264.
165. Neuss, S., Apel, C., Buttler, P., Denecke, B., Dhanasingh, A., Ding, X., Grafahrend, D., Groger, A., Hemmrich, K., Herr, A., Jahnen-Dechent, W., Mastitskaya, S., Perez-Bouza, A., Rosewick, S., Salber, J., Wöltje, M., and Zenke, M. (2008) Assessment of stem cell/biomaterial combinations for stem cell-based tissue engineering, *Biomaterials 29*, 302-313.
166. Aurand, E., Wagner, J., Lanning, C., and Bjugstad, K. (2012) Building Biocompatible Hydrogels for Tissue Engineering of the Brain and Spinal Cord, *Journal of Functional Biomaterials 3*, 839-863.
167. Fan, H., Liu, H., Toh, S. L., and Goh, J. C. H. (2008) Enhanced differentiation of mesenchymal stem cells co-cultured with ligament fibroblasts on gelatin/silk fibroin hybrid scaffold, *Biomaterials 29*, 1017-1027.
168. Hu, X., Lu, Q., Sun, L., Cebe, P., Wang, X., Zhang, X., and Kaplan, D. L. (2010) Biomaterials from Ultrasonication-Induced Silk Fibroin−Hyaluronic Acid Hydrogels, *Biomacromolecules 11*, 3178-3188.

169. Tropepe, V., Hitoshi, S., Sirard, C., Mak, T. W., Rossant, J., and van der Kooy, D. (2001) Direct Neural Fate Specification from Embryonic Stem Cells: A Primitive Mammalian Neural Stem Cell Stage Acquired through a Default Mechanism, *Neuron 30*, 65-78.
170. Kawasaki, H., Mizuseki, K., Nishikawa, S., Kaneko, S., Kuwana, Y., Nakanishi, S., Nishikawa, S.-I., and Sasai, Y. (2000) Induction of Midbrain Dopaminergic Neurons from ES Cells by Stromal Cell–Derived Inducing Activity, *Neuron 28*, 31-40.
171. Cao, H., Feng, Q., Xu, W., Li, X., Kang, Z., Ren, Y., and Du, L. (2010) Genipin Induced Apoptosis Associated with Activation of the c-Jun NH₂-Terminal Kinase and p53 Protein in HeLa Cells, *Biological and Pharmaceutical Bulletin 33*, 1343-1348.
172. Knöchel, S., Schuler-Metz, A., and Knöchel, W. (2000) c-Jun (AP-1) activates BMP-4 transcription in Xenopus embryos, *Mechanisms of Development 98*, 29-36.
173. Saha, K., Keung, A. J., Irwin, E. F., Li, Y., Little, L., Schaffer, D. V., and Healy, K. E. (2008) Substrate Modulus Directs Neural Stem Cell Behavior, *Biophysical journal 95*, 4426-4438.
174. Barinaga, M. (1998) Stroke-Damaged Neurons May Commit Cellular Suicide, *Science 281*, 1302-1303.
175. Fitch, M. T., and Silver, J. (2008) CNS injury, glial scars, and inflammation: Inhibitory extracellular matrices and regeneration failure, *Experimental Neurology 209*, 294-301.
176. Sato, M., Chang, E., Igarashi, T., and Noble, L. J. (2001) Neuronal injury and loss after traumatic brain injury: time course and regional variability, *Brain Research 917*, 45-54.
177. Kikuchi, K., Uchikado, H., Morioka, M., Murai, Y., and Tanaka, E. (2012) Clinical Neuroprotective Drugs for Treatment and Prevention of Stroke, *International Journal of Molecular Sciences 13*, 7739-7761.
178. Jin, K., and Galvan, V. (2007) Endogenous Neural Stem Cells in the Adult Brain, *Journal of Neuroimmune Pharmacology 2*, 236-242.
179. Pakulska, M. M., Ballios, B. G., and Shoichet, M. S. (2012) Injectable hydrogels for central nervous system therapy, *Biomedical Materials 7*, 024101.
180. Uludag, H., De Vos, P., and Tresco, P. A. (2000) Technology of mammalian cell encapsulation, *Advanced Drug Delivery Reviews 42*, 29-64.
181. Foss, C., Merzari, E., Migliaresi, C., and Motta, A. (2012) Silk Fibroin/Hyaluronic Acid 3D Matrices for Cartilage Tissue Engineering, *Biomacromolecules 14*, 38-47.
182. Rutka, J. T., Apodaca, G., Stern, R., and Rosenblum, M. (1988) The extracellular matrix of the central and peripheral nervous systems: structure and function, *Journal of Neurosurgery 69*, 155-170.
183. Hall, P., Lathia, J., Caldwell, M., and ffrench-Constant, C. (2008) Laminin enhances the growth of human neural stem cells in defined culture media, *BMC Neurosci 9*, 1-10.
184. Millaruelo, A. I., Nieto-Sampedro, M., and Cotman, C. W. (1988) Cooperation between nerve growth factor and laminin or fibronectin in promoting sensory neuron survival and neurite outgrowth, *Developmental Brain Research 38*, 219-228.
185. Nomizu, M., Weeks, B. S., Weston, C. A., Kim, W. H., Kleinman, H. K., and Yamada, Y. (1995) Structure-activity study of a laminin α1 chain active peptide segment Ile-Lys-Val-Ala-Val (IKVAV), *FEBS Letters 365*, 227-231.
186. Kubinová, Š., Horák, D., Kozubenko, N., Vaněček, V., Proks, V., Price, J., Cocks, G., and Syková, E. (2010) The use of superporous Ac-CGGASIKVAVS-OH-modified PHEMA scaffolds to promote cell adhesion and the differentiation of human fetal neural precursors, *Biomaterials 31*, 5966-5975.
187. Li, Q., Chow, K. L., and Chau, Y. (2014) Three-dimensional self-assembling peptide matrix enhances the formation of embryoid bodies and their neuronal differentiation, *Journal of Biomedical Materials Research Part A 102*, 1991-2000.

188. Vidal, G., Blanchi, T., Mieszawska, A. J., Calabrese, R., Rossi, C., Vigneron, P., Duval, J.-L., Kaplan, D. L., and Egles, C. (2013) Enhanced cellular adhesion on titanium by silk functionalized with titanium binding and RGD peptides, *Acta Biomaterialia 9*, 4935-4943.
189. Flanagan, L. A., Ju, Y. E., Marg, B., Osterfield, M., and Janmey, P. A. (2002) Neurite branching on deformable substrates, *Neuroreport 13*, 2411-2415.
190. Zhu, H., Liu, N., Feng, X., and Chen, J. (2012) Fabrication and characterization of silk fibroin/bioactive glass composite films, *Materials Science and Engineering: C 32*, 822-829.
191. Motta, A., Migliaresi, C., Faccioni, F., Torricelli, P., Fini, M., and Giardino, R. (2004) Fibroin hydrogels for biomedical applications: preparation, characterization and in vitro cell culture studies, *Journal of biomaterials science. Polymer edition 15*, 851-864.
192. Santin, M., Motta, A., Freddi, G., and Cannas, M. (1999) In vitro evaluation of the inflammatory potential of the silk fibroin, *Journal of Biomedical Materials Research 46*, 382-389.
193. Hopkins, A. M., De Laporte, L., Tortelli, F., Spedden, E., Staii, C., Atherton, T. J., Hubbell, J. A., and Kaplan, D. L. (2013) Silk Hydrogels as Soft Substrates for Neural Tissue Engineering, *Advanced Functional Materials 23*, 5140-5149.
194. Hu, Y., Zhang, Q., You, R., Wang, L., and Li, M. (2012) The Relationship between Secondary Structure and Biodegradation Behavior of Silk Fibroin Scaffolds, *Advances in Materials Science and Engineering 2012*, 5.
195. Hosseinkhani, H., Hiraoka, Y., Li, C.-H., Chen, Y.-R., Yu, D.-S., Hong, P.-D., and Ou, K.-L. (2013) Engineering Three-Dimensional Collagen-IKVAV Matrix to Mimic Neural Microenvironment, *ACS Chemical Neuroscience 4*, 1229-1235.
196. Villard, V., Kalyuzhniy, O., Riccio, O., Potekhin, S., Melnik, T. N., Kajava, A. V., Rüegg, C., and Corradin, G. (2006) Synthetic RGD-containing α-helical coiled coil peptides promote integrin-dependent cell adhesion, *Journal of Peptide Science 12*, 206-212.
197. Srikanth, M., Das, S., Berns, E. J., Kim, J., Stupp, S. I., and Kessler, J. A. (2013) Nanofiber-mediated inhibition of focal adhesion kinase sensitizes glioma stemlike cells to epidermal growth factor receptor inhibition, *Neuro-Oncology 15*, 319-329.
198. Sun, Y., Pollard, S., Conti, L., Toselli, M., Biella, G., Parkin, G., Willatt, L., Falk, A., Cattaneo, E., and Smith, A. (2008) Long-term tripotent differentiation capacity of human neural stem (NS) cells in adherent culture, *Molecular and Cellular Neuroscience 38*, 245-258.
199. Novosel, E. C., Kleinhans, C., and Kluger, P. J. (2011) Vascularization is the key challenge in tissue engineering, *Advanced Drug Delivery Reviews 63*, 300-311.
200. Nomi, M., Atala, A., Coppi, P. D., and Soker, S. (2002) Principals of neovascularization for tissue engineering, *Molecular Aspects of Medicine 23*, 463-483.
201. Dai, J., and Rabie, A. B. M. (2007) VEGF: an Essential Mediator of Both Angiogenesis and Endochondral Ossification, *Journal of Dental Research 86*, 937-950.
202. Ferrara, N., and Davis-Smyth, T. (1997) The Biology of Vascular Endothelial Growth Factor, *Endocrine Reviews 18*, 4-25.
203. Rao, R., Peterson, A., Ceccarelli, J., Putnam, A., and Stegemann, J. (2012) Matrix composition regulates three-dimensional network formation by endothelial cells and mesenchymal stem cells in collagen/fibrin materials, *Angiogenesis 15*, 253-264.
204. Hristov, M., Zernecke, A., Liehn, E. A., and Weber, C. (2007) Regulation of endothelial progenitor cell homing after arterial injury, *Thrombosis and Haemostasis 98*, 274-277.
205. Urbich, C., and Dimmeler, S. (2004) Endothelial Progenitor Cells: Characterization and Role in Vascular Biology, *Circulation Research 95*, 343-353.
206. Santos, M. I., Unger, R. E., Sousa, R. A., Reis, R. L., and Kirkpatrick, C. J. (2009) Crosstalk between osteoblasts and endothelial cells co-cultured on a polycaprolactone–starch scaffold and the in vitro development of vascularization, *Biomaterials 30*, 4407-4415.

207. Rivron, N. C., Liu, J., Rouwkema, J., Boer, J. d., and Blitterswijk, C. A. v. (2008) Engineering vascularised tissues in vitro, *European Cells & Materials 15*, 27-40.
208. Folkman, J., and D'Amore, P. A. (1996) Blood Vessel Formation: What Is Its Molecular Basis?, *Cell 87*, 1153-1155.
209. Davis, G. E., and Senger, D. R. (2005) Endothelial Extracellular Matrix: Biosynthesis, Remodeling, and Functions During Vascular Morphogenesis and Neovessel Stabilization, *Circulation Research 97*, 1093-1107.
210. Au, P., Tam, J., Fukumura, D., and Jain, R. K. (2008) Bone marrow–derived mesenchymal stem cells facilitate engineering of long-lasting functional vasculature, *Blood 111*, 4551-4558.
211. Ghajar, C. M., Kachgal, S., Kniazeva, E., Mori, H., Costes, S. V., George, S. C., and Putnam, A. J. (2010) Mesenchymal cells stimulate capillary morphogenesis via distinct proteolytic mechanisms, *Experimental Cell Research 316*, 813-825.
212. Boomsma, R. A., and Geenen, D. L. (2012) Mesenchymal Stem Cells Secrete Multiple Cytokines That Promote Angiogenesis and Have Contrasting Effects on Chemotaxis and Apoptosis, *PLoS ONE 7*, e35685.
213. Ergul, A., Alhusban, A., and Fagan, S. C. (2012) Angiogenesis: A Harmonized Target for Recovery After Stroke, *Stroke 43*, 2270-2274.
214. Song, Y., Li, Y., and Zheng, Q. (2010) Angiogenesis induced by IKVAV-Containing amphiphile peptide in vivo, *J. Wuhan Univ. Technol.-Mat. Sci. Edit. 25*, 803-806.
215. Fuchs, S., Hermanns, M., and Kirkpatrick, C. (2006) Retention of a differentiated endothelial phenotype by outgrowth endothelial cells isolated from human peripheral blood and expanded in long-term cultures, *Cell Tissue Res 326*, 79-92.
216. Chen, L., Tredget, E. E., Wu, P. Y. G., and Wu, Y. (2008) Paracrine Factors of Mesenchymal Stem Cells Recruit Macrophages and Endothelial Lineage Cells and Enhance Wound Healing, *PLoS ONE 3*, e1886.
217. Marlen Kolbe, Z. X., Eva Dohle, Marcus Tonak, Charles James Kirkpatrick, and Sabine Fuchs. . (2011) Paracrine Effects Influenced by Cell Culture Medium and Consequences on Microvessel-Like Structures in Cocultures of Mesenchymal Stem Cells and Outgrowth Endothelial Cells *Tissue Engineering Part A. 17*, 2199-2212.
218. Köllmer, M., Keskar, V., Hauk, T. G., Collins, J. M., Russell, B., and Gemeinhart, R. A. (2012) Stem Cell-Derived Extracellular Matrix Enables Survival and Multilineage Differentiation within Superporous Hydrogels, *Biomacromolecules 13*, 963-973.
219. Krugliakov, P. V., Sokolova, I. B., Zin'kova, N. N., Viĭde, S. V., Cherednichenko, N. N., Kisliakova, T. V., and Polyntsev, D. G. (2005) The influence of mesenchymal stem cells on bone tissue regeneration upon implantation of demineralized bone matrix, *Tsitologiia 47*, 466-477.